



UNIVERSIDAD NACIONAL AUTÓNOMA DE MÉXICO

POSGRADO EN CIENCIAS BIOLÓGICAS

FACULTAD DE MEDICINA

BIOLOGIA EXPERIMENTAL

**CARACTERIZACIÓN DE LA RESPUESTA INMUNE EN PULMÓN DE RATONES BALB/c
DESPUÉS DE LA INFECCIÓN INTRANASAL CON LOS MORFOTIPOS MICELIAL Y
LEVADURIFORME DE *Histoplasma capsulatum***

TESIS

QUE PARA OPTAR POR EL GRADO DE:

DOCTOR EN CIENCIAS

PRESENTA

JORGE HUMBERTO SAHAZA CARDONA

TUTORA PRINCIPAL DE TESIS: DRA. MARIA LUCIA TAYLOR DA CUNHA E MELLO

FACULTAD DE MEDICINA, UNAM

COMITÉ TUTOR: DRA. INGEBORG DOROTHEA BECKER FAUSER

FACULTAD DE MEDICINA, UNAM

DR. EDUARDO GARCÍA ZEPEDA

INSTITUTO DE INVESTIGACIONES BIOMEDICAS, UNAM

TUTOR INVITADO: DR. ARMANDO PÉREZ TORRES

FACULTAD DE MEDICINA, UNAM

MÉXICO, D.F.

DICIEMBRE 2014



Universidad Nacional
Autónoma de México



UNAM – Dirección General de Bibliotecas
Tesis Digitales
Restricciones de uso

DERECHOS RESERVADOS ©
PROHIBIDA SU REPRODUCCIÓN TOTAL O PARCIAL

Todo el material contenido en esta tesis esta protegido por la Ley Federal del Derecho de Autor (LFDA) de los Estados Unidos Mexicanos (México).

El uso de imágenes, fragmentos de videos, y demás material que sea objeto de protección de los derechos de autor, será exclusivamente para fines educativos e informativos y deberá citar la fuente donde la obtuvo mencionando el autor o autores. Cualquier uso distinto como el lucro, reproducción, edición o modificación, será perseguido y sancionado por el respectivo titular de los Derechos de Autor.



UNIVERSIDAD NACIONAL AUTÓNOMA DE MÉXICO

POSGRADO EN CIENCIAS BIOLÓGICAS

FACULTAD DE MEDICINA

BIOLOGIA EXPERIMENTAL

**CARACTERIZACIÓN DE LA RESPUESTA INMUNE EN PULMÓN DE RATONES BALB/c
DESPUÉS DE LA INFECCIÓN INTRANASAL CON LOS MORFOTIPOS MICELIAL Y
LEVADURIFORME DE *Histoplasma capsulatum***

TESIS

QUE PARA OPTAR POR EL GRADO DE:

DOCTOR EN CIENCIAS

PRESENTA

JORGE HUMBERTO SAHAZA CARDONA

TUTORA PRINCIPAL DE TESIS: DRA. MARIA LUCIA TAYLOR DA CUNHA E MELLO

FACULTAD DE MEDICINA, UNAM

COMITÉ TUTOR: DRA. INGEBORG DOROTHEA BECKER FAUSER

FACULTAD DE MEDICINA, UNAM

DR. EDUARDO GARCÍA ZEPEDA

INSTITUTO DE INVESTIGACIONES BIOMEDICAS, UNAM

TUTOR INVITADO: DR. ARMANDO PÉREZ TORRES

FACULTAD DE MEDICINA, UNAM

MÉXICO, D.F.

DICIEMBRE 2014

Dr. Isidro Ávila Martínez
Director General de Administración Escolar, UNAM
Presente

Me permito informar a usted que el Subcomité de Biología Experimental y Biomedicina del Posgrado en Ciencias Biológicas, en su sesión ordinaria del día 03 de noviembre de 2014, aprobó el jurado para la presentación de su examen para obtener el grado de **DOCTOR EN CIENCIAS** del alumno **SAHAZA CARDONA JORGE HUMBERTO** con número de cuenta **501459750** con la tesis titulada "**CARACTERIZACIÓN DE LA RESPUESTA INMUNE EN PULMÓN DE RATONES BALB/C DESPUÉS DE LA INFECCIÓN INTRANASAL CON LOS MORFOTIPOS MICELIAL Y LEVADURIFORME DE *Histoplasma capsulatum***", realizada bajo la dirección de la **DRA. MARIA LUCIA TAYLOR DA CUNHA E MELLO**:

Presidente: DRA. SARA HUERTA YEPEZ
Vocal: DRA. MARÍA DEL ROCÍO REYES MONTES
Secretario: DRA. INGEBORG DOROTHEA BECKER FAUSER
Suplente: DR. JULIO GRANADOS ARRIOLA
Suplente: DR. ARMANDO PÉREZ TORRES

Sin otro particular, me es grato enviarle un cordial saludo.

ATENTAMENTE
"POR MI RAZA HABLARÁ EL ESPÍRITU"
Cd. Universitaria, D.F., a 24 de noviembre de 2014



DRA. MARÍA DEL CORO ARIZMENDI ARRIAGA
COORDINADORA DEL PROGRAMA



AGRADECIMIENTOS INSTITUCIONALES

Al Posgrado en Ciencias Biológicas de la UNAM por permitirme terminar satisfactoriamente en tiempo y forma el Doctorado en Ciencias.

Al Concejo Nacional de Ciencia y Tecnología (CONACYT) por otorgarme la beca con referencia 245151 durante los semestres 2011-1-2015-1, para la realización de mis estudios de Doctorado.

Al SEP-CONACYT por el financiamiento del proyecto de Doctorado, referencia 166052.

A los miembros del comité Tutor, Dra. Maria Lucia Taylor da Cunha e Mello, Dra. Ingeborg Becker, Dr. Eduardo García Zepeda y Dr. Armando Pérez Torres por sus valiosas contribuciones al proyecto y por el tiempo que dedicaron para analizar y aportar una crítica constructiva a este trabajo.

AGRADECIMIENTOS PERSONALES

A Norela y Paulina, por el tiempo, por soportar la distancia y la ausencia.

A mis padres (Humberto y Noelia)

A mis compañeros y amigos del laboratorio, Antonio G, Antonio R, Amelia, Tania, Claudia, Lisandra (ya PdS), David, por su compañía y sobretodo su calidez humana.

A Daniel, Eugenia, Laura, Dra. Rocio R, Dra. Francisca, Erika, Esperanza, Elba, Gaby, Saúl, Erik, Carolina, Ana C, Natalia.

A mi tutora principal, la Dra. Maria Lucia Taylor, por su paciencia, el tiempo dedicado a la elaboración, escritura y revisión de proyectos, artículos, presentaciones y tesis, por compartir sus conocimientos, creer en mí y sobre todo por hacerme sentir como parte de su familia.

Al Dr. Armando Pérez Torres, Tutor, Maestro, Amigo, Hermano, por los conocimientos transmitidos y sobre todo las buenas charlas compartiendo un café.

A los cuates del sexto, Enrique, Evelyn, Iván, gracias por compartir un pedacito de ustedes conmigo.

A todos los que hacen parte del Posgrado en Ciencias, la Dra. María del Coro Arizmendi, Dra., Yolanda López, Lila Espinoza, Lilia Jiménez, Armando, Rocío Flórez, Maria de Jesús, Patricia Oliva, Rocío Chávez y Erika Rodríguez. Gracias por su apoyo y disposición de servicio, sin ustedes sería muy difícil.

A la Universidad Nacional Autónoma de México.

A México lindo y querido.

DEDICATORIA

Ayer, hoy y siempre, el motor y la vitalidad que impulsan mi vida

Norela y Paulina

“Saber mucho no es lo mismo que ser inteligente. La inteligencia no es sólo información, sino también juicio, la manera en que se recoge y maneja la información.”

“La ciencia es más que un simple conjunto de conocimientos: es una manera de pensar”

Carl Sagan

INDICE

Resumen	1
Abstract	2
CAPÍTULO 1	3
Introducción	4
Planteamiento del problema	6
CAPÍTULO 2	7
Hipótesis	8
Objetivo general	8
Objetivos particulares	8
CAPÍTULO 3	9
Artículo requisito: Sahaza JH , Pérez-Torres A, Zenteno E, Taylor ML. Usefulness of the murine model to study the immune response against <i>Histoplasma capsulatum</i> infection. Comp Immunol Microbiol Infect Dis. 2014;37(3):143-52.	10
CAPÍTULO 4	21
Artículo científico enviado: Suárez-Alvarez R, Sahaza JH , Berzunza-Cruz M, Becker I, Curiel-Quesada E, Pérez-Torres A, Taylor ML. Dimorphism and dissemination of <i>Histoplasma capsulatum</i> occur in the nasal mucosa and cervical lymph nodes of bats and mice in a short-time after intranasal-infection with mycelial propagules. Innate Immunity.	22
CAPÍTULO 5	45
Artículo científico enviado: Sahaza JH , Suárez-Alvarez R, Estrada-Bárceñas DA, Pérez-Torres A, Taylor ML. Profile of cytokines and granulomas development in the lungs of BALB/c mice after <i>Histoplasma capsulatum</i> intra-nasal infection with mycelial propagules. Comp Immunol Microbiol Infect Dis.	46
CAPÍTULO 6	64
Otros resultados obtenidos aun no publicados	65
Determinación de citoquinas en sobrenadantes de homogeneizado de pulmón de ratones BALB/c a diferentes tiempos después de la infección intranasal con propágulos fúngicos del morfotipo-L	65
Perfiles de IL-1 β y TNF- α	65
Perfiles de IL-6, IL-17, IL-22 e IL-23	65
Perfiles de IL-12 e IFN- γ	66

Perfiles de IL-4 e IL-10	66
Evaluación del curso de la respuesta inflamatoria en pulmón de ratones BALB/c obtenidos a diferentes tiempos después de la infección intranasal con propágulos fúngicos del morfotipo-L	67
Figuras 1 a 5	68
CAPÍTULO 7	73
Discusión	74
Conclusiones	77
CAPÍTULO 8	78
Literatura citada	79
ANEXOS	83
Artículos publicados o enviados no asociados al trabajo de tesis	84
Anexo 1	
Artículo publicado: Estrada-Bárceñas DA, Vite-Garín T, Navarro-Barranco H, de la Torre-Arciniega R, Pérez-Mejía A, Rodríguez-Arellanes G, Ramirez JA, Humberto Sahaza J , Taylor ML, Toriello C. Genetic diversity of <i>Histoplasma</i> and <i>Sporothrix</i> complexes based on sequences of their ITS1-5.8S-ITS2 regions from the BOLD System. Rev Iberoam Micol. 2014;31(1):90-4.	85
Anexo 2	
Artículo enviado: Sahaza JH , Reyes-Montes MR, Canteros CE, Taylor ML. Study of temperature sensitivity and doubling time of <i>Histoplasma capsulatum</i> yeast phase using clinical strains from different regions of the Americas. BioMed Research International.	90

Resumen

La infección respiratoria con el hongo dimórfico *Histoplasma capsulatum* resulta de la inhalación de propágulos infectivos de la fase micelial (morfotipo-M) presente en los suelos contaminados. Las manifestaciones de la enfermedad son variables y dependen del estado inmune del huésped, el número de propágulos inhalados y la cepa fúngica. Se dispone de pocos datos en relación con la respuesta inmune pulmonar del huésped después del primer contacto con el morfotipo-M de *H. capsulatum*. Para abordar este planteamiento, se detectó en homogeneizados de pulmón el perfil de 10 citoquinas (IL-1 β , TNF- α , IL-6, IL-17, IL-22, IL-23, IL-12, IFN- γ , IL4 e IL-10) por el sistema MagPix y se estudió la cinética de formación de granulomas en cortes histológicos de pulmón de ratones infectados por vía intranasal con el morfotipo-M o el morfotipo-L (fase levaduriforme) de dos cepas virulentas de *H. capsulatum*, EH-46 de México (del clado filogenético LAm A) y G-217B de Estados Unidos de América (del clado filogenético NAm 2). Los datos de las citoquinas fueron determinados desde el tiempo 0 hasta 28 días post-infección, mientras que los granulomas fueron estudiados primariamente en tiempos tardíos post-infección, 14, 21 y 28 días. Según el morfotipo y las cepas fúngicas utilizadas, los niveles de citoquinas pro-inflamatorias en los homogeneizados pulmonares de los ratones infectados mostraron que, en general, sus concentraciones más elevadas se asociaron con los ratones infectados con el morfotipo-M de la cepa EH-46, a excepción de la IL-22 que reveló niveles elevados durante las primeras horas post-infección con el morfotipo-L de la misma cepa. Mientras que las citoquinas anti-inflamatorias, como IL-4 e IL-10, mostraron niveles similares independientemente del morfotipo pero distintos entre las dos cepas. En muchos casos, la respuesta inflamatoria mostró un comportamiento similar al de las citoquinas en los tiempos estudiados post-infección, resaltando nuevamente las diferencias marcadas por los morfotipos y cepas fúngicas en el desarrollo de la respuesta inflamatoria y, por ende, en la resolución de la infección. Los resultados destacan que la infección inicial con el morfotipo-M generó una respuesta inmune más intensa que la infección inicial con el morfotipo-L, especialmente con la cepa mexicana EH-46 (LAm A). Muchos de los trabajos (publicados y enviados) anexados a esta tesis junto con datos adicionales no publicados reportados en el presente manuscrito apoyan fuertemente los resultados antes mencionado. En conclusión, diferencias tanto en la respuesta inmune mediada por citoquinas así como por la respuesta inflamatoria (granulomas) en pulmón de ratones frente a la infección por *H. capsulatum* dependen de la cepa fúngica utilizada, así como de la plasticidad morfológica asociada al dimorfismo de *H. capsulatum* durante la primera etapa de la infección fúngica.

Abstract

Respiratory infection with the dimorphic fungus *Histoplasma capsulatum* results from inhalation of infective mycelial phase (M-morphotype) propagules present in contaminated soils. The manifestations of the disease are variable and depend on the immune status of the host, the number of inhaled propagules, and the fungal strain. There are few data regarding to the pulmonary host immune response after the first contact with the M-morphotype of *H. capsulatum*. To address this issue, profiles of 10 cytokines (IL-1 β , TNF- α , IL-6, IL-17, IL-22, IL-23, IL-12, IFN- γ , IL4, and IL-10) were detected in lung homogenates by the MagPix system, and the kinetic of granulomas development was studied in lung tissue sections from mice infected intra-nasally with the M-morphotype or the Y-morphotype (yeast phase) of two *H. capsulatum* virulent strains, EH-46 from Mexico (belonging to the phylogenetic clade LAm A) and G-217B from United States of America (belonging to the phylogenetic clade NAm 2). Cytokine data were determined from time 0 until 28 days post-infection, whereas granulomas were studied primarily in delayed post-infection time, 14, 21, and 28 days. Depending on the fungal morphotype and the strain used, pro-inflammatory cytokine levels in lung homogenates from infected mice showed that, in general, their highest concentrations were associated to mice infected with the M-morphotype from EH-46 strain, with the exception of IL-22, which revealed high levels during the first post-infection time with the Y-morphotype of the same strain. Anti-inflammatory cytokines, such as IL-4 and IL-10, showed similar levels irrespective of the morphotype but different levels between the two strains. In most cases, the inflammatory response showed similar behavior of the cytokines in the post-infection times studied, highlighting again particular differences of the fungal morphotypes and strains in the development of the inflammatory response and in the resolution of the disease. Our results highlight that the initial infection with M-morphotype generates a more intense immune response than the initial infection with the Y-morphotype, especially with the EH-46 (LAm A) Mexican strain. Most of the papers (published or submitted) attached to this thesis together with additional unpublished also reported in the present thesis support strongly the afore-mentioned results. In conclusion, differences in the immune response mediated by cytokines or by the inflammatory response (granulomas) in the lung of *H. capsulatum*-infected mice depend on the fungal strain used, as well as on the morphological plasticity associated to *H. capsulatum* dimorphism in the first step of the fungal infection.

CAPÍTULO 1

CAPÍTULO 1

Introducción

La histoplasmosis, micosis sistémica de amplia distribución en las Américas, puede ser considerada como una de las infecciones pulmonares fúngicas más frecuente a nivel mundial. Es causada por el hongo dimórfico *Histoplasma capsulatum* var. *capsulatum* (*H. capsulatum*). Es una enfermedad que afecta principalmente el sistema fagocítico mononuclear y tanto su severidad como sus formas clínicas dependen de las condiciones inmunológicas del huésped, del tamaño del inóculo y de la virulencia de la cepa fúngica. En la mayoría de los pacientes la infección es autolimitada y sólo deja calcificaciones residuales en pulmón (forma benigna). La forma clínica grave es más común después de la exposición masiva y prolongada a los propágulos fúngicos infectivos independientemente del estado inmune del individuo. La infección se adquiere por inhalación de las partículas infectivas aerosolizadas, particularmente, microconidios y fragmentos de hifas producidas por la fase micelial (morfotipo-M) del hongo, la cual se encuentra en suelos contaminados con excretas de murciélagos y aves (fuentes de micro-nutrientes importantes para el desarrollo del morfotipo-M) (Tewari et al. 1998).

Tradicionalmente, se ha sugerido que en los macrófagos alveolares se presenta el cambio dimórfico del morfotipo-M a levadura (morfotipo-L, parasitario y virulento) (Gildea et al. 2001), condición necesaria para el establecimiento y progresión de la infección. Así el pulmón constituye el órgano blanco primario donde las células fagocíticas asociadas a la respuesta inmune innata, principalmente los macrófagos y células dendríticas (CD) alveolares, son las responsables de captar los propágulos infectivos e iniciar además la conexión con la respuesta inmune adaptativa (Newman 1999). Esta última, es primordial para definir el destino final del parásito fúngico. Sin embargo, datos recientes sugieren que la primer línea de defensa del huésped contra *H. capsulatum* involucra el sistema inmune asociado a mucosas del tracto respiratorio superior e inferior, la cual es la vía de entrada de este patógeno, ya que el cambio dimórfico de *H. capsulatum* puede darse desde el contacto inicial entre los propágulos infectivos del morfotipo-M y los componentes de la mucosa nasal a las 2 horas post-infección intranasal de ratones machos BALB/c y murciélagos machos *Artibeus hirsutus* (Sahaza et al. 2014a; Suárez-Alvarez 2010; Suárez-Alvarez et al. 2014).

El papel de la respuesta inmune innata en el proceso infeccioso por *H. capsulatum* no ha sido suficientemente explorado (Medeiros et al. 2004; Patiño et al. 1987). Mientras que la activación de la respuesta inmune adaptativa protectora de tipo Th1, responsable del montaje de la inmunidad mediada por células CD4+, ha sido preferencialmente estudiada con el morfotipo-L (Allen et al. 2006; Allendörfer et al. 1999; Deepe y Seder 1998; Medeiros et al. 2008; Wheat 1996). Tanto en la histoplasmosis experimental y clínica, así como en otras enfermedades fúngicas, la respuesta Th1 en modelos murinos se caracteriza por la producción de las citoquinas IL-12, IFN- γ , TNF- α y GM-CSF que son esenciales para la activación de macrófagos que se encargan de eliminar las levaduras

intracelulares (Allendoerfer y Deepe 1998; Allendoerfer et al. 1997; Cain y Deepe 1998; Clemons et al. 2000; Gildea et al. 2001; Huffnagle y Deepe 2003; Newman 1999; Williams et al. 1978; Zhou et al. 1995). TNF- α parece jugar un papel crítico en la inmunidad protectora de ratones C57BL/6 contra la histoplasmosis inducida por el morfotipo-L, ya que es necesaria para la persistencia de la respuesta de defensa (Deepe y Gibbons 2006).

La respuesta Th2 caracterizada por la producción de IL-4, IL-5 y IL-13 se asocia con una exacerbación de la enfermedad y modula la severidad de la infección. En hongos patógenos de humanos, la respuesta Th2 es importante en el desarrollo y/o mantenimiento de la inmunidad mediada por Th1 (Mencacci et al. 1998). Por lo tanto, en la histoplasmosis, para una buena resolución de la enfermedad es crucial el balance Th1/Th2 ya que la exacerbación de Th1 o la tendencia favorable hacia Th2 puede intervenir en la etiopatogénesis de la enfermedad.

Recientemente, se ha dado importancia a un grupo especial de células T colaboradoras (Th17), las cuales están asociadas a la inmunidad adaptativa contra una gama de patógenos, principalmente, por la producción e inducción de IL-17 e IL-23, respectivamente. Se ha demostrado que IL-17 posee propiedades proinflamatorias y puede regular el equilibrio entre la respuesta Th1/Th2 (Matsuzaki et al. 2007; Ouyang et al. 2008; Romani et al. 2008). En el caso de *H. capsulatum*, se detectó IL-17 en granulomas hepáticos de ratones con histoplasmosis experimental (Heninger et al. 2006). Deepe y Geebans (2009), reportaron que IL-17 podría ser necesaria para la eliminación de *H. capsulatum*, puesto que se detectó una sobrerregulación de ésta en pulmón, durante la infección aguda de ratones C57BL/6 inoculados intranasalmente con el morfotipo-L del hongo; además, anticuerpos monoclonales anti IL-17 fueron capaces de alterar la respuesta inflamatoria, retardando la eliminación del hongo durante la infección primaria, pero no así durante la infección secundaria. Experimentos adicionales revelaron que IL-23 podría prolongar la supervivencia de ratones en la ausencia de IL-12. Este efecto protector fue dependiente de IL-17. Por lo tanto, el eje IL-17/IL-23 favorece la inmunidad durante la infección con *H. capsulatum* (Deepe y Geebans 2009).

Por otro lado, la infección de los macrófagos por *H. capsulatum* induce la formación de granulomas en diferentes tejidos. Como ocurre en otras infecciones, los granulomas son necesarios para contener el crecimiento del hongo, prevenir la diseminación sistémica y proteger los órganos del daño tisular inflamatorio generalizado (Mukhopadhyay y Gal 2010). Se ha demostrado que existen diferencias en la respuesta celular y la formación del granuloma en relación con el tejido afectado, cuando se inoculan ratones con el morfotipo-L de *H. capsulatum* por vía intramuscular o intravenosa (Berry 1969a; 1969b; 1969c; Heninger et al. 2006). La reacción del tejido pulmonar en la infección por *H. capsulatum* puede ser dividida en tres tipos principales: el primero es un infiltrado alveolar mononuclear con pequeños focos inflamatorios y necrosis variable, descrito en la histoplasmosis pulmonar aguda; el segundo es una reacción tisular que se compone de capas de macrófagos, en el intersticio pulmonar, repletos de numerosos organismos, como se ve en la histoplasmosis diseminada; y el tercer tipo es la forma más común de la enfermedad pulmonar relacionada con *H. capsulatum*, la cual se observa como una inflamación granulomatosa necrotizante característica de la

enfermedad pulmonar crónica (Goodwin y Snell 1969; Heninger et al. 2006; Mukhopadhyay y Gal 2010).

La resolución de la infección por *H. capsulatum* requiere de la participación de células y moléculas efectoras del huésped. Los macrófagos, las CD y los linfocitos T son los actores celulares esenciales que actúan en armonía con efectores generados por mecanismos de señalizaciones resultantes de las interacciones de moléculas de superficie del patógeno (PAMPs, del inglés pathogen-associated molecular patterns) con receptores de reconocimiento presentes en las células del huésped (PRRs, del inglés pattern recognition receptors) (Deepe y Geebans 2009). Los productos de estos eventos son, en general, mediadores químicos de la respuesta inmune y células activadas.

En el modelo de *H. capsulatum*, a pesar de saber que su ruta de entrada primordial es la vía inhalatoria y que afecta principalmente los pulmones, se desconocen las consecuencias y aun muchos de los mecanismos y moléculas que interactúan en el reconocimiento inicial del morfotipo-M y durante la transición dimórfica en las primeras etapas de contacto del hongo con el huésped, así como la naturaleza del granuloma debido al morfotipo-L el cual se generó por la inhalación inicial de propágulos del morfotipo-M de *H. capsulatum*.

Planteamiento del problema

A la fecha, son pocos los trabajos que han utilizado la ruta inhalatoria y los propágulos infectivos del morfotipo-M, que simulan la infección natural autolimitada de humanos, utilizando un modelo animal de histoplasmosis. Asimismo, son escasos los estudios comparativos de la respuesta inmune frente a un estímulo intranasal con el morfotipo-M o -L de *H. capsulatum*. Por lo tanto, los eventos primarios de los mecanismos de defensa asociados a la respuesta inmune hacia propágulos de los morfotipos -M o -L pueden diferir en tiempo y forma después de la infección por vía natural, sobre todo considerando que el morfotipo-M debe efectuar en los tiempos iniciales de la infección su cambio dimórfico. Se supone que estos eventos de la respuesta de defensa deben suceder desde el primer contacto del patógeno con el huésped y se pueden prolongar hasta días y semanas después de la infección. Con base en estas inferencias, consideramos prioritario diseñar un modelo experimental con características muy cercanas a la infección natural del humano que permita precisar aspectos importantes de la interacción huésped-parásito en la histoplasmosis, asociados a las moléculas de la respuesta inmune y al proceso inflamatorio involucrados durante las diferentes etapas de la infección inducida por uno u otro morfotipo de *H. capsulatum*.

CAPÍTULO 2

CAPÍTULO 2

Hipótesis

El morfotipo fúngico y la cepa de *H. capsulatum* utilizados para generar una infección intranasal de ratones BALB/c influye sobre el curso e intensidad de la respuesta inmune en la histoplasmosis experimental.

Objetivo general

Caracterizar en pulmón el curso e intensidad de la respuesta inmune de la histoplasmosis experimental en ratones BALB/c, durante y después de la inoculación intranasal de propágulos fúngicos, microconidias y/o fragmentos de hifas (morfotipo-M) o bien de levaduras (morfotipo-L) de distintas cepas de *H. capsulatum*.

Objetivos particulares

- Inducir en ratones BALB/c la histoplasmosis pulmonar utilizando los morfotipos M o L.
- Evaluar el curso de la infección experimental durante cuatro semanas.
- Evaluar el perfil de citoquinas en homogeneizados pulmonares de los ratones infectados.
- Identificar el curso de la respuesta inflamatoria, por medio del estudio histopatológico, en los pulmones de los ratones infectados.

CAPÍTULO 3

CAPÍTULO 3

Artículo requisito

Sahaza JH, Pérez-Torres A, Zenteno E, Taylor ML. Usefulness of the murine model to study the immune response against *Histoplasma capsulatum* infection. *Comp Immunol Microbiol Infect Dis*. 2014;37(3):143-52.



Contents lists available at ScienceDirect

Comparative Immunology, Microbiology and Infectious Diseases

journal homepage: www.elsevier.com/locate/cimid

Review

Usefulness of the murine model to study the immune response against *Histoplasma capsulatum* infection



Jorge H. Sahaza^{a,b}, Armando Pérez-Torres^{c,1}, Edgar Zenteno^d,
Maria Lucia Taylor^{a,*,1}

^a Laboratorio de Inmunología de Hongos, Departamento de Microbiología y Parasitología, Facultad de Medicina, Universidad Nacional Autónoma de México (UNAM), México, DF 04510, Mexico

^b Unidad de Micología Médica y Experimental, Corporación para Investigaciones Biológicas, Medellín, Colombia

^c Laboratorio de Filogenia del Sistema Inmune de Piel y Mucosas, Departamento de Biología Celular y Tisular, Facultad de Medicina, UNAM, México, DF 04510, Mexico

^d Laboratorio de Inmunología, Departamento de Bioquímica, Facultad de Medicina, UNAM, México, DF 04510, Mexico

ARTICLE INFO

Article history:

Received 13 December 2013

Received in revised form 14 March 2014

Accepted 19 March 2014

Keywords:

Histoplasma capsulatum

Histoplasmosis

Murine model

Innate immunity

Adaptive response.

ABSTRACT

The present paper is an overview of the primary events that are associated with the histoplasmosis immune response in the murine model. Valuable data that have been recorded in the scientific literature have contributed to an improved understanding of the clinical course of this systemic mycosis, which is caused by the dimorphic fungus *Histoplasma capsulatum*. Data must be analyzed carefully, given that misinterpretation could be generated because most of the available information is based on experimental host–parasite interactions that used inappropriate proceedings, i.e., the non-natural route of infection with the parasitic and virulent fungal yeast-phase, which is not the usual infective phase of the etiological agent of this mycosis.

Thus, due to their versatility, complexity, and similarities with humans, several murine models have played a fundamental role in exploring the host–parasite interaction during *H. capsulatum* infection.

© 2014 Elsevier Ltd. All rights reserved.

Contents

1. Introduction.....	144
2. Queries regarding the murine histoplasmosis model.....	144
3. Dimorphic transition is required for <i>H. capsulatum</i> pathogenic mechanisms.....	144
4. Fungal cell wall components vs. the first step of host recognition.....	146
5. Fate of <i>H. capsulatum</i> during the host–parasite interaction.....	146
6. Cellular populations involved in the innate immune response to murine histoplasmosis.....	147
7. Cellular populations involved in the adaptive immune response to murine histoplasmosis.....	147
8. Host molecules involved in the interplay of innate and adaptive immune responses to murine histoplasmosis.....	148
9. Other components involved in the host–parasite interaction in murine histoplasmosis.....	149

* Corresponding author. Tel.: +52 55 5623 2462; fax: +52 55 5623 2462.

E-mail addresses: emello@unam.mx, luciataylor@yahoo.com.mx (M.L. Taylor).

¹ These authors participated in the design and coordination of this work.

10. Conclusions.....	149
Conflict of interest.....	149
Acknowledgments.....	149
References.....	149

1. Introduction

Histoplasmosis, which is caused by the dimorphic fungus *Histoplasma capsulatum*, is considered a common systemic mycosis worldwide with well-known endemic geographic areas in many countries, predominantly in the Americas. The disease primarily affects the host mononuclear phagocyte system, and its severity and clinical forms depend on the host's immunological conditions, the infective inoculum size, and the virulence of the involved fungal isolate. In most patients, the infection is self-limited and produces only residual calcifications in the lungs and, sometimes, in the spleen [1,2]. The severe course of histoplasmosis is often associated with its epidemic form. Fungal virulence and exposure to a high concentration of infective propagules, which are primarily present in enclosed spaces that contain bat and bird droppings that foster fungal growth, contribute to the severe outcome of the disease in either immunocompromised or immunocompetent hosts [3–5]. The infection is acquired by the inhalation of airborne infective propagules, mainly microconidia and hyphal fragments, which are produced by the mycelial morphotype (M-phase) of the fungus. The main target organ in the infected host is the lung and, usually, once the infective propagules reach the alveoli they are phagocytosed by alveolar macrophages. Within macrophages, the infective propagules begin their dimorphic transition to the yeast morphotype (Y-phase), which is the parasitic and virulent *H. capsulatum* morphotype [6,7].

Histoplasmosis has been reported in different wild and captive mammals [8–15]; moreover, different mammalian species have been tested in the laboratory as models for experimental histoplasmosis [16–18]. Undoubtedly, mice are the most frequently used animal model to study either histoplasmosis characteristics, such as etiopathogenesis, immunology, diagnosis, and therapy, or fungal characteristics, such as phenotypic variations and genetic diversities. The ability to control numerous characteristics of the animal model allows researchers to mimic the human disease status and to monitor the course of the disease. However, any single experimental model cannot always answer all questions regarding host–parasite interactions because different animal species or distinct routes of infection can produce unexpected results.

To follow the course of experimental histoplasmosis infection different animal species and methodological procedures, involving lung exposure to *H. capsulatum* yeasts, are used. These conditions have distinct strengths and weaknesses concerning fungal infection modeling and the host immune response. There is great variability in animal's susceptibility to fungal infection, which depends on the animal species [19–21]. Sometimes, susceptibility change in the same animal species depends on the animal strain used, as occurs in the murine model,

which could interfere in the outcome of experimental histoplasmosis [22,23]. Host susceptibility also depends on the route of infection (inhalation, involuntary instillation, intra-tracheal, intraperitoneal, and intravenous), the inoculum size, the pathogen's virulence, the discriminated expression of their surface molecules that act as pathogen-associated molecular patterns (PAMPs), and the methodologies that are involved in the selected search.

Human cell-lines, murine cell-lines, and *in vitro* differentiated mammalian-cells have been extensively used as models to study host-*H. capsulatum* interactions. Additionally, *in vivo* models, such as invertebrates (the nematode – *Caenorhabditis elegans* and the insect – *Galleria mellonella*) [24–26] and the protozoa – *Acanthamoeba castellanii* [27], have been employed to explore these interactions. However, the aforementioned models have a critical limitation because they do not develop the complexity of the entire mammalian immune defense.

In the absence of an ideal model, it is more suitable to use mice due to their similarity to the human immune system performance. Based on the aforementioned antecedents, the aims of the present review were: to underline the immunological events that are most frequently detected in mice coursing with *H. capsulatum* infection; and to contribute to a better understanding of the plasticity of the host response in experimental conditions.

2. Queries regarding the murine histoplasmosis model

Several mouse strains have been assessed as experimental models in histoplasmosis, particularly BALB/c, C57BL/6, AKR/J, A/J, and Swiss mice [7,22,23,28–34]. In addition, some mouse strains have been classified as susceptible or resistant to the disease, although this categorization is arbitrary and varies depending on the goal of the study [22,23].

Generally, two atypical conditions have been favored in the laboratory to establish murine systemic histoplasmosis: the use of the parasitic and virulent Y-phase (non-infective) as the inoculum and the handling of intraperitoneal or intravenous infection routes (non-natural routes). In contrast, the natural infection route of histoplasmosis, which is through the inhalation of aerosolized *H. capsulatum* M-phase infective propagules, has been scarcely employed in experimental circumstances [23]. Therefore, results of experimental infections must be analyzed cautiously to avoid incorrect conclusions.

3. Dimorphic transition is required for *H. capsulatum* pathogenic mechanisms

The first line of the host defense against *H. capsulatum* obviously involves the mucosa of the upper and lower

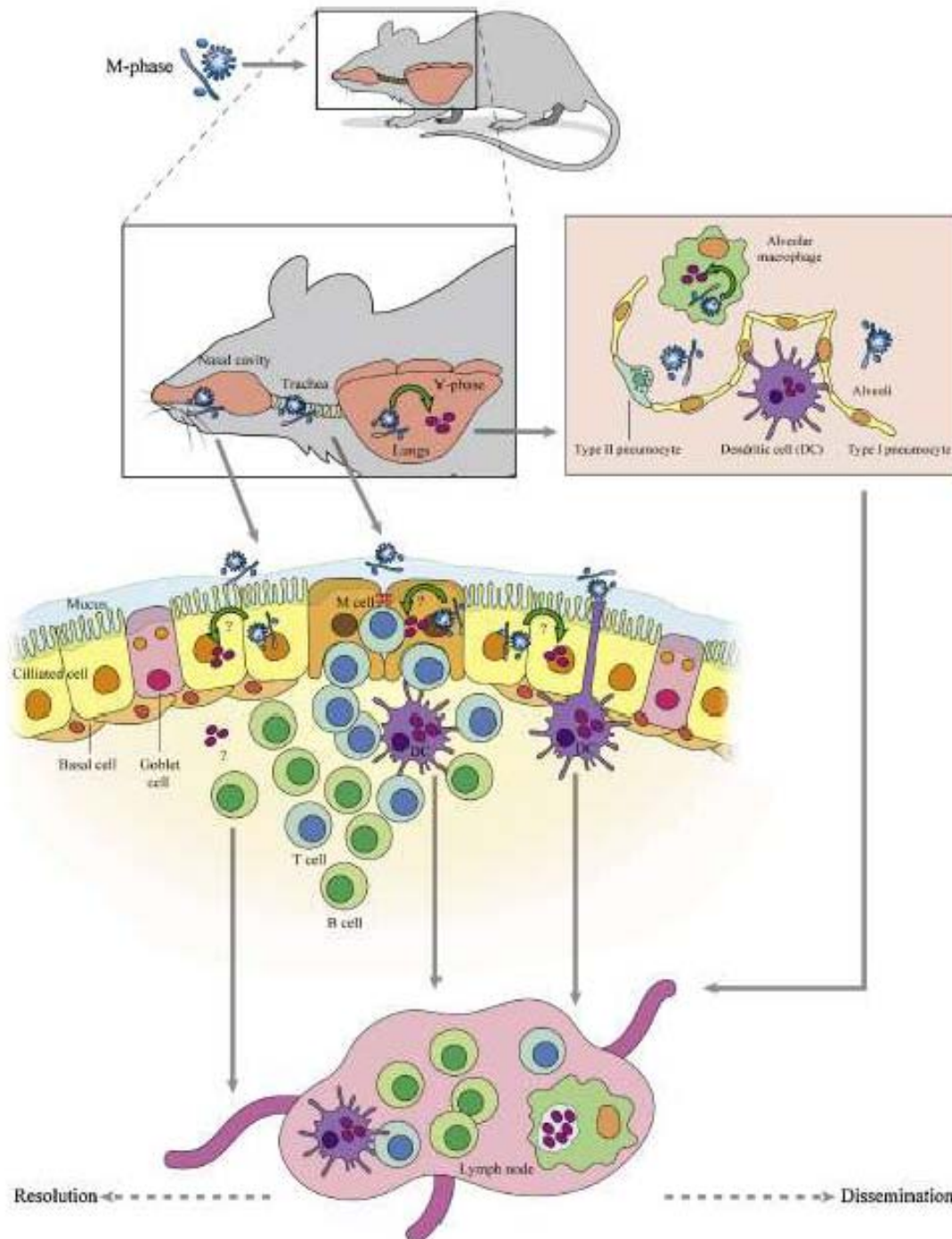


Fig. 1. Anatomic sites where *H. capsulatum* dimorphic transition and dissemination could occur in infected mammalian hosts. The figure highlights the probable cells and tissues of the upper and lower host respiratory tract associated to fungal dimorphic transition, from infective M-phase propagules (hyphae fragments and conidia) to parasitic Y-phase (yeasts). The likely dissemination pathways that are associated to cells and tissues of the host, where yeasts are transported, are also illustrated. Green arrows show the possible *H. capsulatum* dimorphic transition sites in infected hosts.

respiratory tract, including the nasal- and bronchiolar-associated lymphoid tissues, due to its localization along the airway route of this pathogen. It is supposed that the host triggers both innate and adaptive immune responses

to eliminate the pathogen and to control the infection. The *in vitro* infection with *H. capsulatum* M-phase propagules and their subsequent dimorphic transition have been demonstrated in both human or mouse dendritic cells

(DCs) and macrophage cultures [34]. These findings support the role of these cells as crucial players in the innate immune mechanism and in further fungal antigen processing and presentation to T cells [34,35]. These events could occur in the lungs and must involve the upper respiratory mucosa. The anatomic sites where fungal dimorphic transition and dissemination could occur in infected mammalian hosts are depicted in Fig. 1.

4. Fungal cell wall components vs. the first step of host recognition

Different host receptors can recognize their specific fungal-ligand, which is exposed on the external layer (cell wall) of this type of pathogen. Usually, cell wall components are associated with fungal carbohydrate and protein surface molecules. These molecules act as PAMPs and change depending on the fungal strains and their morphotypes, since some PAMPs are morphotype-specific and their expression is controlled by phase-specific genes [36,37].

Carbohydrates are the major structural components of the *H. capsulatum* cell wall, which is primarily composed of chitin and glucans. In the cell wall of the M-phase of this fungus, the presence of β -(1,3)-glucan stands out as the main PAMP. Medeiros et al. [38] suggest that this glucan promotes the recruitment of leukocytes and potentiates the leukotriene-mediated inflammatory pathway in the host, via interactions with β -glucan receptors that are a particular type of pattern recognition receptors (PRR). In contrast, another PAMP, the α -(1,3)-glucan is mainly found on the most external layer of the Y-phase cell wall of some virulent *H. capsulatum* strains, overlapping the β -(1,3)-glucan exposure and blocking β -glucan recognition by Dectin-1 β -glucan receptor, resulting in the inhibition of inflammatory mechanisms as demonstrated in assays with P388D1 murine macrophage-like cells [39,40].

In general, once fungus dimorphism occurs in the infected host, the Y-phase displays several surface molecules that are crucial for *H. capsulatum* virulence, which is considered multi-factorial in this pathogen [37]. Some of these molecules are involved in fungal entry and survival within the host-cells, by promoting modification in the intracellular environment that fosters Y-phase growth. In addition, the *H. capsulatum* Y-phase can circumvent the host defense by avoiding macrophage activation through several mechanisms [7,41].

A specific morphotype protein of *H. capsulatum*, named yeast phase specific-3 (yps3), which is located on the cell wall surface of the Y-phase, interacts with toll-like receptor-2 (TLR2) of microglia cell cultures from wild-type C57BL/6 mice, whereas this interaction was absent in TLR2 knockout mice [42]. For the first time, the interaction between *H. capsulatum* yps3 protein (ligand) and its corresponding host TLR receptor (TLR2) has been described. Thus, in agreement to TLR2 activation, several transcription factors lead to the production of anti- and pro-inflammatory cytokines and chemokines, which potentiate the innate immune response and promote mechanisms that are involved in the interface with the adaptive immune response [42].

A lectin-like activity is associated with a surface component of the *H. capsulatum* Y-phase. This lectin activity is specific to galactosylated residues, mainly β -anomer. The *H. capsulatum* lectin recognizes a 68-kDa molecule (most likely a galactosylated glycoprotein) that is exposed on murine macrophages [43,44]. Through this lectin activity, *H. capsulatum* yeast-cells have the ability to attach and agglutinate erythrocytes from humans [45] and other mammals, such as mouse, rat, horse, and rabbit (ML Taylor, personal communication), which certainly display galactose residues on their membranes. In inhibition assays, yeast-cells that were previously incubated with chondroitin-sulfate A and C, which share galactosyl residues and sialic acid, were unable to attach in either mammalian erythrocytes or peritoneal murine macrophages, suggesting that galactosylated and/or sialylated structures of host-cells are important in the interaction with this fungal lectin [45,46].

On their surface, *H. capsulatum* yeast-cells also exhibit a 50-kDa protein that is the ligand for the 67-kDa murine laminin receptor, suggesting the possible role of this protein in the mechanism of fungal dissemination [47].

Histone H2B, a member of the histone protein family, has been described on the yeast-cell wall of *H. capsulatum*. This protein seems to play a role in the pathogenesis of histoplasmosis; moreover, a protective function of IgM mAb against H2B has been found in C57BL/6 mice that were infected with *H. capsulatum* yeast-cells [48].

At present, it has been well-documented in human cultured macrophages that a fungal heat shock protein 60 (Hsp60), in the cell wall of the *H. capsulatum* Y-phase, is an adhesin able to bind to the subunit CD18 of the β 2 integrin family receptors, CD11a/CD18 (LFA-1), CD11b/CD18 (CR3 or Mac-1), and CD11c/CD18 (p150, 95 or CR4) present on host-macrophages [49]. Moreover, a protein of 20-kDa identified as cyclophilin A, which is distributed on the surface of the *H. capsulatum* Y-phase, has been described as the ligand for the α -5 integrin receptor CD49e or very late antigen-5 (VLA-5), which is expressed on DCs derived from human cultured monocytes [50]. Despite the importance of these findings, similar recognition mechanisms have not yet been described in murine models.

5. Fate of *H. capsulatum* during the host-parasite interaction

The intracellular fate of the fungus could be modulated according to the immune cell type involved in its phagocytosis. Macrophages and DCs play major roles in this affair and participate in either the innate immune response or the interplay with the adaptive immune response, connecting different activation pathways [51].

The process involved in *H. capsulatum* M- or Y-phase internalization by phagocytes and the recognition mechanism via *H. capsulatum* PAMPs and host PRRs could modulate the outcome of the host-pathogen interaction. A very interesting study, published by Dumont [52] many years ago, referred the presence of *H. capsulatum* yeast-cells in infected hamster macrophages within tight and loose phagosomes, resembling the zipper-like or trigger-like internalization process described in bacteria and *Candida*

[53,54], most likely promotes a distinct fate for the phagocytosed microorganism.

Thus, once the fungal dimorphic transition has been completed in the infected host, the fate of the parasite could vary depending on the following aspects: the parasite characteristics, particularly its virulence and infection range; and some mammalian host characteristics, such as age, sex, genetic pattern, and the phagocyte phenotypes that could be associated with a lesser or greater susceptibility to *H. capsulatum* infection [22,55–58].

6. Cellular populations involved in the innate immune response to murine histoplasmosis

Innate effector mechanisms can destroy fungal pathogens and limit their infection, blocking the disease development. The innate response to histoplasmosis can be mediated principally by neutrophils, macrophages, DCs, and natural killer (NK) cells [34,51,59–65].

Concerning the cellular players involved in the host innate response, either murine or human neutrophils have been particularly studied due to their ability to inhibit *H. capsulatum* Y-phase growth, as determined by *in vitro* assays [61–64]. This fungistatic effect was studied during the fungal infection of human neutrophils, which produce azurophil granules that contain defensins [63]. Interestingly, through *in vitro* phagocytosis assays, *H. capsulatum* yeast-cells were able to trigger the oxidative burst of intraperitoneal neutrophils from male BALB/c mice; however, the fungistatic activity prevailed over the fungicidal action under this experimental condition [62]. In addition, Zhou et al. [64] showed that *H. capsulatum* yeast-infected C57BL/6 mice that were depleted of neutrophils increased the fungal burden and accelerated the animal mortality in a short time post-infection. Recent data, described by Medeiros et al. [66], have shown that female Swiss mice that were infected intraperitoneally with *H. capsulatum* Y-phase exhibited less apoptosis of peritoneal neutrophils than non-infected mice, which suggests that this apoptosis inhibition event could be associated with the development of a fungal mechanism to evade the host immune response.

Medeiros et al. [38] demonstrated that Swiss mice intraperitoneally infected with *H. capsulatum* yeasts induced an increase in the number of neutrophils at 4–24 h and recruitment of eosinophils between 24 and 48 h at the inoculation site. Moreover, formalin-killed M-phase induced greater recruitment of neutrophils and eosinophils than formalin-killed *H. capsulatum* Y-phase. The authors have suggested that β -glucan of *H. capsulatum*, which is primarily exposed in the M-phase, is involved in the recruitment of leukocytes through leukotrienes induction. These dissimilar inflammatory responses displayed by both morphotypes of *H. capsulatum* could be associated with differences in the exposed glucans on surfaces of M- and Y-phases. In addition, administration of an inhibitor of leukotriene synthesis favors the death of Swiss mice at day 15 post-infection with *H. capsulatum* Y-phase, in contrast to untreated infected mice [67].

Wolf et al. [68] demonstrated that murine peritoneal macrophages that were infected with heat-killed *H. capsulatum* Y-phase released less leukotriene C4

and prostaglandin E2 (PGE2) than zymosan-treated macrophages. Otherwise, β -glucan of *H. capsulatum* Y-phase cell wall induces lipid body (LB) formation in leukocytes from infected C57BL/6 mice that were CD18, Dectin-1, and TLR2 dependent. LB modulates the generation of lipid mediators, primarily leukotriene B4, and plays a likely role in the innate immunity to histoplasmosis [31]. Nowadays, leukotrienes are considered to be required to control chronic fungal infection by amplifying both innate and adaptive immune responses during murine histoplasmosis [67,69].

In addition, other host-cells are also involved in innate defense mechanisms, such as epithelial cells. For instance, type II pneumocytes produce collectins (surfactant proteins, such as SP-A and SP-D) that contribute to lung defense by binding to *H. capsulatum* yeasts, inducing enhanced permeability of the Y-phase cell wall that promotes a decrease in its viability and growth; in contrast, fast yeast internalization by macrophages avoids these collectin effects [70–74].

7. Cellular populations involved in the adaptive immune response to murine histoplasmosis

In *H. capsulatum*, the adaptive immune response is primarily displayed against the Y-phase because dimorphic transition from infective M-phase to parasitic Y-phase, generally, occurs in the first hours of the host–pathogen interaction and the yeast morphotype predominates and remains along the entire course of the adaptive immune response.

The presence of functional T cells is often required for the successful resolution of infections with intracellular pathogens; nevertheless, the mechanisms by which T cells contribute to fungal pathogen elimination are only partially understood.

The cellular immune response, which is mediated by T cells and their subpopulations, activates the major host defense mechanism in response to *H. capsulatum* Y-phase [41,75–77]. T cells induce and produce cytokines that activate macrophages by enhancing their phagocytosis process and fungicidal activity, allowing for the subsequent protective immunity [6,78].

In athymic nude mice that were infected with *H. capsulatum* Y-phase, a high mortality has been reported associated with a decrease in IFN- γ production due to the lack of CD4+ T cells [75,79]. At the same time, experimental findings in murine histoplasmosis have provided evidence that CD8+ T cells are related to optimal parasite clearance [75,80].

Lin and Wu-Hsieh [77] reported that the intra-tracheal infection of C57BL/6 mice with *H. capsulatum* Y-phase similarly activated CD4+ and CD8+ T cells. CD4+ T cells that express the CD44^{hi} phenotype are responsible for more than 90% of the IFN- γ production required for the optimal cellular immune response in C57BL/6 infected mice. The authors also observed a correlation between IFN- γ production and CD44^{hi} expression throughout the course of the infection [77].

Although the participation of CD4+ and CD8+ T cells is well-documented for the protective immunity against

H. capsulatum, CD4+ T cell subsets (mainly Th1 and Th17) were found to have a role in promoting fungal clearance and protective immunity [75,77,81–85].

In human pathogenic fungi, the Th2 response (another CD4+ T cell subset) is important in the development and/or maintenance of Th1-mediated immunity. Th1/Th2 balance is crucial for the successful outcome of the clinical course of histoplasmosis because exacerbation of Th1 or Th2 could be involved in the etiopathogenesis of the disease [86,87].

Although, the fungal morphotype could affect the optimal function of a particular type of host immune response, this event has not been well-explored in histoplasmosis. The association between fungal morphotypes and Th1/Th2 responses could be vital for generating a Th1-mediated protective inflammatory response or for increasing fungal infection susceptibility involving Th2. This finding has been well-documented by assays using *Candida* yeasts (Y-phase) that trigger a protective Th1 response in experimental conditions, whereas *Candida* hyphae (M-phase) induce an injurious Th2 response [54,88].

Concerning Th17 cells, some studies have demonstrated that their cytokines (mainly IL-17A) are involved in the resistance to primary murine fungal infection [89–91]. Th17 cells induce protection by recruiting and activating neutrophils and macrophages in the alveolar spaces [90,92]. Th17 cells have also been reported to be able to interact with regulatory T cells (Treg) via signaling by CCR5, which is the receptor for some chemokines of the CC family, such as CCL3 (MIP-1 α), CCL4 (MIP-1 β), CCL5 (RANTES), CCL8 (MCP-2), and CCL16 (HCC-4). In experimental histoplasmosis, Th17 cells interaction with Treg is regulated upon the activation of normal T cell by expressing and secreting CCL5, which favors the host's ability to respond effectively to the *H. capsulatum* infection by increasing Th17 cytokines and reducing the number of Treg, as demonstrated by fungal clearance in CCR5-deficient mice [93].

Recently, a subpopulation of CD8+ T cytotoxic cells that is able to produce IL-17 (Tc17 cells) has been involved in the murine protective response associated with *Blastomyces dermatitidis* and *H. capsulatum* infections [85].

8. Host molecules involved in the interplay of innate and adaptive immune responses to murine histoplasmosis

Although the participation of cytokines and chemokines in the innate response to *H. capsulatum* infection is scarcely known, high levels of the chemokine CCL3 in contrast with a low level of the chemokine CCL11 (eotaxin) were detected until 48 h post-infection in female Swiss mice intraperitoneally inoculated with the fungus Y-phase [94]. Using microarray and qRT-PCR analyses, new data have demonstrated the induction of both type I interferon (IFN)-genes, highlighting the production of beta type I IFN (IFN- β) transcripts in C57BL/6 bone marrow-derived macrophages that were infected with *H. capsulatum* M-phase, but not with its Y-phase [95]. Studies regarding the contribution of these innate response mediators in the immunity to histoplasmosis must be encouraged among specialists to elucidate their role in the immune response to fungal pathogens.

Regarding cytokines and chemokines participation in the adaptive immune response, data are more copious. The cytokines IL-12, IFN- γ , TNF- α , and GM-CSF, which are produced by mouse or human lymphocytes and phagocytes, constitute the most crucial molecules associated with the adaptive host defense mechanism [6,64,81,82,96–101]. During the *H. capsulatum* Y-phase sub-lethal infection of C57BL/6 mice, IL-12, IFN- γ , and TNF- α are the major cytokines released, which is in accordance with a Th1 response. In contrast, the absence of these cytokines in these infected mice favors their deaths [81,96,102].

IL-12 is the most important inducer of the Th1 response, and its requirement for the protective immunity in naive C57BL/6 or in SCID mice has been demonstrated, whereas IL-12 neutralization results in the death of these animals [6,96,97].

IFN- γ is the major cytokine involved in mice immune protection and, in accordance with this fact, sub-lethal infections are fatal when this cytokine is neutralized or when IFN- γ knockout mice are tested [64,85,102]. Some reports have documented that mice deficient in IFN- γ are more susceptible to pulmonary than to systemic infection [64,86,102]. Interestingly, the neutralization of IL-4 protects mice from lethal infections and their survival correlates with increased levels of IFN- γ [96].

TNF- α is critical for histoplasmosis control [64,86]. In the C57BL/6 mice pulmonary model, the neutralization of TNF- α abrogates protection and promotes significant increases of Th2 cytokines, primarily IL-4 and IL-10, and their neutralization re-establishes a protective response. An unusual event involves these two cytokines and the apoptosis of lung T cell populations after the intranasal infection of C57BL/6 mice with *H. capsulatum* Y-phase, because IL-4 and IL-10 increase when apoptosis is inhibited, which contributes to the severe outcome of the disease [103].

Normally, IL-4 can inhibit Th1 cytokine production and activity, and IL-4 from the lung of *H. capsulatum*-infected transgenic mice generates higher fungal burden in their lungs than the wild-type infected controls. The adverse effects of IL-4 on *H. capsulatum* elimination were undetectable during the early stage (days 1–3) of the fungal infection, but were maximal at day 7 post-infection, before the induction of cell-mediated immunity. However, the detection of total or lung cytokine levels revealed that IFN- γ and TNF- α production were not inhibited in the presence of excess IL-4 [104], suggesting that the excess production of endogenous IL-4 modulates protective immunity to *H. capsulatum* by delaying fungal clearance, and did not prevent the generation of a Th1 response that, ultimately, controls the infection [104].

Endogenous GM-CSF was found to be significant for mice protective immune response to the first challenge with *H. capsulatum* Y-phase (primary histoplasmosis), whereas GM-CSF neutralization produces a deleterious effect on the immunity to this histoplasmosis infection model, which favors the death of the infected mice, as reported by Deepe et al. [98]. The neutralization of GM-CSF abrogated the levels of Th1 cytokines (IFN- γ and TNF- α) and of reactive nitrogen intermediates, but elevated the levels of Th2 cytokines (IL-4 and IL-10), suggesting that

GM-CSF could participate in the signaling events involved in the balance of Th1 and Th2 responses [98].

The presence of IL-17 support the production of pro-inflammatory cytokines, such as TNF- α and IL-1 β , as well as of chemokines of the CXC family that is involved in the recruitment and activation of macrophages and neutrophils in several types of fungal infections [77,105]. IL-17 has been detected in hepatic granulomas associated with murine histoplasmosis [106], as well as in the lung during the acute infection of mice intranasally inoculated with the *H. capsulatum* Y-phase. In addition, IL-17 might be necessary for the elimination of other fungus, because monoclonal antibodies against IL-17 were able to disturb the mice inflammatory response, delaying the elimination of the fungal pathogen [89].

Chamilos et al. [107] demonstrated that the concentration of cytokines associated with a Th17 response, including IL-6, IL-23, and IL-17, increases gradually in the first week of a murine pulmonary *H. capsulatum* infection and declines thereafter. Moreover, they found that IL-23 prolongs the survival of infected mice in the absence of IL-12, and this protective effect depends on IL-17. Therefore, it is possible that the IL-17/IL-23-axis promotes mice immunity during infection with *H. capsulatum* [107]. Recently, galectin-3 that is known for its immunoregulatory functions in infectious and inflammatory diseases has been found to regulate, negatively, IL-17 responses through the inhibition of the IL-17/IL-23-axis cytokine production by DCs [108].

The major role of chemokines in infections caused by fungi remains to be explored [78,109]. Female Swiss mice, intraperitoneally infected with *H. capsulatum* Y-phase, promote CCL3 production as early as 4 h post-infection [93], whereas in C57BL/6 *H. capsulatum*-infected mice, high concentrations of CCL3 and CCL4 are detected in the lungs at the 3rd day post-infection. In contrast, CCL5 is not up-regulated until 1 week post-infection, which suggests that it is not required for the influx of innate cells to the lungs [78]. Whereas, migration of neutrophils, macrophages, DCs, NK cells and CD8+ T cells to the lungs of C57BL/6 mice after intranasal infection with *H. capsulatum* Y-phase could be promoted by signaling through CCR5, however, CCR5 is not required for fungal resolution [93]. In addition, the absence of CCR2 induces a decreased recruitment of DCs to the lungs of C57BL/6 mice that have been intranasally infected with *H. capsulatum* Y-phase and this finding was associated with the enhancement of IL-4 levels, which produces the life-threatening *H. capsulatum* infection [84].

9. Other components involved in the host–parasite interaction in murine histoplasmosis

In the intricate interactions between fungal pathogens and their mammal hosts, metal homeostasis plays an essential role in both virulence and host defense. Metals, such as iron, zinc, and copper, have several biological functions and play a central role at the host–pathogen interface [110,111]. Among the metals that are involved in histoplasmosis, iron has been well characterized using *in vitro* assays [111–117]. The models of murine pulmonary histoplasmosis that used *H. capsulatum* Y-phase revealed

that *H. capsulatum* produces hydroxamate siderophores, which are required for fungal intracellular survival in macrophages [115,118].

An interesting report using metallomic analysis contributed to understand the role of iron (Fe²⁺ and Fe³⁺) and zinc (Zn²⁺) in the host defense mechanisms mediated by macrophages. *In vitro* assays, performed with C57BL/6 mice macrophages and *H. capsulatum* Y-phase, demonstrated that iron and zinc deprivation in infected macrophages previously treated with GM-CSF, inhibited yeast-cell replication; however, this antifungal effect could be reversed in the presence of IL-4 [119].

10. Conclusions

The resolution of *H. capsulatum* infection requires the participation of host effector cells and molecules. Macrophages, neutrophils, DCs, and T lymphocytes are the essential cellular players that act in harmony with host molecules, generated by these same cellular players, to promote signaling mechanisms as a consequence of the interactions between fungal PAMPs and their PRRs present on the host-cells. Generally, the fates of these recognition events are activated cells and chemical mediators of host cellular immunity, which is the major defense mechanism that contributes to fungal death.

Nowadays, the most important challenge for the experimental models of histoplasmosis is to reproduce faithfully the natural route of infection with M-phase, which is the appropriate fungus infective-inoculum. At present, no ideal pulmonary and systemic histoplasmosis experimental model, which accurately mimics the pathogenesis and the clinical course of the corresponding human disease, has been developed.

The host–parasite interactions during *H. capsulatum* murine infection have allowed the precise elucidation of certain events that occur during histoplasmosis, particularly those associated with the disseminated form of the disease and with the host adaptive immune response. Likewise, murine models have also been advantageous for understanding events that are inherent to the biology and physiology of *H. capsulatum*.

Conflict of interest

None.

Acknowledgments

This research was supported by a grant from Consejo Nacional de Ciencia y Tecnología de México (CONACYT-México, ref-166052). This paper constitutes collateral fulfillment of the requirements of the Graduate Program in Biological Sciences of the UNAM. J.H.S. thanks the Graduate Program in Biological Science of the UNAM and the scholarship of CONACYT (ref-245151). The authors thank Ingrid Mascher for editorial assistance.

References

- [1] Tewari R, Wheat LJ, Ajello L. Agents of histoplasmosis. In: Ajello L, Hay RJ, editors. Medical mycology. Topley & Wilson's, microbiology

- and microbial infections. New York: Arnold and Oxford University Press; 1998. p. 373–407.
- [2] Kauffman CA. Histoplasmosis: a clinical and laboratory update. *Clin Microbiol Rev* 2007;20:115–32.
 - [3] Reyes-Montes MR, Bobadilla-Del Valle M, Martínez-Rivera MA, Rodríguez-Arellanes G, Maravilla E, Sifuentes-Osorio J, et al. Relatedness analyses of *Histoplasma capsulatum* isolates from Mexican patients with AIDS-associated histoplasmosis by using histoplasmin electrophoretic profiles and randomly amplified polymorphic DNA patterns. *J Clin Microbiol* 1999;37:1404–8.
 - [4] Taylor ML, Reyes-Montes MR, Chávez-Tapia CB, Coriel-Quesada E, Duarte-Escalante E, Rodríguez-Arellanes G, et al. Ecology and molecular epidemiology findings of *Histoplasma capsulatum*, in Mexico. In: Benedik M, editor. *Research Advances in Microbiology*. Kerala: Global Research Network; 2000. p. 29–35.
 - [5] Gómez BL. Histoplasmosis epidemiology in Latin America. *Curr Fungal Infect Rep* 2011;5:199–205.
 - [6] Allendoerfer R, Biovin GP, Deepe Jr GS. Modulation of immune responses in murine pulmonary histoplasmosis. *J Infect Dis* 1997;175:905–14.
 - [7] Guimarães AJ, de Cerqueira MD, Nosanchuk JD. Surface architecture of *Histoplasma capsulatum*. *Front Microbiol* 2011;2:225. <http://dx.doi.org/10.3389/fmicb.2011.00225>.
 - [8] Taylor ML, Chávez-Tapia CB, Vargas-Yáñez R, Rodríguez-Arellanes G, Peña-Sandoval GR, Toriello C, et al. Environmental conditions favoring bat infection with *Histoplasma capsulatum* in Mexican shelters. *Am J Trop Med Hyg* 1999;61:914–9.
 - [9] Espinosa-Avilés D, Taylor ML, Reyes-Montes MR, Pérez-Torres A. Molecular findings of disseminated histoplasmosis in two captive snow leopards (*Uncia uncia*). *J Zoo Wildl Med* 2008;39:450–4.
 - [10] Pérez-Torres A, Rosas-Rosas A, París-García A, Juan-Sallés C, Taylor ML. Second case of histoplasmosis in a captive mara (*Dolichotis patagonum*): pathological findings. *Mycopathologia* 2009;168:95–100.
 - [11] Reyes-Montes MR, Rodríguez-Arellanes G, Pérez-Torres A, Rosas-Rosas AG, París-García A, Juan-Sallés C, et al. Identification of the source of histoplasmosis infection in two captive maras (*Dolichotis patagonum*) from the same colony by using molecular and immunologic assays. *Rev Argent Microbiol* 2009;41:102–4.
 - [12] Highland MA, Chaturvedi S, Perez M, Steinberg H, Wallace R. Histologic and molecular identification of disseminated *Histoplasma capsulatum* in a captive brown bear (*Ursus arctos*). *J Vet Diagn Invest* 2011;23:764–9.
 - [13] Keller DL, Steinberg H, Sladky KK. Disseminated histoplasmosis in a Bengal tiger (*Amherstia tigris*). *J Zoo Wildl Med* 2011;42:727–31.
 - [14] Brilhante RS, Coelho CG, Sidrim JJ, de Lima RAC, Ribeiro JF, Cordeiro RA, et al. Feline histoplasmosis in Brazil: clinical and laboratory aspects and a comparative approach of published reports. *Mycopathologia* 2012;173:193–7.
 - [15] González-González AE, Aliouat-Denis CM, Carreto-Binaghi LE, Ramirez JA, Rodríguez-Arellanes G, Demanche C, et al. An Hcp100 gene fragment reveals *Histoplasma capsulatum* presence in lungs of *Tadarida brasiliensis* migratory bats. *Epidemiol Infect* 2012;8:1–9.
 - [16] Al-Doory Y, Vice TE, Kalher SS. Experimental histoplasmosis in the baboon (*Papio sp.*). *Mycopathol Mycol Appl* 1969;38:83–92.
 - [17] Bauman DS, Chick EW. An experimental model for studying extra-pulmonary dissemination of *Histoplasma capsulatum* in hamsters. *Am Rev Respir Dis* 1969;100:79–81.
 - [18] Ebert JW, Jones V, Jones RD, Weeks RJ, Tosh FE. Experimental canine histoplasmosis and blastomycosis. *Mycopathol Mycol Appl* 1971;45:285–300.
 - [19] Gonzalez Ochoa A, Navarrete F. Comparative susceptibility of the hamster and mouse to *Histoplasma capsulatum* infection. *Rev Inst Salubr Enferm Trop* 1956;16:9–15.
 - [20] Schlitzer RL, Chandler FW, Larsh HW. Primary acute histoplasmosis in guinea pigs exposed to aerosolized *Histoplasma capsulatum*. *Infect Immun* 1981;33:575–82.
 - [21] Daniels LS, Berliner MD, Campbell CC. Varying virulence in rabbits infected with different filamentous types of *Histoplasma capsulatum*. *J Bacteriol* 1968;96:1525–9.
 - [22] Wu-Hsieh BA. Relative susceptibilities of inbred mouse strains C57BL/6 and A/J to infection with *Histoplasma capsulatum*. *Infect Immun* 1989;57:3788–92.
 - [23] Smulian AG. Invasive models of histoplasmosis. In: Brand AC, MacCallum DM, editors. *Host-fungus interactions: methods and protocols series. Methods in molecular biology*, vol. 845. New York: Springer Humana Press; 2012. p. 519–25.
 - [24] Johnson CH, Ayyadevara S, McEwen JE, Shmookler Reis RJ. *Histoplasma capsulatum* and *Caenorhabditis elegans*: a simple nematode model for an innate immune response to fungal infection. *Med Mycol* 2000;47:808–13.
 - [25] Arvanitis M, Glavis-Bloom J, Mylonakis E. Invertebrate models of fungal infection. *Biochim Biophys Acta* 2013;1832:1378–83.
 - [26] Thomaz L, Garcia-Rodas R, Guimarães AJ, Taborda CP, Zaragoza O, Nosanchuk JD. *Galleria mellonella* as a model host to study *Paracoccidioides lutzii* and *Histoplasma capsulatum*. *Virulence* 2013;4:139–46.
 - [27] Steenbergen JN, Nosanchuk JD, Malliaris SD, Casadevall A. Interaction of *Blastomyces dermatitidis*, *Sporothrix schenckii*, and *Histoplasma capsulatum* with *Acanthamoeba castellanii*. *Infect Immun* 2004;72:3478–88.
 - [28] Wolf JE, Abegg AL, Travis SJ, Kobayashi GS, Little JR. Effects of *Histoplasma capsulatum* on murine macrophage functions: inhibition of macrophage priming, oxidative burst, and antifungal activities. *Infect Immun* 1989;57:513–9.
 - [29] Wolf JE, Massof SE. In vivo activation of macrophage oxidative burst activity by cytokines and amphotericin B. *Infect Immun* 1990;58:1296–300.
 - [30] Wu-Hsieh BA. Resistance mechanisms in murine experimental histoplasmosis. *Arch Med Res* 1993;24:233–8.
 - [31] Soegi CA, Secatto A, Fontanari C, Turato WM, Belangêr C, Medeiros AI, et al. *Histoplasma capsulatum* cell wall β -glucan induces lipid body formation through CD18, TLR2, and Dectin-1 receptors: correlation with leukotriene B₄ generation and role in HIV-1 infection. *J Immunol* 2009;182:4025–35.
 - [32] Tagliari I, Toledo MS, Lacerda TG, Suzuki E, Straus AH, Takahashi HK. Membrane microdomain components of *Histoplasma capsulatum* yeast forms, and their role in alveolar macrophage infectivity. *Biochim Biophys Acta* 2012;1818:458–66.
 - [33] Tristão FS, Leonello PC, Nagashima LA, Sano A, Ono MA, Itano EN. Carbohydrate-rich high-molecular-mass antigens are strongly recognized during experimental *Histoplasma capsulatum* infection. *Rev Soc Bras Med Trop* 2012;45:232–7.
 - [34] Nosanchuk JD, Gacser A. *Histoplasma capsulatum* at the host pathogen interface. *Microb Infect* 2008;10:573–7.
 - [35] Newman SL, Lemen W, Smulian AG. Dendritic cells restrict the transformation of *Histoplasma capsulatum* conidia into yeasts. *Med Mycol* 2011;49:356–64.
 - [36] Netea MG, Van der Meer JW, Kullberg BJ. Role of the dual interaction of fungal pathogens with pattern recognition receptors in the activation and modulation of host defence. *Clin Microbiol Infect* 2006;12:404–9.
 - [37] Holbrook ED, Rappleye CA. *Histoplasma capsulatum* pathogenesis: making a lifestyle switch. *Curr Opin Microbiol* 2008;11:318–24.
 - [38] Medeiros AI, Silva CL, Malheiro A, Maffei CML, Jacrioli LH. Leukotrienes are involved in leukocyte recruitment induced by live *Histoplasma capsulatum* or by the β -glucan present in their cell wall. *Br J Pharmacol* 1999;128:1529–37.
 - [39] Rappleye CA, Engle JT, Goldman WE. RNA interference in *Histoplasma capsulatum* demonstrates a role for α -(1,3)-glucan in virulence. *Mol Microbiol* 2004;53:153–65.
 - [40] Rappleye CA, Eisenberg LG, Goldman WE. *Histoplasma capsulatum* α -(1,3)-glucan blocks innate immune recognition by the β -glucan receptor. *Proc Natl Acad Sci USA* 2007;104:1366–70.
 - [41] Mihu MR, Nosanchuk JD. *Histoplasma* virulence and host responses. *Int J Microbiol* 2012;2012:268123. <http://dx.doi.org/10.1155/2012/268123>.
 - [42] Aravalli RN, Hu S, Woods JP, Lokensgard JR. *Histoplasma capsulatum* yeast phase-specific protein Yps3p induces Toll-like receptor 2 signaling. *J Neuroinflammation* 2008;5:30. <http://dx.doi.org/10.1186/1742-2094-5-30>.
 - [43] Taylor ML, Duarte-Escalante E, Reyes-Montes MR, Eizencord N, Maldonado G, Zenteno E. Interaction of murine macrophage-membrane proteins with components of the pathogenic fungus *Histoplasma capsulatum*. *Clin Exp Immunol* 1998;113:423–8.
 - [44] Duarte-Escalante E, Zenteno E, Taylor ML. Interaction of *Histoplasma capsulatum* yeasts with galactosylated surface molecules of murine macrophages. *Arch Med Res* 2003;34:176–83.
 - [45] Taylor ML, Duarte-Escalante E, Pérez A, Zenteno E, Toriello C. *Histoplasma capsulatum* yeast cells attach and agglutinate human erythrocytes. *Med Mycol* 2004;42:287–92.
 - [46] Mendes-Giannini M, Taylor ML, Bouchara JB, Burger E, Calich VL, Escalante ED, et al. Pathogenesis II: fungal responses to host responses: interaction of host cells with fungi. *Med Mycol* 2000;38:113–23.
 - [47] McMahon JP, Wheat J, Sobel ME, Pasula R, Downing JF, Martin II WJ. Murine laminin binds to *Histoplasma capsulatum*. A possible mechanism of dissemination. *J Clin Invest* 1995;96:1010–7.

- [48] Nosanchuk JD, Steenbergen JN, Shi L, Deepe Jr GS, Casadevall A. Antibodies to a cell surface histone-like protein protect against *Histoplasma capsulatum*. *J Clin Invest* 2003;112:1164–75.
- [49] Long KH, Gomez IJ, Morris RE, Newman SL. Identification of heat shock protein 60 as the ligand on *Histoplasma capsulatum* that mediates binding to CD18 receptors on human macrophages. *J Immunol* 2003;170:487–94.
- [50] Gildea LA, Morris RE, Newman SL. *Histoplasma capsulatum* yeasts are phagocytosed via very late antigen-5, killed, and processed for antigen presentation by human dendritic cells. *J Immunol* 2001;166:1049–56.
- [51] Newman SL, Bucher C, Rhodes JC, Bullock WE. Phagocytosis of *Histoplasma capsulatum* yeasts and microconidia by human cultured macrophages and alveolar macrophages. Cellular cytoskeleton requirement for attachment and ingestion. *J Clin Invest* 1990;85:223–30.
- [52] Dumont A, Robert A. Electron microscopic study of phagocytosis of *Histoplasma capsulatum* by hamster peritoneal macrophages. *Lab Invest* 1970;23:278–86.
- [53] Kumari S, Swetha MG, Mayor S. Endocytosis unplugged: multiple ways to enter the cell. *Cell Res* 2010;20:256–75.
- [54] Romani L. Immunity to fungal infections. *Nat Rev Immunol* 2004;4:1–23.
- [55] Taylor ML, Reyes-Montes MR, Casasola González-GR, Hernández-Ramírez JA. Immune response changes with age and sex as factors of variation in resistance to *Histoplasma* infection. In: Baxter M, editor. Proceedings VIII Congress of ISHAM. Palmerston North: Massey University Press; New Zealand; 1982. p. 260–4.
- [56] Reyes-Montes MR, Casasola J, Elizondo NE, Taylor ML. Relationship between age and cellular suppressive activity in resistance to *Histoplasma capsulatum* infection. *Sabouraudia* 1985;23:251–60.
- [57] Reyes-Montes MR, García-Camacho MP, Casasola J, Taylor ML. Immunosuppression transfer by spleen cells from young to adult mice previous to *Histoplasma capsulatum* infection. *Mycopathologia* 1988;101:69–75.
- [58] Deepe Jr GS, Gibbons RS, Smulian AG. *Histoplasma capsulatum* manifests preferential invasion of phagocytic subpopulations in murine lungs. *J Leukoc Biol* 2008;84:669–78.
- [59] Patiño MM, Williams D, Ahrens J, Graybill JR. Experimental histoplasmosis in the beige mouse. *J Leukoc Biol* 1987;41:228–35.
- [60] Suchyta MR, Smith JC, Graybill JR. The role of natural killer cells in histoplasmosis. *Am Rev Respir Dis* 1988;138:578–82.
- [61] Brummer E, Kurita N, Yoshida S, Nishimura K, Miyaji M. Fungistatic activity of human neutrophils against *Histoplasma capsulatum*: correlation with phagocytosis. *J Infect Dis* 1991;164:158–62.
- [62] Kurita N, Terao K, Brummer E, Ito E, Nishimura K, Miyaji M. Resistance of *Histoplasma capsulatum* to killing by human neutrophils. Evasion of oxidative burst and lysosomal-fusion products. *Mycopathologia* 1991;115:207–13.
- [63] Newman SL, Gootee L, Gabay JE. Human neutrophil-mediated fungistasis against *Histoplasma capsulatum*. Localization of fungistatic activity to the azurophilic granules. *J Clin Invest* 1993;92:624–31.
- [64] Zhou P, Miller G, Seder RA. Factors involved in regulating primary and secondary immunity to infection with *Histoplasma capsulatum*: TNF- α plays a critical role in maintaining secondary immunity in the absence of IFN- γ . *J Immunol* 1998;160:1359–68.
- [65] Newman SL, Gootee L, Gabay JE, Selsted ME. Identification of constituents of human neutrophil azurophilic granules that mediate fungistasis against *Histoplasma capsulatum*. *Infect Immun* 2000;68:5668–72.
- [66] Medeiros AL, Bonato VL, Malheiro A, Dias AR, Silva CL, Faccioli LH. *Histoplasma capsulatum* inhibits apoptosis and Mac-1 expression in leucocytes. *Scand J Immunol* 2002;56:392–8.
- [67] Medeiros AL, Sá-Nunes A, Soares EG, Peres CM, Silva CL, Faccioli LH. Blockade of endogenous leukotrienes exacerbates pulmonary histoplasmosis. *Infect Immun* 2004;72:1637–44.
- [68] Wolf JE, Massof SE, Peters SP. Alterations in murine macrophage arachidonic acid metabolism following ingestion of nonviable *Histoplasma capsulatum*. *Infect Immun* 1992;60:2559–64.
- [69] Secatto A, Rodrigues LC, Serezani CH, Ramos SG, Dias-Baruffi M, Faccioli LH, et al. 5-Lipoxygenase deficiency impairs innate and adaptive immune responses during fungal infection. *PLoS ONE* 2012;7:e31701. <http://dx.doi.org/10.1371/journal.pone.0031701>.
- [70] Crouch EC. Collectins and pulmonary defense. *Am J Respir Cell Mol Biol* 1998;19:177–201.
- [71] Crouch EC. Surfactant protein-D and pulmonary host defense. *Respir Res* 2000;1:93–108.
- [72] McCormack FX, Gibbons R, Ward SR, Kuzmenko A, Wu H, Deepe Jr GS. Macrophage-independent fungicidal action of the pulmonary collectin. *J Biol Chem* 2003;278:36250–6.
- [73] Kuroki Y, Takahashi M, Nishitani C. Pulmonary collectins in innate immunity of the lung. *Cell Microbiol* 2007;9:1871–9.
- [74] Brunner E, Stevens DA. Collectins and fungal pathogens: roles of surfactant proteins and mannose binding lectin in host resistance. *Med Mycol* 2010;48:16–28.
- [75] Allendorfer R, Brunner GD, Deepe Jr GS. Complex requirements for nascent and memory immunity in pulmonary histoplasmosis. *J Immunol* 1999;162:7389–96.
- [76] Tewari RP, Von Behren LA. Immune responses in histoplasmosis, a prototype of respiratory mycoses. *Indian J Chest Dis Allied Sci* 2000;42:265–9.
- [77] Lin JS, Wu-Hsieh BA. Functional T cells in primary immune response to histoplasmosis. *Int Immunol* 2004;16:1663–73.
- [78] Kroetz DN, Deepe Jr GS. An aberrant thymus in CCR5-/- mice is coupled with an enhanced adaptive immune response in fungal infection. *J Immunol* 2012;186:5949–55.
- [79] Gomez AM, Bullock WE, Taylor CL, Deepe Jr GS. Role of LIT4+ T cells in host defense against *Histoplasma capsulatum*. *Infect Immun* 1988;56:1685–91.
- [80] Deepe Jr GS. Role of CD8+ T cells in host resistance to systemic infection with *Histoplasma capsulatum* in mice. *J Immunol* 1994;153:3461–500.
- [81] Cain JA, Deepe Jr GS. Evolution of the primary immune response to *Histoplasma capsulatum* in murine lung. *Infect Immun* 1998;66:1473–81.
- [82] Allen HL, Deepe Jr GS. B cells and CD4+ CD8- T cells are key regulators of the severity of reactivation histoplasmosis. *J Immunol* 2006;177:1763–71.
- [83] Medeiros AL, Sá-Nunes A, Turato WM, Secatto A, Frantz FG, Sorgi CA, et al. Leukotrienes are potent adjuvant during fungal infection: effects on memory T cells. *J Immunol* 2008;181:8544–51.
- [84] Szymczak WA, Deepe Jr GS. Antigen-presenting dendritic cells rescue CD4-depleted CCR2-/- mice from lethal *Histoplasma capsulatum* infection. *Infect Immun* 2010;78:2125–37.
- [85] Nanjappa SG, Heninger E, Wüthrich M, Casper DJ, Klein BS. Tc17 cells mediate vaccine immunity against lethal fungal pneumonia in immune deficient hosts lacking CD4+ T cells. *PLoS Pathog* 2012;8:e1002771. <http://dx.doi.org/10.1371/journal.ppat.1002771>.
- [86] Allendorfer R, Deepe Jr GS. Blockade of endogenous TNF- α exacerbates primary and secondary pulmonary histoplasmosis by differential mechanisms. *J Immunol* 1998;160:6072–82.
- [87] Peng JK, Lin JS, Kung JT, Finkelman FD, Wu-Hsieh BA. The combined effect of IL-4 and IL-10 suppresses the generation of, but does not change the polarity of type-1 T cells in *Histoplasma* infection. *Int Immunol* 2005;17:193–205.
- [88] Romani L, Bistoni F, Puccetti P. Adaptation of *Candida albicans* to the host environment: the role of morphogenesis in virulence and survival in mammalian hosts. *Curr Opin Microbiol* 2003;6:338–43.
- [89] Rudner NL, Happel KI, Young EA, Shellito JE. Interleukin-23 (IL-23)-IL-17 cytokine axis in murine *Pneumocystis carinii* infection. *Infect Immun* 2007;75:3055–61.
- [90] Deepe Jr GS, Gibbons RS. Interleukins 17 and 23 influence the host response to *Histoplasma capsulatum*. *J Infect Dis* 2009;200:142–51.
- [91] Werner JL, Metz AE, Horn D, Schoeb TR, Hewitt MM, Schwiebert LM, et al. Requisite role for the dectin-1 β -glucan receptor in pulmonary defense against *Aspergillus fumigatus*. *J Immunol* 2009;182:4938–46.
- [92] Wüthrich M, Gern B, Hung CY, Ersland K, Rocco N, Pick-Jacobs J, et al. Vaccine-induced protection against 3 systemic mycoses endemic to North America requires Th17 cells in mice. *J Clin Invest* 2011;121:554–68.
- [93] Kroetz DN, Deepe Jr GS. CCR5 dictates the equilibrium of proinflammatory IL-17+ and regulatory Foxp3+ T cells in fungal infection. *J Immunol* 2010;184:5224–31.
- [94] Medeiros AL, Jose PJ, Malheiro A, Conroy DM, Williams TJ, Faccioli LH. Differential release of MIP-1 α and actaxin during infection of mice by *Histoplasma capsulatum* or inoculation of β -glucan. *Inflamm Res* 2004;53:351–4.
- [95] Inglis DO, Berkes CA, Hocking Murray DR, Sil A. Conidia but not yeast cells of the fungal pathogen *Histoplasma capsulatum* trigger a type I interferon innate immune response in murine macrophages. *Infect Immun* 2010;78:3871–82.
- [96] Zhou P, Sieve MC, Bennett J, Kwon-Chung KJ, Tewari RP, Gazzinelli RT, et al. IL-12 prevents mortality in mice infected with

- Histoplasma capsulatum* through induction of IFN- γ . *J Immunol* 1995;155:785–95.
- [97] Zhou P, Sieve MC, Tewari RP, Seder RA. Interleukin-12 modulates the protective immune response in SCID mice infected with *Histoplasma capsulatum*. *Infect Immun* 1997;65:936–42.
- [98] Deepe Jr GS, Gibbons R, Woodward E. Neutralization of endogenous granulocyte-macrophage colony-stimulating factor subverts the protective immune response to *Histoplasma capsulatum*. *J Immunol* 1999;163:4985–93.
- [99] Cain JA, Deepe Jr GS. Interleukin-12 neutralization alters lung inflammation and leukocyte expression of CD80, CD86, and major histocompatibility complex class II in mice infected with *Histoplasma capsulatum*. *Infect Immun* 2000;68:2069–76.
- [100] Deepe Jr GS. Modulation of infection with *Histoplasma capsulatum* by inhibition of tumor necrosis factor- α activity. *Clin Infect Dis* 2005;1(41 (Suppl. 3)):S204–7.
- [101] Deepe Jr GS, Gibbons R. Recombinant murine granulocyte-macrophage colony-stimulating factor modulates the course of pulmonary histoplasmosis in immunocompetent and immunodeficient mice. *Antimicrob Agents Chemother* 2000;44:3328–36.
- [102] Clemons KV, Darbonne WC, Curmutte JT, Sobel RA, Stevens DA. Experimental histoplasmosis in mice treated with anti-murine interferon- γ antibody and in interferon- γ gene knockout mice. *Microbes Infect* 2000;2:997–1001.
- [103] Allen HR, Deepe Jr GS. Apoptosis modulates protective immunity to the pathogenic fungus *Histoplasma capsulatum*. *J Clin Invest* 2005;115:2875–85.
- [104] Gildea LA, Gibbons R, Finkelman FD, Deepe Jr GS. Overexpression of interleukin-4 in lungs of mice impairs elimination of *Histoplasma capsulatum*. *Infect Immun* 2003;71:3787–93.
- [105] Hsiang W, Na L, Fidel PL, Schwarzenberger P. Requirement of interleukin-17A for systemic anti-*Candida albicans* host defense in mice. *J Infect Dis* 2004;190:624–31.
- [106] Heninger E, Hogan LH, Karman J, Macvilay S, Hill R, Woods JP, et al. Characterization of the *Histoplasma capsulatum*-induced granuloma. *J Immunol* 2006;177:3303–13.
- [107] Chamilos G, Ganguly D, Lande R, Gregorio J, Meller S, Goldman WE, et al. Generation of IL-23 producing dendritic cells (DCs) by airborne fungi regulates fungal pathogenicity via the induction of TH-17 responses. *PLOS ONE* 2010;5(9):e12955. <http://dx.doi.org/10.1371/journal.pone.0012955>
- [108] Wu SY, Yu JS, Liu FT, Miaw SC, Wu-Hsieh BA. Galectin-3 negatively regulates dendritic cell production of IL-23/IL-17-axis cytokines in infection by *Histoplasma capsulatum*. *J Immunol* 2013;190:3427–37.
- [109] Traynor TR, Huffnagle GB. Role of chemokines in fungal infections. *Med Mycol* 2001;39:41–50.
- [110] Silva MG, Schrank A, Bailão EF, Bailão AM, Borges CL, Staats CC, et al. The homeostasis of iron, copper, and zinc in *Paracoccidioides brasiliensis*, *Cryptococcus neoformans* var. *grubii*, and *Cryptococcus gattii*: a comparative analysis. *Front Microbiol* 2011;2(49). <http://dx.doi.org/10.3389/fmicb.2011.00049>.
- [111] Howard DH. Acquisition, transport, and storage of iron by pathogenic fungi. *Clin Microbiol Rev* 1999;12:394–404.
- [112] Lane TE, Wu-Hsieh BA, Howard DH. Iron limitation and the gamma interferon-mediated antihistoplasma state of murine macrophages. *Infect Immun* 1991;59:2274–8.
- [113] Newman SL, Gootee L, Brunner G, Deepe Jr GS. Chloroquine induces human macrophage killing of *Histoplasma capsulatum* by limiting the availability of intracellular iron and is therapeutic in a murine model of histoplasmosis. *J Clin Invest* 1994;93:1422–9.
- [114] Newman SL, Gootee L, Stroobant V, van der Goot H, Boelaert JR. Inhibition of growth of *Histoplasma capsulatum* yeast cells in human macrophages by the iron chelator VUF 8514 and comparison of VUF 8514 with deferasamine. *Antimicrob Agents Chemother* 1995;39:1824–9.
- [115] Howard DH, Rafie R, Tiwari A, Faulk KE. Hydroxamate siderophores of *Histoplasma capsulatum*. *Infect Immun* 2000;68:2338–43.
- [116] Newman SL, Smulian AG. Iron uptake and virulence in *Histoplasma capsulatum*. *Curr Opin Microbiol* 2013. <http://dx.doi.org/10.1016/j.mib.2013.09.001>, pii: S1369-5274(13)00152-5.
- [117] Hilty J, Smulian AG, Newman SL. The *Histoplasma capsulatum* vacuolar ATPase is required for iron homeostasis, intracellular replication in macrophages and virulence in a murine model of histoplasmosis. *Mol Microbiol* 2008;70:127–39.
- [118] Hilty J, Smulian AG, Newman SL. *Histoplasma capsulatum* utilizes siderophores for intracellular iron acquisition in macrophages. *Med Mycol* 2011;49:613–42.
- [119] Winters MS, Chan Q, Caruso JA, Deepe Jr GS. Metallomic analysis of macrophages infected with *Histoplasma capsulatum* reveals a fundamental role for zinc in host defenses. *J Infect Dis* 2010;202:1136–45.

CAPÍTULO 4

CAPÍTULO 4

Artículo original enviado

Suárez-Alvarez R, **Sahaza JH**, Berzunza-Cruz M, Becker I, Curiel-Quesada E, Pérez-Torres A, Taylor ML. Dimorphism and dissemination of *Histoplasma capsulatum* occur in the nasal mucosa and cervical lymph nodes of bats and mice in a short-time after intranasal-infection with mycelial propagules. *Innate Immunity*.

ScholarOne Manuscripts™

Maria Lucia Taylor ▾

Instructions & Forms

Help

Log Out

Innate Immunity

 SAGE track

Main Menu / Author Dashboard / **Submission Confirmation**

Submission Confirmation

Thank you for submitting your manuscript to *Innate Immunity*.

Manuscript ID: INI-14-0064


Title: Dimorphism and dissemination of *Histoplasma capsulatum* occur in the nasal mucosa and cervical lymph nodes of bats and mice in a short-time after intranasal-infection with mycelial propagules

Suárez-Álvarez, Roberto
Sahaza, Jorge
Berzunza-Cruz, Miriam

Authors: Becker, Ingeborg
Curiel-Quesada, Everardo
Pérez-Torres, Armando
Taylor, Maria Lucia

Date Submitted: 07-Nov-2014

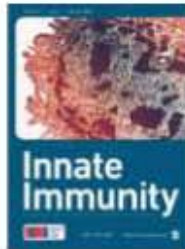
 Print

 Return to Dashboard

SCHOLARONE™

 THOMSON REUTERS™

© Thomson Reuters | © ScholarOne, Inc., 2014. All Rights Reserved.
ScholarOne Manuscripts and ScholarOne are registered trademarks of ScholarOne, Inc.
ScholarOne Manuscripts Patents #7,257,767 and #7,263,655.



Dimorphism and dissemination of *Histoplasma capsulatum* occur in the nasal mucosa and cervical lymph nodes of bats and mice in a short-time after intranasal-infection with mycelial propagules

Journal:	<i>Innate Immunity</i>
Manuscript ID:	Draft
Manuscript Type:	Original Manuscript
Date Submitted by the Author:	n/a
Complete List of Authors:	Suárez-Alvarez, Roberto; Universidad Nacional Autónoma de México, Microbiología y Parasitología, Facultad de Medicina Sahaza, Jorge; Universidad Nacional Autónoma de México, Microbiología y Parasitología, Facultad de Medicina Berzunza-Cruz, Miriam; Universidad Nacional Autónoma de México (UNAM), Medicina Experimental, Facultad de Medicina Becker, Ingeborg; Universidad Nacional Autónoma de México (UNAM), Medicina Experimental, Facultad de Medicina Curiel-Quesada, Everardo; Escuela Nacional de Ciencias Biológicas, Instituto Politécnico Nacional, Bioquímica Pérez-Torres, Armando; Universidad Nacional Autónoma de México (UNAM), Biología Celular-Tisular Taylor, María Lucía; Universidad Nacional Autónoma de México, Microbiología y Parasitología, Facultad de Medicina
Keywords:	Dimorphism, dissemination, <i>H. capsulatum</i> , mycelial propagules, respiratory tract response
Abstract:	The present results describe, for the first time, the role of the nasal mucosa (NM) and cervical lymph nodes (CLN) as initial sites for <i>Histoplasma capsulatum</i> dimorphic transition and its subsequent dissemination. Bats and mice were intranasally infected with <i>H. capsulatum</i> mycelial propagules and killed at 10, 20, 40 min and 1, 2, 3 h after infection. The NM and CLN were monitored for the fungal presence. Yeasts compatible with <i>H. capsulatum</i> were detected within NM and CLN dendritic cells at 2-to-3-h post-infection, using immunohistochemistry. <i>H. capsulatum</i> was isolated by culture at 28°C from the CLN of bats and of one mouse after infection. These fungal isolates were the same as the original strain inoculum based on their RAPD-PCR patterns. Novel RT-PCR assays were designed to detect fungal dimorphism, using the expression of mycelial specific (MS8) and yeast specific (YPS3) genes. This strategy supported the fast fungal dimorphism under in vivo conditions, which began in the NM at 1 h post-infection (a time point when MS8 and YPS3 specific genes were expressed) and was completed in 3 h (a time point when only the YPS3 transcripts were detected), in both bats and mice.

1
2
3
4
5
6
7
8
9
10
11
12
13
14
15
16
17
18
19
20
21
22
23
24
25
26
27
28
29
30
31
32
33
34
35
36
37
38
39
40
41
42
43
44
45
46
47
48
49
50
51
52

Dimorphism and dissemination of *Histoplasma capsulatum* occur in the nasal mucosa and cervical lymph nodes of bats and mice in a short-time after intranasal-infection with mycelial propagules

Roberto O. Suárez-Álvarez^{1,2,§}, Jorge H. Sahaza^{1,3,§}, Miriam Berzunza-Cruz⁴,
Ingeborg Becker⁴, Everardo Curiel-Quesada⁵, Armando Pérez-Torres^{6,0} and Maria-
Lucia Taylor^{1,0}

¹Departamento de Microbiología-Parasitología, Facultad de Medicina, Universidad Nacional Autónoma de México (UNAM), México DF, Mexico

²Departamento Micología, INEI ANLIS "Dr. Carlos G. Malbrán", Buenos Aires, Argentina

³Unidad de Micología Médica y Experimental, Corporación para Investigaciones Biológicas, Medellín, Colombia

⁴Departamento de Medicina Experimental, Facultad de Medicina, UNAM, México DF Mexico

⁵Departamento de Bioquímica, Escuela Nacional de Ciencias Biológicas, Instituto Politécnico Nacional, México DF, Mexico

⁶Departamento Biología Celular-Tisular, Facultad de Medicina, UNAM, México DF Mexico

[§]These authors contributed equally to this article

⁰These authors participated in the design and supervision of this article

Corresponding author:

Maria-Lucia Taylor, Departamento de Microbiología-Parasitología, Facultad de Medicina, UNAM, Av. Universidad 3000, Circuito Escolar s/n, Ciudad Universitaria, México DF 04510, Mexico. Phone/Fax: (+52) (55) 5623-2462

Email: emello@unam.mx

Abstract

The present results describe, for the first time, the role of the nasal mucosa (NM) and cervical lymph nodes (CLN) as initial sites for *Histoplasma capsulatum* dimorphic transition and its subsequent dissemination. Bats and mice were intranasally infected with *H. capsulatum* mycelial propagules and killed at 10, 20, 40 min and 1, 2, 3 h after infection. The NM and CLN were monitored for the fungal presence. Yeasts compatible with *H. capsulatum* were detected within NM and CLN dendritic cells at 2-to-3-h post-infection, using immunohistochemistry. *H. capsulatum* was isolated by culture at 28°C from the CLN of bats and of one mouse after infection. These fungal isolates were the same as the original strain inoculum based on their RAPD-PCR patterns. Novel RT-PCR assays were designed to detect fungal dimorphism, using the expression of mycelial specific (*MSS*) and yeast specific (*YPS3*) genes. This strategy supported the fast fungal dimorphism under *in vivo* conditions, which began in the NM at 1 h post-infection (a time point when *MSS* and *YPS3* specific genes were expressed) and was completed in 3 h (a time point when only the *YPS3* transcripts were detected), in both bats and mice.

Keywords

Dimorphism, dissemination, *H. capsulatum*, mycelial propagules, respiratory tract response

Introduction

Histoplasma capsulatum is the etiologic agent of the respiratory and systemic granulomatous mycosis histoplasmosis, which has different clinical presentations that depend on host susceptibility and the conditions prevailing in the infection process.¹

H. capsulatum is a dimorphic fungus widespread in the world. In special environments, it grows as a saprobe mycelial (M)-phase and produces infective propagules, mainly microconidia and small hyphal fragments. Once aerosolized and inhaled by hosts, these propagules can cause an infection associated with a mild-to-severe clinical course mostly in immunosuppressed individuals or in susceptible persons who work in places with

1
2
3
4
5 a high risk of infection.

6
7 It has been proposed that after inhalation, the infective M-phase propagules
8 accumulate in lung alveoli and convert to the *H. capsulatum* yeast (Y)-phase within
9 alveolar macrophages. Usually, immunocompetent hosts are able to resolve this type of
10 infection. Under some circumstances, however, this parasite can multiply within the hostile
11 intracellular macrophage microenvironment, allowing the fungus to persist within alveolar
12 macrophages, leading to macrophage destruction and the subsequent dissemination of its Y-
13 phase.^{2,3}

14
15
16
17
18
19
20
21
22
23
24
25
26
27
28
29
30
31
32
33
34
35
36
37
38
39
40
41
42
43
44
45
46
47
48
49
50
51
52
53
54
55
H. capsulatum develops in different host cells including macrophages, neutrophils,
dendritic cells (DCs), and epithelial cells.²⁻⁷ In general, processing and presentation of *H.*
capsulatum antigens to T-lymphocytes is more effective in DCs than in macrophages, a
necessary step to trigger the adaptive immune response.^{2,6,8}

A resident DC subpopulation in the lungs with the phenotype CD11⁺, F4/80⁻,
CD11b⁺, Ly6C⁺, CD205⁺ has been reported to be responsible for the phagocytosis of *H.*
capsulatum yeasts in C57BL/6 mice.⁹ Recently, Newman et al.¹⁰ found that transition of
conidia (M-phase) to yeasts (Y-phase) was restricted in human and murine cultured lung
DCs.

Given that *H. capsulatum* infects the host through the airways, the nasal mucosa
(NM), nasal associated lymphoid tissue (NALT), and cervical lymph nodes (CLN) could
participate as the first step in fungal capture and dissemination, which likely occurs through
their constitutive DCs that are located strategically in the NM and CLN.

The aims of this study were to determine the roles played by the NM, NALT, and
CLN during the early hours of *H. capsulatum* intranasal infection of two different
mammalian hosts, as well as to advise other initial host's anatomic sites for *H. capsulatum*
M-to-Y morphotype transition and its subsequent dissemination, probably within DCs. For
this purpose, pioneering strategies were implemented using bats (natural wild host) and
mice (laboratory experimental host) as models, as well as the expression of two
morphotype protein specific genes for *H. capsulatum*, *MSS* (mold-specific) expressed only
in the fungal M-phase^{11,12} and *YPS3* (yeast-phase specific) expressed only in the Y-phase.¹³

Materials and methods

Histoplasma capsulatum

The EH-53 strain, which was isolated from a patient infected in a cave in the state of Hidalgo, Mexico, was selected for the study. This strain was characterized as LAm A phylogenetic species by Kasuga et al.¹⁴ and it is considered as reference of our laboratory research team. It is deposited in the *H. capsulatum* Culture Collection of the Fungal Immunology Laboratory of the Department of Microbiology and Parasitology, School of Medicine, UNAM (www.histoplas-mex.unam.mx), which is registered in the database of the World Data Centre for Microorganisms (WDCM) under number [LIH-UNAM WDCM817](#). The M-phase of the EH-53 strain was cultured at 28°C in mycobiotic-agar (Bioxon, Becton-Dickinson, México DF, MX). The Y-phase was maintained at 37°C in brain-heart infusion broth (BHI) (Bioxon) supplemented with 0.1% L-cysteine and 1% glucose.

Animal models

Bats were selected because of their possible evolutionary history with the pathogen *H. capsulatum* over the course of millions of years in shared habitats in nature, whereas naïve mice used in laboratory assays did not exhibit this singular characteristic. Adult male *Tadarida brasiliensis* bats were captured in the “El Salitre” cave, Mezquitlán municipality, state of Hidalgo, Mexico, with a chiropteran mist-net. This bat species was chosen based on its high susceptibility to *H. capsulatum* infection and due to its behavior to form large colonies.¹⁵ Bats were transported alive from their shelter to the Fungal Immunology Laboratory, UNAM, where they were housed and maintained for a short period with coleopteran larvae and acidified water, until required for different assays. Eight-week-old male BALB/c mice were maintained at the animal facilities of the School of Medicine, UNAM, and provided with Purina chow (Purina de México, México DF, MX) and water *ad*

4
5
6
7
8
9
10
11
12
13
14
15
16
17
18
19
20
21
22
23
24
25
26
27
28
29
30
31
32
33
34
35
36
37
38
39
40
41
42
43
44
45
46
47
48
49
50
51
52
53
54
55
56
57

libitum. Both animal models were treated in accordance with the suggestions of the Ethics Committee of the School of Medicine, UNAM, to project numbers: 112-2009 (approved on January 05, 2010) and 049-2011 (approved on June 14, 2011), and following the recommendations of the Animal Care and Use Committee of the UNAM and the Mexican Official Guide (NOM 062-ZOO-1999).

Fungal inoculum

Mycelium cultured in mycobiotic-agar was transferred to non-supplemented BHI-agar plates and incubated at 28°C for 4 weeks. After incubation, conidia and hyphae were harvested by gently washing the fungal culture surface with sterile saline-solution (SS). The fungal suspension was filtered through Whatman grade 40 filter paper (General Electric, Healthcare Bio-Sciences Corp. Piscataway, NJ, USA) to homogenize the inoculum, and then centrifuged at 800 *g*-15 min. After removing the supernatant, the pellet was suspended in 1 ml SS and observed under light microscopy for the presence of microconidia and small hyphal fragments. The mycelial propagules viability was tested with trypan blue (0.05%) and, to confirm the viability, a sample was cultured in non-supplemented BHI-agar at 28°C. The propagules suspension was carefully prepared in SS and adjusted to 0.5 optical density units and the desired inoculum was quantified with a hemocytometer. The fungal inoculum (8×10^7 mycelial propagules/100 μ l) was processed as most homogeneously as possible, containing 90% microconidia and 10% small mycelial fragments, approximately. All procedures were performed under strict biosafety and sterile conditions.

Intranasal infection

Fourteen animals of each species were infected with the above mentioned standardized inoculums (20 μ l) dispensed in each animal's nostril at intervals of approximately 30 s, until completing 100 μ l. Bats and mice were euthanized appropriately, as recommended by the Animal Care and Use Committee of the UNAM, at 10, 20, 40 min and 1, 2, 3 h post-infection. NM (including the NALT) and CLN were harvested to monitor the fungal

3
4
5 infection. Each tissue sample was washed three times in SS prior to any assay. The
6 infection assays were processed in duplicate for each studied time. Non-infected animals
7 were used as negative controls.
8
9

10 11 *Fungal recovering from infected animals*

12
13
14
15 Saline-solution-washed fragments of NM and CLN from bats and mice were incubated on
16 mycobiotic-agar (Bioxon), for 3-4 weeks at 28°C, to facilitate fungal growth and
17 identification according to Taylor et al.¹⁶ Genomic DNA from each M-phase of the
18 recovered fungal isolates was evaluated by RAPD-PCR as described by Taylor et al.¹⁷ and
19 Canteros et al.¹⁸ to confirm the polymorphic DNA-pattern of *H. capsulatum*.
20
21
22
23

24 25 *Paraffin-embedded sections*

26
27
28
29 Nasal mucosa and CLN samples, taken at the different post-infection times studied, were
30 fixed with 4% paraformaldehyde in 0.1 M Tris-HCl (pH 7.4) buffer for 8 h, and then
31 washed in the same buffer. The nasal cavity and its bony framework, including the
32 nasopharyngeal duct, were dissected after the removal of the soft tissue and bones of the
33 animal's head. The resulting bony block was decalcified by immersion in 10% EDTA
34 prepared in 0.1 M phosphate-buffered saline (pH 7.2) for 2 weeks. All specimens were
35 paraffin-embedded to obtain tissue sections. Serial frontal sections were used to localize the
36 NALT in the NM for each studied animal. All tissue sections were processed for periodic
37 acid Schiff (PAS), hematoxylin-eosin (H&E), and immunohistochemistry (IHC).
38
39
40
41
42
43
44

45 46 47 *Detection of *H. capsulatum* and DCs in NM and CLN sections by IHC using* 48 *immunoperoxidase staining*

49
50
51
52 Tissue sections (3- μ m) were mounted on positively-charged slides Superfrost plus®
53 (Shandon Inc. Pittsburgh, PA, USA), dewaxed with xylene, rehydrated with 0.1 M Tris-
54 HCl (pH 7.2) buffer, and treated with 0.1 M citrate buffer (pH 6.0) for antigen retrieval.
55
56
57

4 The sections were processed using a conventional immunoperoxidase method to detect *H.*
5 *capsulatum* as described by Espinosa-Avilés et al.¹⁹ and Pérez-Torres et al.²⁰ with minor
6 modifications. A specific *H. capsulatum* rabbit hyperimmune serum diluted 1:50 in Tris-
7 HCl (pH 7.2) was used as the primary antibody, and a biotinylated goat anti-rabbit IgG
8 (Zymed Laboratories Inc., San Francisco, CA, USA) as the secondary antibody. Finally, a
9 streptavidin-biotin-horseradish peroxidase complex, an aminoethylcarbazole (Zymed)
10 chromogen solution, and hydrogen peroxide were added to reveal the reaction.
11

12 Double staining was also performed to detect *H. capsulatum* and DCs in the same
13 tissue section. After staining for *H. capsulatum*, peroxidase was blocked again as described
14 by Pérez-Torres et al.²⁰ Then, a second immunoperoxidase staining was performed to
15 identify the DEC-205 receptor on DCs. The rat anti-DEC-205 monoclonal NLDC-145
16 (Serotec Co., Oxford, UK) diluted 1:40 in Tris-HCl (pH 7.2) was used as the primary
17 antibody and a biotinylated goat anti-rat IgG (Zymed) was used as the secondary antibody.
18 Afterwards, the streptavidin-biotin-horseradish peroxidase complex was processed as above
19 mentioned, using 3,3'-diaminobenzidine (Zymed) as chromogen.
20

21 All IHC slides were counterstained with Mayer's hematoxylin for 30 s and mounted
22 with hydrosoluble resin (Biocare Medical Co., Concord, CA, USA).
23

24 Sections of the peripancreatic lymph node from a disseminated histoplasmosis
25 clinical case containing a high number of intracellular yeasts and sections of the thymus
26 containing NLDC-145-positive corticomedullar interdigitating DCs were used as positive
27 controls in every IHC assay for the detection of *H. capsulatum* and DCs, respectively.
28

29 Negative controls for all tissue sections assayed were treated as above, using rabbit
30 normal serum as the primary antibody.
31

32 Photomicrographs were taken with an automatic Olympus SC 35 camera connected
33 to a BX 50 microscope (Olympus American Inc., Miami, FL, USA).
34

35 *Expression of H. capsulatum phase-specific genes by reverse transcription-polymerase* 36 *chain reaction (RT-PCR)* 37

38 Total RNA from the NM and CLN of each infected animal, at the different post-infection
39
40
41
42
43
44
45
46
47
48
49
50
51
52
53
54
55
56
--

3
4
5
6
7
8
9
10
11
12
13
14
15
16
17
18
19
20
21
22
23
24
25
26
27
28
29
30
31
32
33
34
35
36
37
38
39
40
41
42
43
44
45
46
47
48
49
50
51
52
53
54
55
56

times studied, were extracted using the TRIzol[®] Reagent (Invitrogen Life Technologies, San Diego, CA, USA). Briefly, 1 ml TRIzol was added to 10 mg of NM or CLN samples and each suspension was incubated at room temperature for 20 min, vortexing every 5 min. Then, 200 µl chloroform were gently mixed at room temperature for 3 min. Each sample was centrifuged at 12,000 *g*-15 min at 4°C and the water-soluble phase was recovered, followed by the addition of 500 µl isopropanol. Samples were incubated at room temperature for 10 min and centrifuged at 12,000 *g*-10 min at 4°C. The supernatant was removed and each pellet was suspended in 75% ethanol. Samples were again centrifuged at 7,500 *g*-5 min at 4°C and each pellet was dried, dissolved in 13 µl of milli-Q water, and finally incubated at 60°C for 10 min. The RNA from each sample was fluorometrically quantified and immediately processed.

Purified RNA samples (1 µg) from the NM or CLN, taken at each infection time, were used for cDNA synthesis and amplification of each *H. capsulatum* phase-specific gene with the SuperScript III One-Step RT-PCR System (Invitrogen). Based on previous reports for *MS8*¹¹ and *YPS3*²¹ genes, we designed two sets of specific primers (10 pmol for each primer), with each set corresponding to a particular fungal morphotype. The M-phase specific (*MS8*) primers, *MS8-FWD* (5'-GGGTTCTTCGAACTTCCTTG-3') and *MS8-REV* (5'-TGAAGATATGCGGTACAACA-3') generated a 153-bp fragment of the *MS8* gene, which encodes a predicted 21-kDa structural protein necessary for hyphal cell wall formation.¹² The Y-phase specific (*YPS3*) primers, *YPS-FWD* (5'-TCTGCGGCACCTGCAACCCTAT-3') and *YPS-REV* (5'-CGGCTTCGTGTTATCGTCGC-3') generated a 230-bp fragment of the *YPS3* gene, which encodes a 20-kDa protein localized in the yeast cell wall.²²⁻²⁴

The following thermocycling conditions were used for cDNA synthesis and amplification: one cycle at 50°C for 30 min and one cycle at 94°C for 2 min, followed by 35 cycles at 94°C for 15 s, 55°C for 30 s, 72°C for 1 min, and a final extension cycle at 72°C for 7 min.

RT-PCR of β-actin from the NM and CLN samples of each animal were processed as positive controls of the assay with tissue samples and the following primers (10 pmol each) were used: *FWD* (5'-CCAACTGGGACGACATGG-3') and *REV* (5'-

4 GGTGGTACCACCAGACAGC-3'), which generated a 648-bp fragment. RNA extracted
5 from each M- or Y-phase of *H. capsulatum* EH-53 strain suitable cultures was processed
6 only as a control to standardize the optimal conditions to detect the expression of the M- or
7 Y-phase specific genes for each morphotype, in individual cultures. Milli-Q water and/or
8 RNA from the NM or CLN of non-infected animals processed by the One-Step RT-PCR
9 System were used as negative controls.
10
11
12
13
14

15 The amplification products were electrophoresed on 1.5% agarose in 1X TAE buffer
16 at 100 V for 50 min. A 123-bp DNA ladder (Gibco, Life Technologies, Carlsbad, CA,
17 USA) was used as a molecular size marker. The bands were visualized as described above.
18
19
20
21
22

23 Results

24 *Fungal recovering from infected animals*

25
26
27 Three *H. capsulatum* mycelial cultures grown on mycobiotic-agar were isolated from the
28 CLN of two bats killed at 2 and 3 h and of one mouse killed at 3 h post-infection. *H.*
29 *capsulatum* was identified by its typical macro- and micromorphology and each recovered
30 isolate was confirmed to be the same as the original inoculum (EH-53 strain), as evidenced
31 by comparison of their RAPD-PCR polymorphic patterns (data not shown).
32
33
34
35
36
37
38
39
40

41 *Histological findings*

42
43
44 The NALT from the bats and mice were identified using transversal decalcified
45 nasopharynx sections stained by PAS and H&E, and fungal cells compatible with *H.*
46 *capsulatum* yeasts were observed in the ciliated pseudostratified columnar epithelium
47 associated with the NALT, in bats at 2 h and in mice at 3 h post-infection (Figure. 1A, B).
48
49
50
51

52 *H. capsulatum* yeast-like cells were observed by IHC in NM, non-associated to
53 NALT, in either bats at 2 and 3 h (Figure 2A) or mice at 3 h (Figure 2B) post-infection. In
54 general, fewer numbers of yeast-like cells were observed in the NM epithelial cells of bats
55
56
57

4
5
6
7
8
9
10
11
12
13
14
15
16
17
18
19
20
21
22
23
24
25
26
27
28
29
30
31
32
33
34
35
36
37
38
39
40
41
42
43
44
45
46
47
48
49
50
51
52
53
54
55
56
57

than in those of mice. In most cases, yeast-like cells were observed intracellularly, although they were occasionally found extracellularly. Likewise, intracellular and/or extracellular yeast-like cells were observed by IHC in the CLN sections of bats at 2 and 3 h and in mice at 3 h post-infection (Figure 2C). Several yeast-like cells were found in the cytoplasm of phagocytes located in the paracortical zone of CLN, which most likely correspond to interdigitating DCs (Figure 2D). Double IHC staining, for *H. capsulatum* and DCs, provided support for yeast phagocytosis by DCs (Figure 2D).

Numerous intracellular and extracellular yeasts were observed in peripancreatic lymph node sections from a clinical case of a fatal histoplasmosis that was used as positive control for *H. capsulatum* infection. Besides, IHC of thymus sections confirmed the usefulness of the assay to detect DCs in tissues.

In all IHC assays, controls with normal serum were always negative.

Detection of H. capsulatum phase-specific genes by RT-PCR

First, the expression of each morphotype-specific gene was standardized using RNA of each *H. capsulatum* morphotype cultures. Overall, concentration of the total RNA was 194 µg/ml for the M-phase culture and 228 µg/ml for the Y-phase culture. RT-PCR was performed on the total RNA extracted from each of the morphotypes to generate the cDNA for phase-specific genes. After resolving the cDNA products on agarose gel electrophoresis, the morphotypes of *H. capsulatum* were confirmed by the observation of the corresponding cDNA bands of the two phase-specific genes: *MSS*, a 153-bp product specific to the M-morphotype; and *YPS3*, a 230-bp product specific to the Y-morphotype (data not shown).

Afterwards, RT-PCR assays were conducted with tissues from infected bats and mice. In bats NM, the cDNA band matching the *MSS* gene (M-phase) was detectable from 40 min to 1 h after the infection (Figure 3A), whereas the band corresponding to the *YPS3* gene (Y-phase) was only detectable after 1 h post-infection and remained detectable for up to 3 h post-infection (Figure 3B). In mice NM, the band matching the *MSS* cDNA was not detectable during the initial stage of infection (Figure 4A), but was revealed from 1 to 2 h

3
4
5
6
7
8
9
10
11
12
13
14
15
16
17
18
19
20
21
22
23
24
25
26
27
28
29
30
31
32
33
34
35
36
37
38
39
40
41
42
43
44
45
46
47
48
49
50
51
52
53
54
55
56
57
58

post-infection (Figure 4B), whereas the band corresponding to the *YPS3* cDNA was also found after 1 h post-infection and remained detectable during the assayed post-infection times (Figure 4B).

Regarding the phase-specific transcript expressions in the CLN of both bats and mice, the 153-bp band corresponding to the *MSS* cDNA was never detectable in any of the animals when analyzed at different post-infection times (Figure 3C, D, and Figure 4C). In contrast, the 230-bp band corresponding to the *YPS3* cDNA was detectable at 2 and 3 h post-infection in both bats (Figure 3C, D) and mice (Figure 4C).

The 648-bp band corresponding to the β -actin cDNA (positive control) was revealed in all assays. The RT-PCR assay performed with milli-Q water and RNA from the tissues of non-infected animals systematically yielded negative results.

Discussion

Host response to M-morphotype of *H. capsulatum* has been scarcely analyzed, despite the fact that Inglis et al.²⁵ reported that type I interferon responsive genes were induced during infection of murine alveolar macrophages with conidia but not with yeasts, which suggests that different host innate immune responses could be associated with each of the *H. capsulatum* morphotypes. However, the interaction between *H. capsulatum* morphotypes and the host response associated with the upper respiratory tract has not been explored.

The NM represents the first site of host defense against entry of airborne pathogens into the upper and lower respiratory tracts. Most of the NM displays cylindrical-pseudostratified and ciliated epithelium with caliciform cells. In the lamina propria, macrophages, neutrophils, and DCs are present. The interaction between diverse microorganisms and these phagocytes, in combination with the overall immunological state of the host, can define the clinical course of the infection. The upper airways, particularly the highly vascular NM, have an important protective function that includes humidification and heating of inspired air to 37°C.²⁶ The NM may also present optimal conditions that facilitate the M-to-Y morphotype transition of certain dimorphic fungal pathogens, such as

3
4
5
6
7
8
9
10
11
12
13
14
15
16
17
18
19
20
21
22
23
24
25
26
27
28
29
30
31
32
33
34
35
36
37
38
39
40
41
42
43
44
45
46
47
48
49
50
51
52
53
54
55
56

H. capsulatum. This transition is a crucial event for the virulence and the survival of the fungus in hostile intra- and extracellular host environments. In this study, molecular methods were addressed at evaluating the dimorphic transition and subsequent dissemination of *H. capsulatum* after intranasal infection with a mycelial inoculum in either bats or mice, expecting to determine, in both animal models, the roles played by the NM, NALT, and CLN in response to the challenge with a pathogen directly associated to the respiratory tract.

In mice, the NALT is well-known,^{27,28} whereas in bats, the NALT was described for the first time by Suárez-Alvarez et al.²⁹ It has an appearance similar to a paired lymphoid tissue distributed on both sides of the nasal septum, within the angle formed between the palate-bone and the lower-comet.

Double IHC demonstrated that *H. capsulatum* yeast-like cells were present within the subepithelial DCs of NM and the paracortical DCs of the CLN, in both bats and mice. Unfortunately, there are few studies of histoplasmosis conducted in bats model; whereas the mice model has been more explored.³⁰ It is important to highlight that this is the only study that has employed bats as an experimental model for *H. capsulatum* dimorphism and dissemination. The findings herein described, suggest differences between the two animal models regarding the time required for the dimorphic transition and subsequent dissemination of the fungus, as well as the amount of fungal cells present in the NM, NALT, and CLN host environments, which could induce slight discrepancies in their immune response to histoplasmosis infection. These discrepancies could be associated with a special bat and fungus relationship in nature, which has favored the interplay between this kind of wild host and the pathogen *H. capsulatum*.³¹ Under this assumption, bats have been able to resolve the *H. capsulatum* infection through a more effective response at the first contact with the fungus that could differ from the mice defense mechanisms. To support this statement, low inflammatory responses have been reported in the lungs of infected bats that show histological findings and culture evidences of *H. capsulatum* infection, as reported by Taylor et al.¹⁶

The recovery of *H. capsulatum*, on mycobiotic-agar, from the CLN of bats and mice, killed at 2-to-3 h and 3 h post infection, respectively, demonstrated the success of the

4 infectious process and confirmed the viability of the inocula, as well as the occurrence of
5 fungal dissemination in these two animal models. Although the *H. capsulatum* M-to-Y
6 transition and further dissemination is assumed to occur within alveolar macrophages,^{3,8} the
7 present study shows that particular sites of the upper respiratory tract may also be involved
8 in both processes. The dimorphic transition of *H. capsulatum* has been widely studied *in*
9 *vitro* using special culture media,^{32,33} however, the findings of the current research
10 contribute with new data on the *in vivo* dimorphism and subsequent yeasts dissemination of
11 this pathogen in infected hosts. Besides, the time required for *in vivo* dimorphic transition
12 was shorter than in another study performed under experimental conditions using *H.*
13 *capsulatum* and cultured alveolar or peritoneal macrophages.³⁴

22 The unequivocal expression by RT-PCR assays of morphotype-specific *MSS* and
23 *YPS3* genes, in M- or Y-phase *H. capsulatum* cultures, demonstrated that both markers
24 were undoubtedly specific for their respective morphotypes, supporting the finding that
25 fungal cultures did not contain a mixture of both *H. capsulatum* morphotypes, since a
26 unique and specific cDNA band was revealed for each morphotype culture.

31 RT-PCR analyses also demonstrated that the morphotype-specific *MSS* and *YPS3*
32 genes were expressed in infected bats and mice, albeit with some differences in their time-
33 points. Thus, in bats the *MSS* transcript was detectable from 40 min until 1 h post-infection
34 in the NM, suggesting that the mycelial propagules of the fungus persisted during this
35 period of time. Inversely, the *YPS3* transcript was detectable only at 1 h after the infection,
36 suggesting that the fungal yeast-like cells appeared at this time and persisted subsequently.
37 In contrast, the expression of the *MSS* transcripts in the NM was delayed in mice and
38 disappeared altogether at 2 h post-infection, whereas the expression of the *YPS3* gene was
39 similar to that observed in bats. In consequence, our findings suggest that the dimorphic
40 transition of *H. capsulatum* occurs earlier in bats than in mice and, furthermore, the first 2 h
41 after infection could be proposed as a necessary time for the fungal morphotype-transition
42 process, which was completed at 3 h post-infection, under the *in vivo* conditions used.

52 Interestingly, the *MSS* gene was no longer expressed in the NM from either bats or
53 mice during the latest infection time analyzed, suggesting that all the mycelial propagules
54 that were able to cross the NM were converted to their Y-morphotype prior to their arrival
55
56
57

4
5 to the CLN. The identification of only the Y-phase in CLN suggests that phagocytes
6 associated with the NM and NALT, usually the DCs, transport the fungus through the blood
7 and lymphatic vessels that drain these tissues towards the CLN. Thus, some extra- or
8 intracellular yeast cells that were not processed in the CLN could continue to be transported
9 by hematic and/or lymphatic routes, thus facilitating the spread of the Y-morphotype to
10 other host tissues.
11

12
13
14
15 The role of DCs in the recognition, transport, processing, and fate of *H. capsulatum*
16 has been studied, and the interaction of this fungus with the DCs is achieved mainly by the
17 very late antigen-5 molecule of the integrin family,² which recognizes a 20-kDa protein
18 identified as cyclophilin A on the *H. capsulatum* yeast surface.⁶ The interaction of the DC
19 toll-like receptor-2 (TLR-2) with this fungus was first documented by Aravalli et al.³⁵ who
20 determined that the Yps3 protein induces signaling through TLR-2. Sorgi et al.³⁶ also found
21 an interaction of TLR-2 with *H. capsulatum*.
22

23
24
25
26
27 The presented findings suggest that DCs are the ideal candidates to be involved in
28 the mobilization of the fungus from the NM of infected animals to their CLN. The
29 identification of intracellular yeast-like cells within the subepithelial and interstitial DCs of
30 the NM as well as within the interdigitating DCs of the CLN in both animal models
31 provides additional support for this statement. Although other mechanisms are involved in
32 the dissemination of *H. capsulatum*,³⁷⁻³⁹ a DC-based mechanism appears to be the easiest
33 route for this pathogen to arrive at the CLN, where it can initiate its dissemination to
34 several other organs.
35

36
37
38
39
40
41
42 Given the involvement of the NM and NALT observed in this study, it would be
43 interesting to show that either NM or NALT are rich in lymphoid tissue and could generate
44 an effective defense response, because they have all the necessary elements required to
45 mount a competent local immune response. The effectiveness of this defense would depend
46 on diverse factors, including the fungal inoculum, the virulence of the *H. capsulatum* strain,
47 the animal model, the route of infection, and the whole immunological state of the host.
48

49
50
51
52
53 The current findings do not exclude the classic route involved in *H. capsulatum*
54 infection, in which aerosolized infective M-phase propagules have a direct arrival route into
55 the lungs, where the dimorphic transition and initiation of dissemination has been suggested
56
57

3
4
5
6
7
8
9
10
11
12
13
14
15
16
17
18
19
20
21
22
23
24
25
26
27
28
29
30
31
32
33
34
35
36
37
38
39
40
41
42
43
44
45
46
47
48
49
50
51
52
53
54
55
56
--

to occur.^{2,3} However, fungal dimorphism and dissemination in infected animals may also occur in the NM without necessarily requiring that the fungal propagules arrive to the lungs.

In addition, we would like to underline that our indigenous EH-53 *H. capsulatum* strain, classified previously as LAm A phylogenetic species, was able to induce the *YPS3* transcript either in fungal culture or in infected tissue, as detected by RT-PCR assays in the present study. Besides, the purified Yps3 protein from EH-53 strain has been detected by Western-blot, revealed with anti-*H. capsulatum* human antibodies (Curiel-Quesada E and Taylor ML, pers. comm.). These findings are relevant because neither the *YPS3* transcript nor its protein has been previously identified in *H. capsulatum* LAm A phylogenetic species.

In conclusion, our results of morphological, immunohistochemical, and molecular assays, performed on the tissues of infected bats and mice, suggest the following: first, in the infected host, *H. capsulatum* has alternative sites for initiating its dimorphic transition and dissemination, including the NM and CLN; second, fungal dimorphism and dissemination to internal organs initiates earlier than previously reported in the literature; and finally, the time required for *H. capsulatum* dimorphic transition under our *in vivo* infection conditions, which mimics the natural route of pulmonary histoplasmosis, was shorter than those reported by most other studies performed under non-natural conditions, such as using non-appropriated hosts, non-infective *H. capsulatum* propagules, and inaccurate route of fungal infection.

Funding

This research was supported by two grants from CONACYT-Mexico (Reference Numbers, 182501 and 166052).

Acknowledgments

5
6
7
8
9
10
11
12
13
14
15
16
17
18
19
20
21
22
23
24
25
26
27
28
29
30
31
32
33
34
35
36
37
38
39
40
41
42
43
44
45
46
47
48
49
50
51
52
53
54
55
56
57

This paper constitutes collateral fulfillment of the requirements of the Graduate Program in Biological Sciences of the UNAM. Jorge Humberto Sahaza thanks the Graduate Program in Biological Sciences of the UNAM and the scholarship of the *Consejo Nacional de Ciencia y Tecnología-México* (CONACYT-Mexico, Reference Number, 245151). Everardo Curiel-Quesada is a fellow of the *Comisión de Operación y Fomento de Actividades Académicas* (COFAA) and *Estímulo al Desempeño en Investigación* (EDI). The authors thank Ingrid Mascher for editorial assistance.

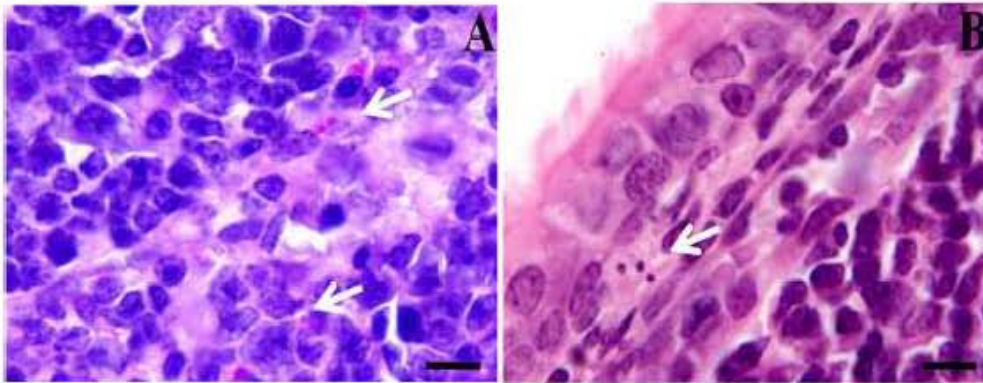
References

1. Tewari R, Wheat LJ and Ajello L. Agents of histoplasmosis. In: Ajello L and Hay RJ (eds). *Microbiology and microbial infections. Medical mycology. Topley and Wilson's*. New York: Arnold and Oxford University Press Inc., 1998, pp. 373-393.
2. Gildea LA, Morris RE and Newman SL. *Histoplasma capsulatum* yeasts are phagocytosed via very late antigen-5, killed, and processed for antigen presentation by human dendritic cells. *J Immunol* 2001; 166: 1049-1056.
3. Newman SL. Interaction of *Histoplasma capsulatum* with human macrophages, dendritic cells, and neutrophils. *Methods Mol Med* 2005; 118: 181-191.
4. Eissenberg LG and Goldman WE. *Histoplasma* variation and adaptive strategies for parasitism: new perspectives on histoplasmosis. *Clin Microbiol Rev* 1991; 4: 411-421.
5. Eissenberg LG, Goldman WE and Schlesinger PH. *Histoplasma capsulatum* modulates the acidification of phagolysosomes. *J Exp Med* 1993; 177: 1605-1611.
6. Gomez FJ, Pilcher-Roberts R, Alborzi A and Newman SL. *Histoplasma capsulatum* cyclophilin A mediates attachment to dendritic cell VLA-5. *J Immunol* 2010; 181: 7106-7114.
7. Newman SL, Gootee L and Gabay JE. Human neutrophil-mediated fungistasis against *Histoplasma capsulatum*. Localization of fungistatic activity to the azurophil

- 3
4
5
6
7
8
9
10
11
12
13
14
15
16
17
18
19
20
21
22
23
24
25
26
27
28
29
30
31
32
33
34
35
36
37
38
39
40
41
42
43
44
45
46
47
48
49
50
51
52
53
54
55
56
57
58
- granules. *J Clin Invest* 1993; 92: 624-631.
8. Newman SL. Macrophages in host defense against *Histoplasma capsulatum*. *Trends Microbiol* 1999; 7: 67-71.
 9. Deepe GS Jr, Gibbons RS and Smulian AG. *Histoplasma capsulatum* manifests preferential invasion of phagocytic subpopulations in murine lungs. *J Leuk Biol* 2008; 84: 669-678.
 10. Newman SL, Lemen W and Smulian AG. Dendritic cells restrict the transformation of *Histoplasma capsulatum* conidia into yeasts. *Med Mycol* 2011; 49: 356-364.
 11. Tian X and Shearer G Jr. Cloning and analysis of mold-specific genes in the dimorphic fungus *Histoplasma capsulatum*. *Gene* 2001; 275: 107-114.
 12. Tian X and Shearer G Jr. The mold-specific MS8 gene is required for normal hypha formation in the dimorphic pathogenic fungus *Histoplasma capsulatum*. *Eukaryot Cell* 2002; 1: 249-256.
 13. Keath EJ, Painter AA, Kobayashi GS and Medoff G. Variable expression of a yeast-phase-specific gene in *Histoplasma capsulatum* strains differing in thermotolerance and virulence. *Infect Immun* 1989; 57: 1384-1390.
 14. Kasuga T, White TJ, Koenig G, et al. Phylogeography of the fungal pathogen *Histoplasma capsulatum*. *Mol Ecol* 2003; 12: 3383-3401.
 15. González-González AE, Aliouat-Denis CM, Carreto-Binaghi LE, et al. An *Hcp100* gene fragment reveals *Histoplasma capsulatum* presence in lungs of *Tadarida brasiliensis* migratory bats. *Epidemiol Infect* 2012; 140: 1955-1963.
 16. Taylor ML, Chávez-Tapia CB, Vargas-Yañez R, et al. Environmental conditions favoring bat infection with *Histoplasma capsulatum* in Mexican shelters. *Am J Trop Med Hyg* 1999; 61: 914-919.
 17. Taylor ML, Chávez-Tapia CB and Reyes-Montes MR. Molecular typing of *Histoplasma capsulatum* isolated from infected bats, captured in Mexico. *Fungal Genet Biol* 2000; 30: 207-212.
 18. Canteros CE, Iachini RH, Rivas MC, et al. Primer aislamiento de *Histoplasma capsulatum* de murciélago urbano *Eumops bonariensis*. *Rev Argent Microbiol* 2005; 37: 46-56.

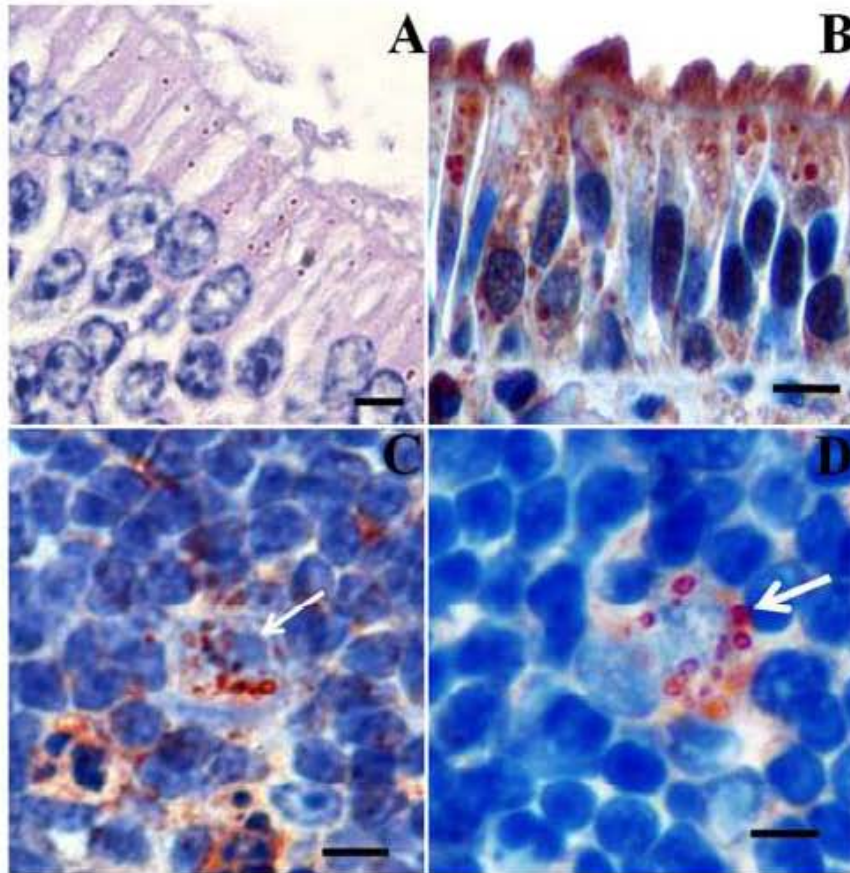
- 4
5 19. Espinosa-Avilés D, Taylor ML, Reyes-Montes MR and Pérez-Torres A. Molecular
6 findings of disseminated histoplasmosis in two captive snow leopards (*Uncia uncia*).
7 *J Zoo Wildl Med* 2008; 39: 450-454.
- 8
9 20. Pérez-Torres A, Rosas-Rosas A, Parás-García A, et al. Second case of histoplasmosis
10 in a captive mara (*Dolichotis patagonum*): pathological findings. *Mycopathologia*
11 2009; 168: 95-100.
- 12
13 21. Keath EJ and Abidi FE. Molecular cloning and sequence analysis of yps-3, a yeast-
14 phase-specific gene in the dimorphic fungal pathogen *Histoplasma capsulatum*.
15 *Microbiology* 1994; 140: 759-767.
- 16
17 22. Weaver CH, Kathleen CF, Sheehan KCF and Keath EJ. Localization of a yeast-
18 phase-specific gene product to the cell wall in *Histoplasma capsulatum*. *Infect Immun*
19 1996; 64: 3048-3054.
- 20
21 23. Bohse ML and Woods JP. Surface localization of the Yps3p protein of *Histoplasma*
22 *capsulatum*. *Eukaryot Cell* 2005; 4: 685-693.
- 23
24 24. Bohse ML and Woods JP. Expression and interstrain variability of the *YPS3* gene of
25 *Histoplasma capsulatum*. *Eukaryot Cell* 2007; 6: 609-615.
- 26
27 25. Inglis DO, Berkes CA, Hocking Murray DR and Sill A. Conidia but not yeast cells of
28 the fungal pathogen *Histoplasma capsulatum* trigger a type I interferon innate
29 immune response in murine macrophages. *Infect Immun* 2010; 78: 3871-3882.
- 30
31 26. McCaffrey TV. Nasal function and evaluation. In: Bailey BJ, Calhoun KH, Healy
32 GB, Pillsbury HC III, Johnson JT, Tardy ME Jr and Jackler RK (eds). *Head and neck*
33 *surgery-otolaryngology*. Philadelphia: Lippincott Williams and Wilkins, 2001, pp.
34 261-271.
- 35
36 27. Heritage PL, Underdown BJ, Arsenault AL, et al. Comparison of murine nasal-
37 associated lymphoid tissue and Peyer's patches. *Am J Respir Crit Care Med* 1997;
38 156: 1256-1262.
- 39
40 28. Heritage PL, Brook MA, Underdown BJ and McDermontt MR. Intranasal
41 immunization with polymer-grafted microparticles activates the nasal-associated
42 lymphoid tissue and draining lymph nodes. *Immunology* 1998; 93: 249-256.
- 43
44 29. Suárez-Alvarez RO, Taylor ML and Pérez-Torres A. Identificación histológica del
45
46
47
48
49
50
51
52
53
54
55
56
57

- 4
5 tejido linfoide asociado a la nariz (NALT) en el murciélago migratorio *Tadarida*
6 *brasiliensis*. *LAB-acta* 2009; 21: 5-8.
- 7
8
9
10
11 30. Sahaza JH, Pérez-Torres A, Zenteno E and Taylor ML. Usefulness of the murine
12 model to study the immune response against *Histoplasma capsulatum* infection.
13 *Comp Immunol Microbiol Infect Dis* 2014; 37: 143-152.
- 14
15 31. González-González AE, Aliouat-Denis CM, Ramírez-Bárceñas JA, et al. *Histoplasma*
16 *capsulatum* and *Pneumocystis* spp. co-infection in wild bats from Argentina, French
17 Guyana, and Mexico. *BMC Microbiol* 2014; 14:23, doi: 10.1186/1471-2180-14-23.
- 18
19 32. Maresca B and Kobayashi GS. Dimorphism in *Histoplasma capsulatum*: a model for
20 the study of cell differentiation in pathogenic fungi. *Microbiol Rev* 1989; 53: 186-
21 209.
- 22
23 33. Medoff G, Kobayashi GS, Painter A and Travis S. Morphogenesis and pathogenicity
24 of *Histoplasma capsulatum*. *Infect Immun* 1989; 55: 1355-1358.
- 25
26 34. Kimberlin C, Harri A, Hempel H and Goodman N. Interactions between *Histoplasma*
27 *capsulatum* and macrophages from normal and treated mice. Comparison of the
28 mycelial and yeast phases in alveolar and peritoneal macrophages. *Infect Immun*
29 1981; 34: 6-10.
- 30
31 35. Aravalli RN, Hu S, Woods J and Lokensgard JR. *Histoplasma capsulatum* yeast
32 phase-specific protein Yps3p induces Toll-like receptor 2 signaling. *J*
33 *Neuroinflammation* 2008; 5: 1-7.
- 34
35 36. Sorgi CA, Secatto A, Fontanari C, et al. *Histoplasma capsulatum* cell wall β -glucan
36 induces lipid body formation through CD18, TLR2, and dectin-1 receptors:
37 correlation with leukotriene B4 generation and role in HIV-1 infection. *J Immunol*
38 2009; 182: 4025-4035.
- 39
40 37. McMahon JP, Wheat J, Sobel ME, et al. Murine laminin binds to *Histoplasma*
41 *capsulatum*. A possible mechanism of dissemination. *J Clin Invest* 1995; 96: 1010-
42 1017.
- 43
44 38. Mendes-Giannini MJ, Taylor ML, Bouchara JB, et al. Pathogenesis II: Fungal
45 responses to host responses: interaction of host cells with fungi. *Med Mycol* 2000; 38:
46 113-123.
- 47
48 39. Taylor ML, Duarte-Escalante E, Pérez A, et al. 2004. *Histoplasma capsulatum* yeast
49 cells attach and agglutinate human erythrocytes. *Med Mycol* 2004; 42: 287-292.
50
51
52
53
54
55
56



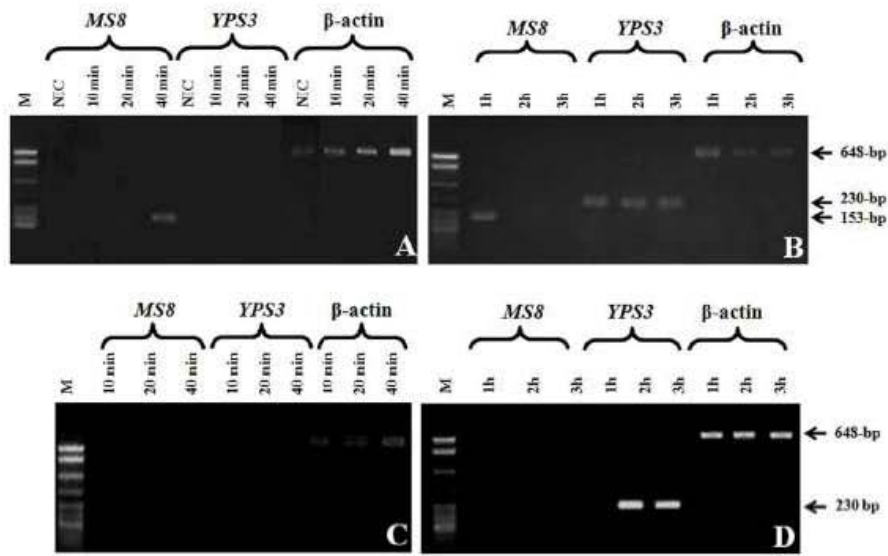
H. capsulatum yeast-like cells in the NALT of bats and mice after infection with mycelial propagules. (A) In bat NALT at 2 h, PAS staining; (B) in mouse NALT at 3 h, H&E staining. Arrows indicate yeast-like cells. Bars = 10 μ m.

199x80mm (300 x 300 DPI)



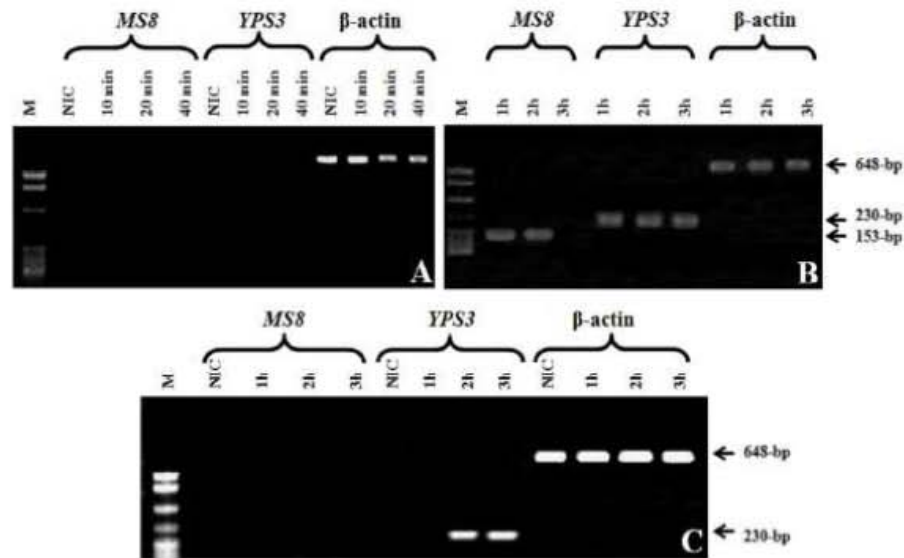
H. capsulatum yeast-like cells in the NM and CLN of bats and mice at 3 h post-infection with mycelial propagules. (A) In bat NM; (B) in mouse NM; (C) within bat CLN phagocytes; (D) within mouse CLN paracortical DC. All tissue sections were IHC stained: the yeast-like cells were observed in red color using aminoethylcarbazole as chromogen; whereas DCs were observed in brown color using 3,3'-diaminobenzidine as chromogen. The IHC sections were counterstained with Mayer's hematoxylin. The selected NM sections did not enclose NALT tissue. Arrows indicate yeast-like cells. Bars = 20 μ m.

236x239mm (300 x 300 DPI)



Representative expression of the MS8 and YPS3 phase-specific genes in NM and CLN of infected bats at different times after infection. RT-PCR was used to identify the *H. capsulatum* phase-specific genes in each tissue sample and the resulting cDNAs were resolved on agarose gel electrophoresis (details are provided in the Materials and Methods section). Gel electrophoresis of bats NM: (A) from 10 to 40 min; (B) from 1 to 3 h. Gel electrophoresis of bats CLN: (C) from 10 to 40 min; (D) from 1 to 3 h. M: molecular marker (123-bp DNA ladder); NIC: Non-infected control. NM or CLN β -actin cDNAs were used as an internal control for RT-PCR assays. Arrows indicate the amplified products of each RT-PCR reaction corresponding to the cDNA for the MS8 (153-bp), YPS3 (230-bp), and β -actin (648-bp) genes.

160x99mm (300 x 300 DPI)



Representative expression of the MS8 and YPS3 phase-specific genes in NM and CLN of infected mice at different times after infection. RT-PCR was used to identify the *H. capsulatum* phase-specific genes in each tissue sample and the resulting cDNAs were resolved on agarose gel electrophoresis (details are provided in the Materials and Methods section). Gel electrophoresis of mice NM: (A) from 10 to 40 min; (B) from 1 to 3 h. Gel electrophoresis of mice CLN: (C) from 1 to 3 h post-infection. M: molecular marker (123-bp DNA ladder); NIC: Non-infected control. NM or CLN β -actin cDNAs were used as an internal control for RT-PCR assays. Arrows indicate the amplified products of each RT-PCR reaction corresponding to the cDNA for the MS8 (153-bp), YPS3 (230-bp), and β -actin (648-bp) genes.

160x99mm (300 x 300 DPI)

CAPÍTULO 5

CAPÍTULO 5

Artículo original enviado

Sahaza JH, Suárez-Alvarez R, Estrada-Bárceñas DA, Pérez-Torres A, Taylor ML. Profile of cytokines and granulomas development in the lungs of BALB/c mice after *Histoplasma capsulatum* intra-nasal infection with mycelial propagules. *Comp Immunol Microbiol Infect Dis*.

Profile of cytokines and granulomas development in the lungs of BALB/c mice after *Histoplasma capsulatum* intra-nasal infection with mycelial propagules.

Jorge Humberto Sahaza^{a,b,◇,§}, Roberto Suárez-Alvarez,^{c,◇} Daniel Alfonso Estrada-Bárceñas^{a,d}, Armando Pérez-Torres^{e,§}, Maria Lucia Taylor^{a,§,*}

^a*Laboratorio de Inmunología de Hongos, Unidad de Micología, Departamento de Microbiología y Parasitología, Facultad de Medicina, Universidad Nacional Autónoma de México (UNAM), México DF, 04510, Mexico*

^b*Unidad de Micología Médica y Experimental, Corporación para Investigaciones Biológicas, Medellín, Colombia*

^c*Departamento Micología, INEI ANLIS “Dr. Carlos G. Malbrán”, Buenos Aires, Argentina*

^d*Colección Nacional de Cultivos Microbianos, Centro de Investigación y de Estudios Avanzados, Instituto Politécnico Nacional, México DF, 07360, Mexico*

^e*Laboratorio de Filogenia del Sistema Inmune de Piel y Mucosas, Departamento de Biología Celular y Tisular, Facultad de Medicina, UNAM, México DF, 04510, Mexico*

*Corresponding author. Tel/Fax: +52 55 5623 2462.

E-mail address: emello@unam.mx (M. L. Taylor).

◇These authors contributed equally to this article.

§These authors participated in the design and supervision of this article.

ABSTRACT

Few data are available concerning the host pulmonary response to the dimorphic fungus *Histoplasma capsulatum* after the earliest contact with infective mycelial propagules (M-phase). To address this problem, we report the profile of cytokines detected by the MagPix system in lung homogenates from mice that were intra-nasally infected with the M-phase of two virulent *H. capsulatum* strains EH-46 from Mexico and G-217B from the USA. Cytokines that are primarily involved in the innate response, such as IL-1 β and TNF- α , show increase in their concentrations of up to 16- and 26-fold compared with the control group at 14 days and 6 hours post-infection with the EH-46 and G-217B strains, respectively. Among the cytokines associated to the innate-adaptive interface, the highest levels of IL-6 and IL-17 were found on the 14th day in lung homogenates of EH-46 infected mice. The levels of IL-22 were variable in lung homogenates at all assayed post-infection times for both strains studied, while an early increase in IL-23 levels detected between 12 and 24 hours, was only found in EH-46 infected mice. Regarding IL-12, IFN- γ , IL-4, and IL-10 cytokines which are primarily involved in the adaptive response, the greatest increases were

associated with EH-46 infected mice. Histological panoramic view of mice lungs revealed, only in the EH-46 infected mice, evidence of incipient granulomas at the 14th day and numerous well developed granulomas distributed in several lung-lobes at the 21st day after infection. Thus, mice lung defense against *H. capsulatum* mediated by cytokine and inflammatory responses depends on the fungal strain used and its morphological plasticity during the first step of the infection with M-phase.

Keywords: Cytokines; *H. capsulatum*; mycelial propagules; intra-nasal infection

1. Introduction

Histoplasma capsulatum causes the most important systemic mycosis in the world. Both the severity of the disease and its clinical spectrum depend on the immunological status of the host, the inoculum size, and the virulence of the fungal isolate. In most patients, the infection is self-limiting. In natural conditions, aerosolized infective propagules of the mycelial morphotype (M-phase) from this dimorphic fungus can produce a respiratory infection when inhaled by humans and other mammals. In the host environment, *H. capsulatum* changes to its parasitic and virulent yeast morphotype (Y-phase), which is found preferentially within host phagocytes [1,2].

H. capsulatum has evolved to primarily attack the lungs. There are few studies that have used the inhalation route and M-phase propagules to simulate a natural infection for the development of experimental histoplasmosis. The major events of the inflammatory mechanisms associated to the immune response against M-phase propagules are unknown, especially during the initiation of the fungal dimorphic transition in the infected host; instead, host interaction with the Y-phase has been more thoroughly studied.

The innate response to histoplasmosis can be mediated by cellular players, such as neutrophils, macrophages, dendritic cells and natural killer cells [3-9]. In contrast, the host molecules of the innate response are less studied in histoplasmosis. Innate mechanisms can destroy *H. capsulatum* or limit its infection blocking disease development [10-12]. The host immune response is primarily displayed against the Y-phase, because the dimorphic transition from the infective M-phase to the parasitic Y-phase takes place in the first hours of the host-pathogen interaction. This transition could occur in the mucosa of the upper and lower respiratory tract, including the nasal- and bronchiolar-associated lymphoid tissues as has been suggested by Sahaza et al. [13]. The cellular immune response, mediated by T cells and their subsets, activates the major host defense mechanisms in response to the Y-phase, which remains throughout the entire course of the adaptive immune response [5,14].

The infective propagules of the M-phase (conidia and hyphal fragments) of *H. capsulatum* has been rarely employed in either *in vivo* or *in vitro* assays to study the first step of the host defense mechanisms against this pathogen [15,16]. Due to the few data available on this subject, our laboratory has developed a model of pulmonary disease in BALB/c mice using M-phase propagules and the natural route of fungal infection (intra-nasal), which mimics the course of pulmonary

histoplasmosis in humans, to characterize the major host events associated to the course of the immune response to the initial inoculum with M-phase that is able to induce a self-limiting infection.

The major aim of the present study was to assess, over four weeks, the profiles of cytokines production and granuloma development in the lung of mice after intra-nasal fungal challenge with *H. capsulatum* infective M-phase propagules.

2. Materials and methods

2.1. *Histoplasma capsulatum* inocula

Two virulent fungal strains were used: EH-46 (Mexico) from the *H. capsulatum* Culture Collection of the Fungal Immunology Laboratory of the Department of Microbiology and Parasitology, School of Medicine-UNAM (www.histoplas-mex.unam.mx), which is registered in the database of the World Data Centre for Microorganisms under the number [LIH-UNAM WDCM817](#), and G-217B (USA) from the American Type Culture Collection (ATCC-26032). EH-46 and G-217B strains were previously phylogenetically classified as LAm A and NAM 2, respectively, as reported by Kasuga et al. [17].

The strains were cultured for 3-4 weeks at 28 °C in potato-dextrose-agar (PDA, Bioxón, Becton Dickinson, Mexico City, MX). The M-phase of each strain was harvested in saline solution (SS) and centrifuged at 800 x g-10 min at 4 °C to remove large mycelium fragments and macroconidia. Microconidia and small hyphal fragments were suspended in SS and counted in a hemocytometer, and the inoculum of each strain was adjusted to 3×10^6 infective propagules/mL. The inoculum viability was tested with trypan blue (0.05%) and cultured in PDA at 28 °C. Biosafety standards regarding the secure manipulation of *H. capsulatum*, which require a Level 3 Biosecurity Laboratory, were in place in the Mycology Unit, Department of Microbiology-Parasitology, School of Medicine, UNAM.

2.2. Animal infection

Isogenic male BALB/c mice (6 weeks-old) were kept under optimal environmental conditions and fed *ad libitum* with mouse chow (Purina de México, Mexico City, MX) and acidified distilled water.

The mice were intra-nasally inoculated with SS-suspended *H. capsulatum* inoculum ($3 \times 10^6/40 \mu\text{L}$), after intramuscular injection with a mix of ketamine-xylazine (v/v) to facilitate the intra-nasal fungal infection process. The anesthetized animals were held in the supine position, and 40 μL of the fungal inoculum was placed on the nares to encourage animal instillation. Six mice, per each *H. capsulatum* strain, were processed at 0, 1, 3, 6, 12, 24, and 48 hours as well as at 5, 7, 14, 21, and

28 days per time point post-infection. Non-infected control mice were inoculated similarly with 40 μ L of SS for each time point tested. A total of 216 animals, including infected and control mice, were processed at each time point post-infection, and they were euthanized according to protocols approved by the Ethics Committee of the School of Medicine, UNAM (project number 049-2011). The recommendations of the Animal Care and Use Committee of the UNAM and the Mexican Official Guide (NOM 062-ZOO-1999), in agreement with the international rules of the Guide for the Care and Use of Laboratory Animal National Research Council, were strictly followed. Lungs from each animal tested, at different time points post-infection, were aseptically removed. Moreover, the lungs of each group of infected animals and non-infected animals (controls) were destined to different procedures, cytokine determinations and histological studies. For histopathological procedures, mouse lungs were processed after intra-cardiac and intra-tracheal perfusion with 10% buffered formalin.

2.3. Cytokine determination

For this procedure, lungs were homogenized in 1 mL SS using an Ultra-Turrax T8 (IKA®Works, Inc., Wilmington, NC, USA). Each homogenate was centrifuged at 14 000 $\times g$ -15 min at 4 °C and, the supernatant, was harvested. Then, 0.2 mL of protease inhibitor cocktail (cOmplete mini protease inhibitor tablets, Roche Applied Science, Mannheim, DE) was added. The proteins were normalized and, subsequently, each homogenate was frozen at -196 °C until required.

Cytokines in lung homogenate supernatants were quantified using a MagPix magnetic beads platform (Luminex xMAP, Austin, TX, USA). Panels containing magnetic beads covered with fluorescent dyed conjugated to a monoclonal antibody specific for each target cytokine were used to quantify IL-1 β , IL-4, IL-6, IL-10, IL-12p40, IL-12p70, IL-17, IL-22, IL-23, TNF- α , and IFN- γ cytokines according to the manufacturer's instructions (Milliplex MAG, Millipore, Billerica, MA, USA).

2.4. Histological procedure

Formalin-perfused lungs, of infected and non-infected mice, were paraffin-embedded, and tissue sections (3 μ m) were processed for histological observations using periodic acid Schiff (PAS) staining. Transverse sections, which provided an overview of several lobes of the mice lung, were semi-microscopically photographed using a Canon EOS T5i adapted to a Stand-Multiphot with a macro-lens HL-1X.

2.4. Statistics

All data were statistically analyzed using STATISTICA version 6.1 (StatSoft, www.statsoft.com). Analyses were performed using the Kruskal-Wallis test with multiple comparisons of mean ranks for all mice groups studied. Differences in cytokines production

between infected and non-infected animals (controls) were used for the statistical comparisons and, P values ≤ 0.05 were considered significant.

3. Results

Overall, cytokine measurements in lung homogenate supernatants revealed substantial differences between EH-46 and G-217B *H. capsulatum* strains used for the infection assays. The lowest detection limits of cytokines were 32 pg/mL for IL-23 and 3.2 pg/mL for the others cytokines tested by the MagPix magnetic beads system.

3.1. Cytokine determination in mice lung homogenate supernatants at different time points post-infection with *M-phase* fungal propagules

3.1.1 IL-1 β and TNF- α profiles

IL-1 β production, at the studied time points after intra-nasal infection of mice with the EH-46 strain showed a progressive increase, with high levels from 6 hours up to 21 days. The highest concentration of IL-1 β (16-fold greater than the control group) was reached at the 14th day post-infection ($P \leq 0.01$), while the G-217B strain did not show significant concentrations at any time point post-infection (Fig. 1A).

The TNF- α levels were lower in mice infected with the EH-46 strain compared with those infected with the G-217B strain until 12 hours post-infection. After this time, from 24 hours to 14 days post-infection, TNF- α levels induced by the EH-46 strain were continuously higher than those detected in mice infected with the G-217B strain. In contrast, for the G-217B infected mice, the production of TNF- α was high, with significant increases of 18- and 26-fold at 3 hours ($P \leq 0.05$) and 6 hours ($P \leq 0.01$) post-infection, respectively, when compared with the control group. After 24 hours post-infection, TNF- α levels did not show significant differences. Both strains caused the decrease of TNF- α in mice after 21 days post-infection (Fig. 1B).

3.1.2. IL-6, IL-17, IL-22, and IL-23 profiles

An increase in the levels of IL-6, to 40- and 49-fold greater than the control group was detected in mice infected with the EH-46 strain at 3 hours ($P \leq 0.01$) and 14 days ($P \leq 0.01$) post-infection, respectively. Whereas, in mice infected with the G-217B strain, IL-6 showed an increase of 35-fold compared with the control group at only 6 hours post-infection ($P \leq 0.01$) (Fig. 2A).

Regarding the IL-17 levels (Fig. 2B), only mice infected with the EH-46 strain increased the production of this cytokine, slightly between 12 hours to 7 days post-infection, and considerably at 14th days post-infection (42-fold greater than the control group).

In mice infected with the EH-46 strain, the production of IL-22 was variable throughout the post-infection period assayed. However, significant differences ($P \leq 0.01$) in IL-22 levels were found from 6 to 12 hours and from 48 hours to 28 days post-infection times. In general, the increase in the levels of this cytokine was not more than 5-fold greater than the levels obtained for the control group (Fig. 2C). Mice infected with the G-217B strain produced also a variable level of this cytokine during the assayed post-infection time; however, the production of this cytokine in mice infected with the G-217B strain was always lower than that detected in mice infected with the EH-46 strain. At 28 days post-infection the levels of IL-22 production remained detectable, for both strains used, and were significant for mice infected with the EH-46 strain ($P \leq 0.01$) (Fig. 2C).

A significant increase of IL-23 between 12 and 24 hours ($P \leq 0.05$) post-infection was detected only in mice infected with the EH-46 strain, corresponding to 154- and 109-fold increases compared with the control group, respectively (Fig. 2D).

3.1.3. IL-12 and IFN- γ profiles

IL-12, represented by the production of the peptides IL-12p40 and IL-12p70, showed a sustained increase throughout the post-infection time points in mice infected with the EH-46 strain. High levels IL-12 peptides were noted from 6 hours up to 21 days post-infection, with significant P values at several points in their profiles (Fig. 3A,B). The maximum production of IL-12 peptides occurred at 24 hours and 7 days post-infection; at these time points, both IL12-p40 and IL-12p70 were approximately 15-fold increased compared with the control group. In contrast, very low levels of both IL-12 peptides were detected in mice infected with the G-217B strain, with IL-12 p40 and IL-12p70 increasing only 5- and 2-fold compared with the control group, respectively (Fig. 3A,B). Decreases of IL12-p40 level, after 14 and 21 days post-infection, were detected in mice infected with G-217B and EH-46 strains, respectively.

Regarding IFN- γ production, only mice infected with the EH-46 strain showed a significant level ($P \leq 0.01$) of IFN- γ with a concentration 200-fold greater than that of the control group at the 14th day post-infection. The mice infected with the G-217B strain never showed significant levels of IFN- γ , which was always lesser than 2-fold with respect to the control group, at all time points post-infection assayed (Fig. 3C).

3.1.4. IL-4 and IL-10 profiles

IL-4 levels detected in mice infected with the EH-46 strain (Fig. 4a), showed significant differences at 24 hours, 5 and 7 days post-infection (P values ≤ 0.01). Besides, significant increase in levels of IL-10 were only detected in mice infected with the EH-46 strain (Fig. 4B), from 6 to 24 hours post-infection, with 9- to 11-fold more than in the control group (P values ≤ 0.01), and at 5, 7 and 21 days post-infection, with 16-, 20-, and 15-fold more than the control group (P values ≤ 0.01), respectively. Whereas, in mice infected with the G-217B strain neither IL-4 nor IL-10 reached significant levels at any post-infection time assayed.

3.2. Histopathological observations

Panoramic overviews of lung sections of infected mice showed incipient granulomas at the 14th day after EH-46 infection (Fig. 5A) and numerous well-developed granulomas distributed in several lung-lobes at the 21st day after infection (Fig. 5B), while granulomas decreased in number at 28th day (Fig. 5C). In contrast, G-217B infected mice showed a diffuse peribronchiolar and alveolar inflammatory infiltration at the 14th, 21st, and 28th days post-infection (Fig. 5D,E,F). As expected, no tissue responses were observed in non-infected control mice (Fig. 5G,H,I).

4. Discussion

In the present study, in a model of male BALB/c immunocompetent mice, we mimic a natural pulmonary histoplasmosis infection using the intra-nasal route and infective M-phase propagules of two different virulent strains of *H. capsulatum*: EH-46 (LAm A) and G-217B (NAm 2). Fungal infective propagules are able to cross several host barriers and can endure different types of stresses that are involved in *H. capsulatum* dimorphism and dissemination before the arrival of infective propagules to the host lungs [13]. We evaluated cytokine productions in lung homogenates of the host at different time points post-infection, such that both innate and adaptive immune defense mechanisms are engaged throughout the assayed period.

Our results emphasize that the LAm A EH-46 strain from Mexico induces a higher cytokines response than the NA 2 G-217B strain from the USA with regard to their production, appearance and persistence in the lung tissue. Differences in the pathogenicity process and animal mortality associated with *H. capsulatum* strains from North America (USA) and Latin America (Brazil), have been documented by Durkin et al. [18]. Recently, Schoffelen et al. [19] reported distinct cytokine patterns in human cultured peripheral blood mononuclear cells infected with different heat-killed cryptococcal species, emphasizing that *Cryptococcus gattii* induces a marked inflammatory cytokine response. Both of the above-mentioned reports support our findings with regard to the differences detected in the cytokines response using either the LAm A or the NA 2 *H. capsulatum* strains.

Another interesting aspect of our findings is the role of the infective fungal morphotype associated with cytokine profiles in the early host lung response to the infection. It is likely that, when the host response is first induced by the infective M-morphotype, the outcome of the *H. capsulatum* infection varies over time and depends on the host cells involved, the cytokine profiles, the type of fungal strain, and the changes in the fungal surface components associated with the *in vivo* fungal dimorphism. Obviously, under natural conditions, the first line of the host defense against *H. capsulatum* involves the production of cytokines that are initially stimulated by the pathogen-associated molecular patterns (PAMPs) of the infective M-morphotype, which remains as soon as the fungal transition to the Y-morphotype occurs. The time and course of the infection depend on how long the pathogen takes to complete the morphotype transition [13].

Due to their pleiotropic activities during the host immune response, we categorized the studied cytokines according to their closest association with the innate (IL-1 β and TNF- α), innate-adaptive (IL-6, IL-17, IL-22, and IL-23), and adaptive (IL-12, IFN- γ , IL-4 and IL-10) responses.

Regarding the IL-1 β and TNF- α profiles, and in compliance with their possible involvement with the innate immune response and with the innate-adaptive interface response, our data revealed that both cytokines were produced continuously from 24 hours to 21 days, primarily in mice infected with the EH-46 strain. Both cytokines produced during this time interval, might be involved in the development of lung granulomas as we observed in our histopathological findings and in accordance with prior reports, suggesting a role for TNF- α in the formation and maintenance of granulomas in *H. capsulatum* infected mice [20-22].

Although the IL-6, IL-17, and IL-23 cytokines are considered to be primarily engaged in the innate-adaptive interface response to different pathogens, they have rarely been studied in *H. capsulatum* experimental infection [23-25]. Overall, these cytokines play an important role in controlling the progression of the clinical course of histoplasmosis [23-25]. Our results with respect to the profiles of these cytokines along the experimental course of mice infected with M-phase propagules of EH-46 *H. capsulatum* strain emphasize that IL-6 and IL-17 are at their highest levels at the 14th day post-infection, while high levels of IL-23 are observed from the beginning of infection. Interestingly, IL-23 was one of the assayed cytokines that reached the highest level of production compared with the control group. The implication of this finding, in the histoplasmosis infection course needs to be further explored. With respect to the IL-23/IL-17-axis over the course of our experiments, the increase in IL-23 prior to the enhancement of IL-17 is a new event that must be considered in further studies examining the course of histoplasmosis infection with M-phase propagules and cytokines production.

IL-17 levels were increased, considerably, at the 14th day post-infection only in mice infected with the EH-46 strain, which is in agreement with the *Mycobacterium* infection process, in which IL-17 is necessary for infection control and granuloma formation in the lungs [26,27]. However, an early response of IL-17 during the first week of the mice infection with *H. capsulatum* yeast cells has been reported by Deepe and Gibbons [23].

Although Th17 cells are the major CD4⁺ T cell population responsible for IL-17 production, this cytokine is considered one of the most important cytokines engaged in the interface of the innate-adaptive response, because it is produced by different cell populations of the innate and adaptive immune systems [27,28].

IL-22 has been reported to be important to protect mucosa epithelia and to repair lung epithelia damaged by pathogens [28,29]. IL-22 can be produced by several types of cells [28], and its participation via the IL-23/IL-22-axis is important for inhibition of fungal growth in infected hosts [30]. Although, in histoplasmosis infection the IL-22 was never previously considered, the present results indicate, for the first time, that this cytokine is present in mice lung homogenates at all post-infection time tested. In our point of view, the persistence of this cytokine throughout the *H.*

capsulatum infection process using two different strains may be associated to any type of event triggered by the host response, either in the defense or tissue repair processes.

Among Th1 pro-inflammatory cytokines, IL-12 is necessary to generate a protective immunity against *H. capsulatum* infection due to its role in the synthesis of IFN- γ by CD4⁺ T and NK cells [31]. As for other cytokines, their increase during the infection process could depend on the type of fungal strain used, because the levels of IL-12 production varied in the lung homogenates of EH-46 and G-217B infected mice, however, in contrast to other cytokines its level remains detectable up to 28 days post-infection times.

IFN- γ was the cytokine that presented the highest levels, showing up to a 200-fold increase on the 14th day, revealing its importance in controlling *H. capsulatum* infection. Obviously, this is in accordance with its role in murine histoplasmosis, because IFN- γ is the most potent activator of phagocytes at the site of infection and it can inhibit intracellular growth of *H. capsulatum* [7,21,22].

Concerning the Th2 anti-inflammatory cytokines evaluated in the present study, IL-4 and IL-10 are most likely involved in the regulation of the pro-inflammatory response according the type of *H. capsulatum* strain used. It is feasible that modulation of the Th1/Th2 balance could be associated with the more intense inflammatory response developed by the EH-46 strain.

With respect to the development of granulomas under the experimental conditions in the current study, it was found that both *H. capsulatum* strains also differ in the number, size and distribution of pulmonary granulomas. Granulomas in processing were primarily observed in the lungs of EH-46 infected mice from the 14th to 21st day post-infection, and at 28th day the semi-microscopic photography showed a decrease in the number of granulomas, suggesting the beginning of the infection self-limiting process. Interestingly, these data correlate with the highest levels of IL-1 β , IL-6, IL-17, and IFN- γ detected on the 14th day post-infection using the EH-46 strain. This finding is in agreement with reports described in experimental tuberculosis studies, which have determined that IL-17 and IFN- γ are necessary during the granulomas organization [27].

5. Conclusions

Host recognition mechanisms mediated by the immune response against *H. capsulatum* depend on different PAMPs exposed on the surface of the fungus, firstly on the infective M-phase and, subsequently, on the parasitic Y-phase derived from the dimorphic process that must be triggered during the early time points of infection. Thus, the production of cytokines necessary to control *Histoplasma* infection in susceptible hosts must be modulated by the high morphological plasticity of this dimorphic fungal pathogen.

Conflict of Interest

The authors declare that there is no potential, personal, academic, financial, or intellectual conflict of interest among them.

Acknowledgments

This paper constitutes partial fulfillment of the requirements of the Graduate Program in Biological Science of the UNAM. Jorge Humberto Sahaza thanks the Graduate Program in Biological Science of the UNAM and the scholarship of the *Consejo Nacional de Ciencia y Tecnología-México* (CONACyT-México, Reference Number, 245151). This research was financially supported by a grant provided by CONACyT-México, Reference Number, 166052. The authors thank Dr. Felipe Vadillo-Ortega and Dr. Noemi Meraz-Cruz of the Unidad de Vinculación de la Facultad de Medicina en el Instituto Nacional de Medicina Genómica, UNAM, all the facilities for allowing use of the MagPix platform. The authors thank Ingrid Mascher for editorial assistance.

References

- [1]Tewari R, Wheat LJ, Ajello L. Agents of histoplasmosis. In: Ajello L, Hay RJ, eds. Topley & Wilson's. Microbiology and Microbial Infections. Medical mycology. New York: Arnold & Oxford University Press Inc., 1998:373-93.
- [2]Taylor ML, Reyes-Montes MR, Chávez-Tapia CB, Curiel-Quesada E, Duarte-Escalante E, Rodríguez-Arellanes G, et al. Ecology and molecular epidemiology findings of *Histoplasma capsulatum*, in Mexico. In: Benedik M, ed. Research Advances in Microbiology. Kerala: Global Research Network, 2000:29-35.
- [3]Brummer E, Kurita N, Yoshida S, Nishimura K, Miyaji M. Fungistatic activity of human neutrophils against *Histoplasma capsulatum*: correlation with phagocytosis. J Infect Dis 1991;164:158-62.
- [4]Kurita N, Terao K, Brummer E, Ito E, Nishimura K, Miyaji M. Resistance of *Histoplasma capsulatum* to killing by human neutrophils. Evasion of oxidative burst and lysosomal-fusion products. Mycopathologia 1991;115:207-13.
- [5]Newman SL, Gootee L, Gabay JE. Human neutrophil-mediated fungistasis against *Histoplasma capsulatum*. Localization of fungistatic activity to the azurophil granules. J Clin Invest 1993;92:624-31.
- [6]Newman SL, Gootee L, Gabay JE, Selsted ME. Identification of constituents of human neutrophil azurophil granules that mediate fungistasis against *Histoplasma capsulatum*. Infect Immun 2000;68:5668-72.
- [7]Zhou P, Miller G, Seder RA. Factors involved in regulating primary and secondary immunity to infection with *Histoplasma capsulatum*: TNF- α plays a critical role in maintaining secondary immunity in the absence of IFN- γ . J Immunol 1998;160:1359-68.

- [8] Patiño MM, Williams D, Ahrens J, Graybill JR. Experimental histoplasmosis in the beige mouse. *J Leukoc Biol* 1987;41:228-35.
- [9] Suchyta MR, Smith JG, Graybill JR. The role of natural killer cells in histoplasmosis. *Am Rev Respir Dis* 1988;138:578-82.
- [10] Medeiros AI, Silva CL, Malheiro A, Maffei CML, Faccioli LH. Leukotrienes are involved in leukocyte recruitment induced by live *Histoplasma capsulatum* or by the β -glucan present in their cell wall. *Br J Pharmacol* 1999;128:1529-37.
- [11] Newman SL, Bucher C, Rhodes JC, Bullock WE. Phagocytosis of *Histoplasma capsulatum* yeasts and microconidia by human cultured macrophages and alveolar macrophages. Cellular cytoskeleton requirement for attachment and ingestion. *J Clin Invest* 1990;85:223-30.
- [12] Nosanchuk JD, Gacser A. *Histoplasma capsulatum* at the host pathogen interface. *Microb Infect* 2008;10:973-7.
- [13] Sahaza JH, Pérez-Torres A, Zenteno E, Taylor ML. Usefulness of the murine model to study the immune response against *Histoplasma capsulatum* infection. *Comp Immunol Microbiol Infect Dis* 2014;37:143-52.
- [14] Schnur RA, Newman SL. The respiratory burst response to *Histoplasma capsulatum* by human neutrophils. Evidence for intracellular trapping of superoxide anion. *J Immunol* 1990;144:4765-72.
- [15] Inglis DO, Berkes CA, Hocking Murray DR, Sil A. Conidia but not yeast cells of the fungal pathogen *Histoplasma capsulatum* trigger a type I interferon innate immune response in murine macrophages. *Infect Immun* 2010;78:3871-82.
- [16] Newman SL, Lemen W, Smulian AG. Dendritic cells restrict the transformation of *Histoplasma capsulatum* conidia into yeasts. *Med Mycol* 2011;49:356-64.
- [17] Kasuga T, White TJ, Koenig G, McEwen J, Restrepo A, Castañeda E, et al. Phylogeography of the fungal pathogen *Histoplasma capsulatum*. *Mol Ecol* 2003;12:3383-401.
- [18] Durkin MM, Connolly PA, Karimi K, Wheat E, Schnizlein-Bick C, Allen SD, et al. Pathogenic differences between North American and Latin American strains of *Histoplasma capsulatum* var. *capsulatum* in experimentally infected mice. *J Clin Microbiol* 2004;42:4370-3.
- [19] Schoffelen T, Illnait-Zaragozi M-T, Joosten LAB, Netea MG, Boekhout T, Meis JF, Sprong T. *Cryptococcus gattii* induces a cytokine pattern that is distinct from other cryptococcal species. *PLoS One* 2013;8:e55579.
- [20] Smith JG, Magee DM, Williams DM, Graybill JR. Tumor necrosis factor-alpha plays a role in host defense against *Histoplasma capsulatum*. *J Infect Dis* 1990;162:1349-53.
- [21] Allendoerfer R, Deepe GS Jr. Blockade of endogenous TNF- α exacerbates primary and secondary pulmonary histoplasmosis by differential mechanisms. *J Immunol* 1998;160:6072-82.
- [22] Heninger E, Hogan LH, Karman J, Macvilay S, Hill B, Woods JP, et al. Characterization of the *Histoplasma capsulatum*-induced granuloma. *J Immunol* 2006;177:3303-13.
- [23] Deepe GS Jr, Gibbons RS. Interleukins 17 and 23 influence the host response to *Histoplasma capsulatum*. *J Infect Dis* 2009;200:142-51.
- [24] Kroetz DN, Deepe GS Jr. CCR5 dictates the equilibrium of proinflammatory IL-17+ and regulatory Foxp3+ T cells in fungal infection. *J Immunol* 2010;184:5224-31.

- [25] Wu SY, Yu JS, Liu FT, Miaw SC, Wu-Hsieh BA. Galectin-3 negatively regulates dendritic cell production of IL-23/IL-17-axis cytokines in infection by *Histoplasma capsulatum*. J Immunol. 2013;190:3427-37.
- [26] Okamoto Yoshida Y, Umemura M, Yahagi A, O'Brien RL, Ikuta K, Kishihara K, et al. Essential role of IL-17A in the formation of a mycobacterial infection-induced granuloma in the lung. J Immunol 2010;184:4414-22.
- [27] Torrado E, Cooper AM. IL-17 and Th17 cells in tuberculosis. Cytokine Growth Factor Rev 2010;21:455-62.
- [28] Zelante T, Iannitti R, De Luca A, Romani L. IL-22 in antifungal immunity. Eur J Immunol 2011;41:270-5.
- [29] Pociask DA, Scheller EV, Mandalapu S, McHugh KJ, Enelow RI, Fattman CL, et al. IL-22 is essential for lung epithelial repair following influenza infection. Am J Pathol 2013;182:1286-96.
- [30] De Luca A, Zelante T, D'Angelo C, Zagarella S, Fallarino F, Spreca A, et al. IL-22 defines a novel immune pathway of antifungal resistance. Mucosal Immunol 2010;3:361-73.
- [31] Marth T, Kelsall BL. Regulation of interleukin-12 by complement receptor 3 signaling. J Exp Med 1997;185:1987-95.

Figures

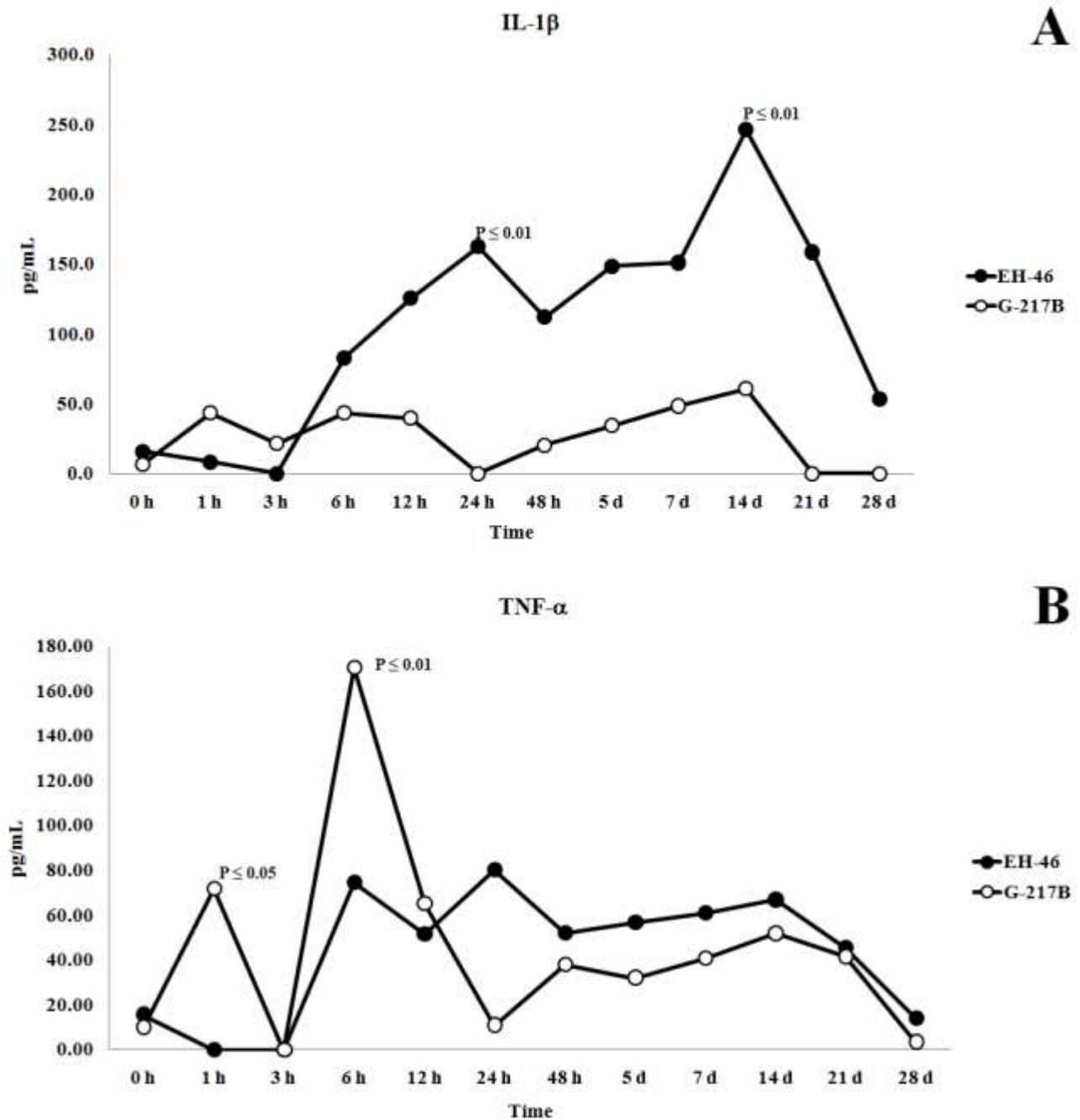


Fig. 1. IL-1 β and TNF- α profiles. Cytokine levels (pg/mL) were detected using a MagPix system in lung homogenates from mice intra-nasally infected with M-phase propagules of EH-46 or G-217B *H. capsulatum* strains. Each cytokine level represented in the figure was previously subtracted from the basal level given by MagPix readings of lung homogenates from non-infected mice (control). (A) IL-1 β and (B) TNF- α detection was performed at different time points post-infection (h= hour; d= day). Significant *P* values are presented in the figure (details are provided in the Materials and methods section).

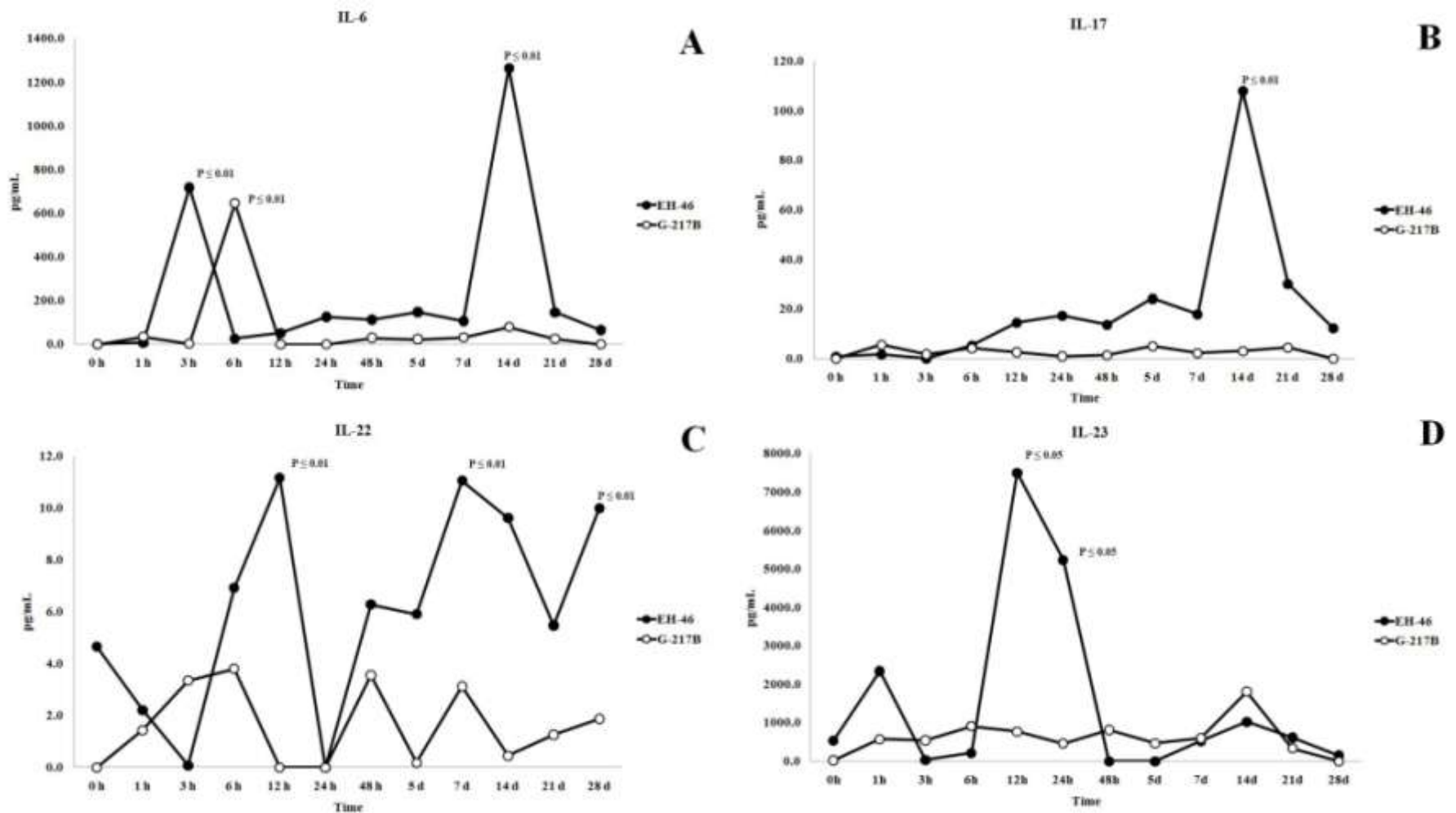


Fig. 2. IL-6, IL-17, IL-22, and IL-23 profiles. Cytokine levels (pg/mL) were detected using a MagPix system in lung homogenates from mice intranasally infected with M-phase propagules of EH-46 or G-217B *H. capsulatum* strains. Each cytokine level represented in the figure was previously subtracted from the basal level given by MagPix readings of lung homogenates from non-infected mice (control). (A) IL-6, (B) IL-17, (C) IL-22, and (D) IL-23 detection was performed at different time points post-infection (h= hour; d= day). Significant *P* values are presented in the figure (details are provided in the Materials and methods section).

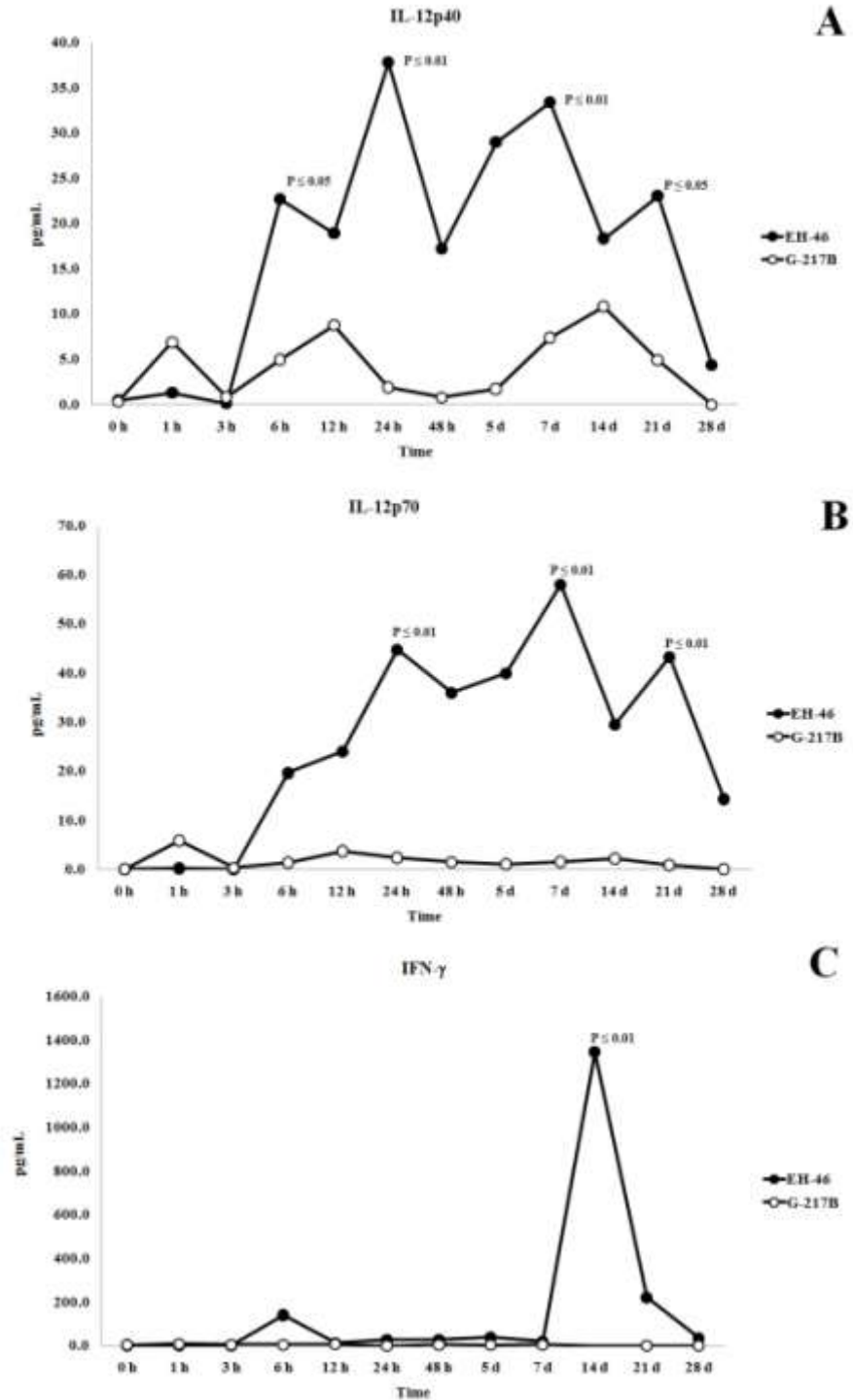


Fig. 3. IL-12p40, IL-12p70, and IFN- γ profiles. Cytokine levels (pg/mL) were detected using a MagPix system in lung homogenates from mice intra-nasally infected with M-phase propagules of EH-46 or G-217B *H. capsulatum* strains. Each cytokine level represented in the figure was previously subtracted from the basal level given by MagPix readings of lung homogenates from non-infected mice (control). (A) IL-12p40, (B) IL-12p70, and (C) IFN- γ detection was performed at different time points post-infection (h= hour; d= day). Significant *P* values are presented in the figure (details are provided in the Materials and methods section).

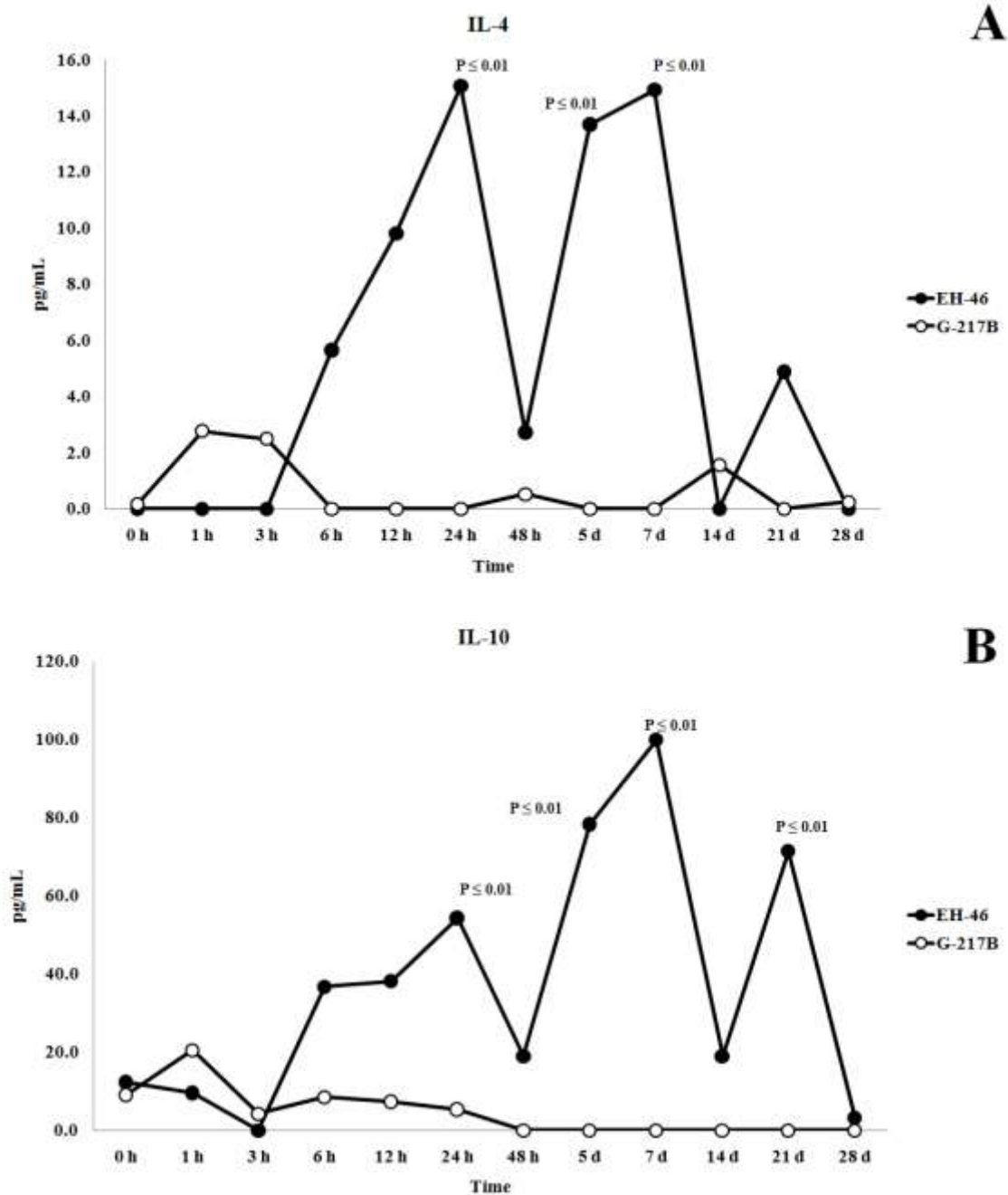


Fig. 4. IL-4, IL-10 profiles. Cytokine levels (pg/mL) were detected using a MagPix system in lung homogenates from mice intra-nasally infected with M-phase propagules of EH-46 or G-217B *H. capsulatum* strains. Each cytokine level represented in the figure was previously subtracted from the basal level given by MagPix readings of lung homogenates from non-infected mice (control). (A) IL-4 and (B) IL-10 detection was performed at different time points post-infection (h= hour; d= day). Significant *P* values are presented in the figure (details are provided in the Materials and methods section).

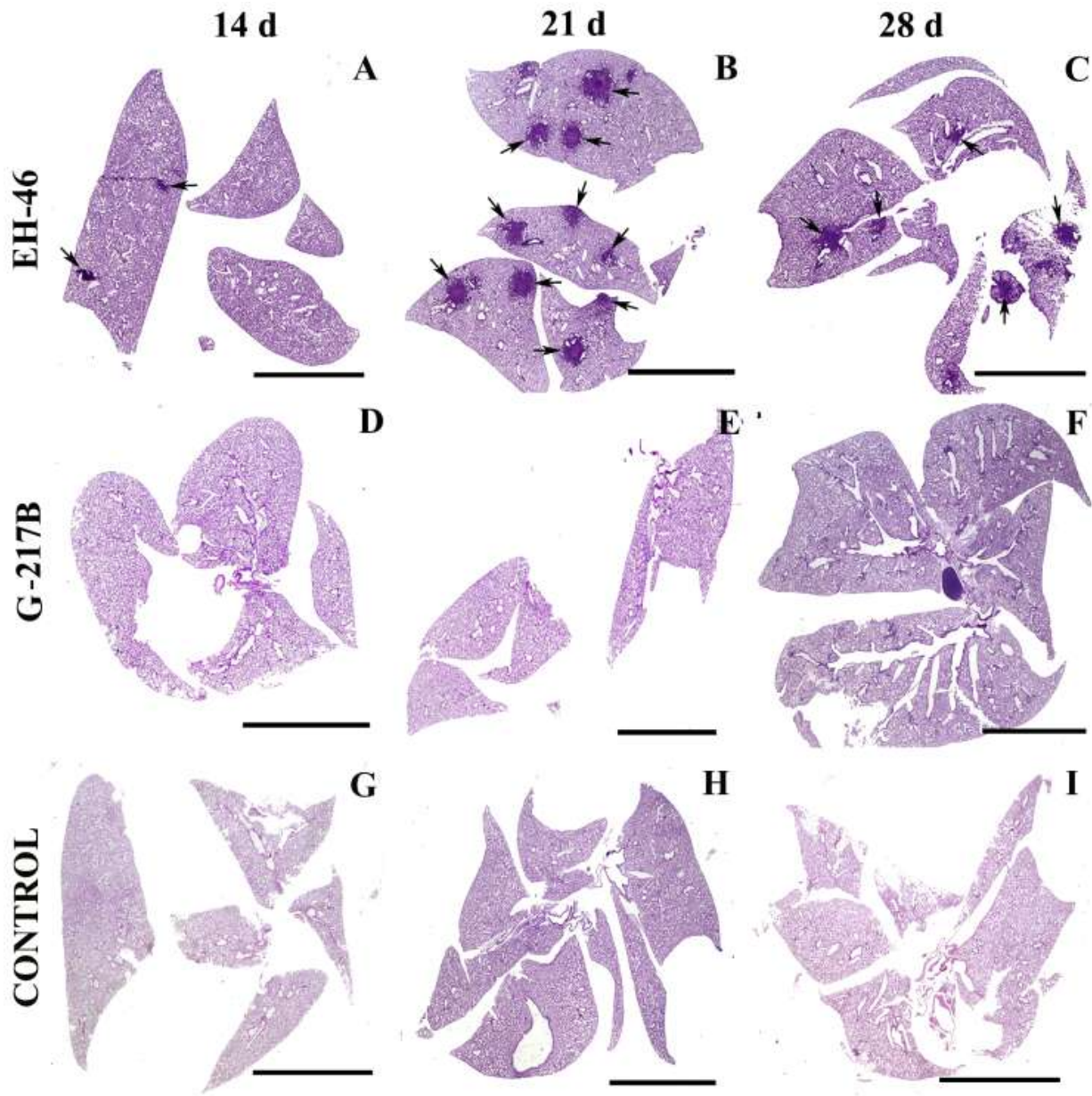


Fig. 5. Panoramic overview of mice lung sections at 14, 21 and 28 days after *H. capsulatum* infection. (A, B, C) EH-46 strain; (D, E, F) G-217B strain; (G, H, I) non-infected mice (control). Arrows show: (A) incipient granulomas at the 14th day post-infection, (B) well-developed granulomas distributed in all lung-lobes at the 21st day, and (C) granulomas in remission at 28th day after infection. PAS staining, Bars = 0.5 mm, (d= day).

CAPÍTULO 6

CAPÍTULO 6

Otros resultados obtenidos aun no publicados

Siguiendo el mismo protocolo descrito por Sahaza et al. (2014b), se utilizó el morfotipo-L de las cepas, EH-46 y G-217B, para realizar un análisis similar y comparar los resultados de ambos morfotipos. De modo similar a la utilización del morfotipo-M, las mediciones de citoquinas en los sobrenadantes de homogeneizado de pulmón infectados con el morfotipo-L revelaron diferencias sustanciales entre las cepas de *H. capsulatum* utilizadas. Igualmente se comparó la respuesta inflamatoria (desarrollo de granulomas).

Determinación de citoquinas en sobrenadantes de homogeneizados de pulmón de ratones BALB/c obtenidos a diferentes tiempos después de la infección intranasal con propágulos fúngicos del morfotipo-L

Perfiles de IL-1 β y TNF- α

En los tiempos estudiados post- infección intranasal de ratones con la cepa EH-46, la producción de IL-1 β mostró variaciones. Se detectaron niveles altos de IL-1 β desde 1 h hasta 7 d. La mayor concentración de IL-1 β (14 veces más que el grupo testigo) se alcanzó en el séptimo día después de la infección ($P \leq 0.01$), mientras que la cepa G-217B no generó en los ratones concentraciones significativas de IL-1 β en cualquier tiempo posterior a la infección (Fig. 1A).

Los niveles de TNF- α para los ratones infectados con la cepa EH-46 presentaron valores bajos a excepción de las 6 h donde se detectó un incremento de hasta 25 veces más ($P \leq 0.01$) que el testigo de esta citoquina, mientras que en los ratones infectados con la cepa G-217B los niveles de TNF- α fueron bajos durante todos los tiempos post-infección (Fig. 1B).

Perfiles de IL-6, IL-17, IL-22 e IL-23

Un aumento significativo en los niveles de IL-6, 28 veces más que el grupo testigo ($P \leq 0.01$), fue detectado en ratones infectados con la cepa EH-46 a las 3 h post-infección. Por el contrario, en los ratones infectados con la cepa G-217B, la IL-6 no reveló valores significativos en comparación con el grupo testigo (Fig. 2A).

Los niveles de IL-17 mostraron una cinética similar para ambas cepas estudiadas, sin embargo llama la atención los niveles iniciales, tiempo 0 y 1 h, para los animales infectados con la cepa EH-46, los cuales fueron 8 y 6 veces más altos que el grupo testigo, respectivamente. En general, los niveles de

IL-17 para la cepa EH-46 fueron considerablemente más altos a los encontrados para los ratones infectados con la cepa G-217B (Fig. 2B).

En los ratones infectados con la cepa EH-46, la producción de IL-22 varió a lo largo de los tiempos post-infección. Sin embargo, destacan el incremento de 16 y 11 veces en relación con el grupo testigo a las 3 h y 5 d post-infección, respectivamente ($P \leq 0.01$). No se encontraron diferencias significativas en niveles de IL-22 en los ratones infectados con la cepa G-217B (Fig. 2C).

IL-23 presentó principalmente un aumento importante en sus niveles en el día 21 post-infección (23 veces más que el grupo testigo) en los animales inoculados con la cepa EH-46. Sin embargo, esta citoquina fue una de las pocas que desarrolló niveles altos en los animales infectados con la cepa G-217B, detectándose a las 24 h y 21 d post-infección valores de 34 y 21 veces más altos que el grupo testigo, respectivamente (Fig. 2D).

Perfiles de IL-12 e IFN- γ

IL-12 está representada por la cuantificación de los péptidos IL-12p40 e IL-12p70. En ratones infectados con la cepa EH-46, IL-12p40 mostró un rápido aumento en sus niveles durante la primera hora después de la infección (29 veces más que el grupo testigo) que decayó luego de 24 h post-infección, volviendo a incrementarse significativamente entre los 5 y 7 d post-infección (15 veces más que el grupo testigo, $P \leq 0.01$). Con la cepa G-217B no se detectaron concentraciones significativas en los homogeneizados de pulmón en cualquier tiempo posterior a la infección de los ratones (Fig. 3A). Con relación a IL-12p70, en los animales infectados con la cepa EH-46, su producción máxima fue a las 24 h y 5 d post-infección, siendo sus niveles de 14 y 10 veces más que el grupo testigo ($P \leq 0.01$), respectivamente. En contraste, niveles bajos de IL-12p70 fueron detectados en ratones infectados con la cepa G-217B, sólo aumentando 7 y 8 veces más que el grupo testigo a las 6 y 12 h post-infección ($P \leq 0.01$), respectivamente (Fig. 3B).

La producción de IFN- γ sólo fue detectada en los ratones infectados con la cepa EH-46 que mostraron niveles significativos ($P \leq 0.01$) de IFN- γ con incremento de sus valores 6 y 11 veces más que el grupo testigo a las 48 h y 7 d post-infección. Los ratones infectados con la cepa G-217B nunca mostraron niveles significativos de IFN- γ en todos los tiempos post-infección ensayados (Fig. 3C).

Perfiles de IL-4 e IL-10

IL-4 presentó niveles detectables sólo en ratones infectados con la cepa EH-46, que mostraron diferencias significativas en los tiempos 0 y 1 h así como en el día 5 (3 veces más que el grupo testigo) post-infección (Fig. 4A).

Aumentos significativos en los niveles de IL-10 se detectó en ratones infectados con la cepa EH-46 a las 24 h (24 veces más que el grupo testigo) y a los 5 d después de la infección (10 veces más que el grupo testigo) (Fig. 4B).

En ratones infectados con la cepa G-217B ni IL-4 ni IL-10 alcanzaron niveles significativos en cualquier tiempo post-infección (Fig. 4A y 4B).

Resultados de la evaluación del curso de la respuesta inflamatoria en pulmón de ratones BALB/c obtenidos a diferentes tiempos después de la infección intranasal con propágulos fúngicos del morfotipo-L

La observación microscópica a bajo aumento de cortes de pulmón de ratones infectados con el morfotipo-L de *H. capsulatum* a los 14, 21 y 28 d, reveló al utilizar la cepa EH-46: 1) un infiltrado celular difuso en el día 14 post-infección (Fig. 5A); 2) numerosas reacciones inflamatorias sugiriendo granulomas incipientes distribuidos en varios lóbulos pulmonares a los 21 d después de la infección (Fig. 5B); 3) escasos cúmulos de infiltrado celular (Fig. 5C) en el día 28 post-infección. En contraste, los cortes de pulmón de ratones infectados con el morfotipo-L de la cepa G-217B mostraron una respuesta inflamatoria peribronquiolar en el 14 d, mientras que en el 21 y 28 d post-infección no se observaron reacciones inflamatorias (Fig. 5D, E, F). En los ratones testigos no infectados (Fig. 5G, H, I), no se observaron ningún tipo de respuesta inflamatoria.

Figuras

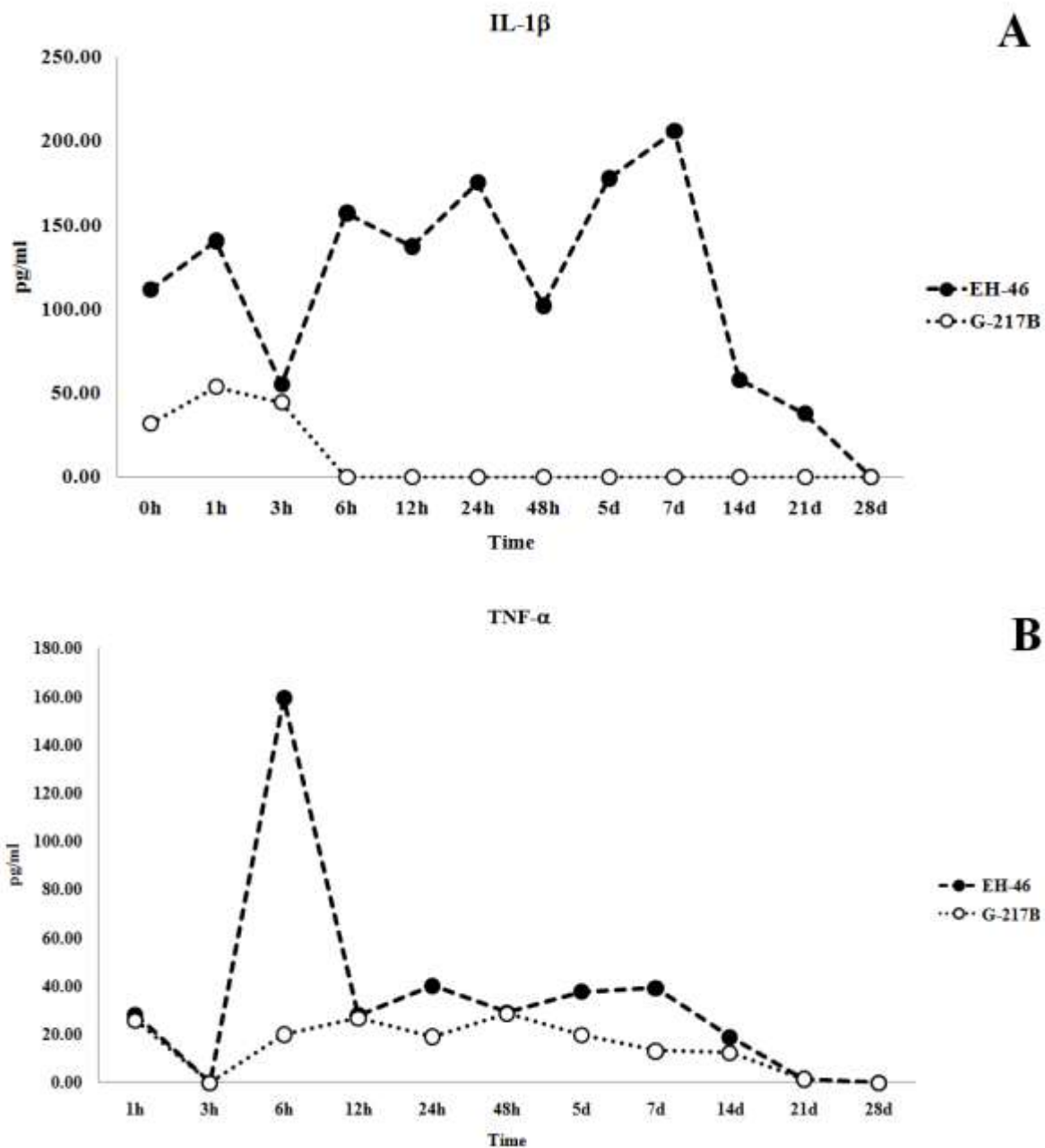


Fig. 1. Perfiles de IL-1 β y TNF- α en homogeneizado de pulmón de ratones infectados por vía intranasal con propágulos del morfotipo-L. Se utilizaron las cepas de *H. capsulatum* EH-46 o G-217B. Los niveles de citoquinas (pg/ml) fueron detectados por el sistema MagPix. Cada valor de citoquina graficado fue corregido con sus respectivos valores basales determinados por el sistema MagPix en homogeneizados de pulmón de ratones no infectados (testigo). (A) IL-1 β y (B) TNF- α . Las lecturas de citoquinas se realizaron a diferentes tiempos después de la infección. (h = horas, d = días).

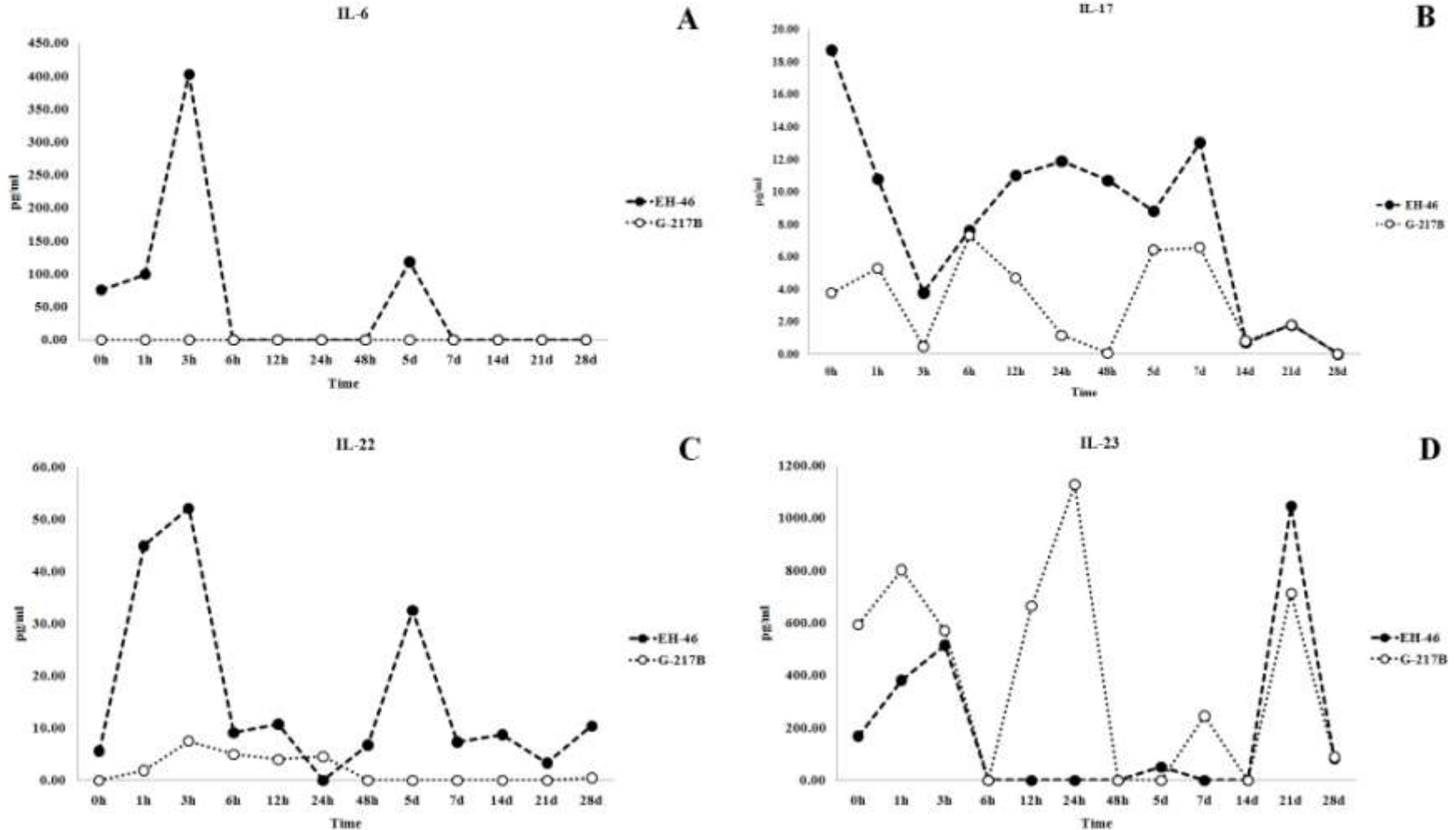


Fig. 2. Perfiles de IL-6, IL-17, IL-22 e IL-23 en homogeneizado de pulmón de ratones infectados por vía intranasal con propágulos del morfotipo-L. Se utilizaron las cepas de *H. capsulatum* EH-46 o G-217B. Los niveles de citoquinas (pg/ml) fueron detectados por el sistema MagPix. Cada valor de citoquina graficado fue corregido con sus respectivos valores basales determinados por el sistema MagPix en homogeneizados de pulmón de ratones no infectados (testigo). (A) IL-6, (B) IL-17, (C) IL-22 y (D) IL-23. Las lecturas de citoquinas se realizaron a diferentes tiempos después de la infección. (h = horas, d = días).

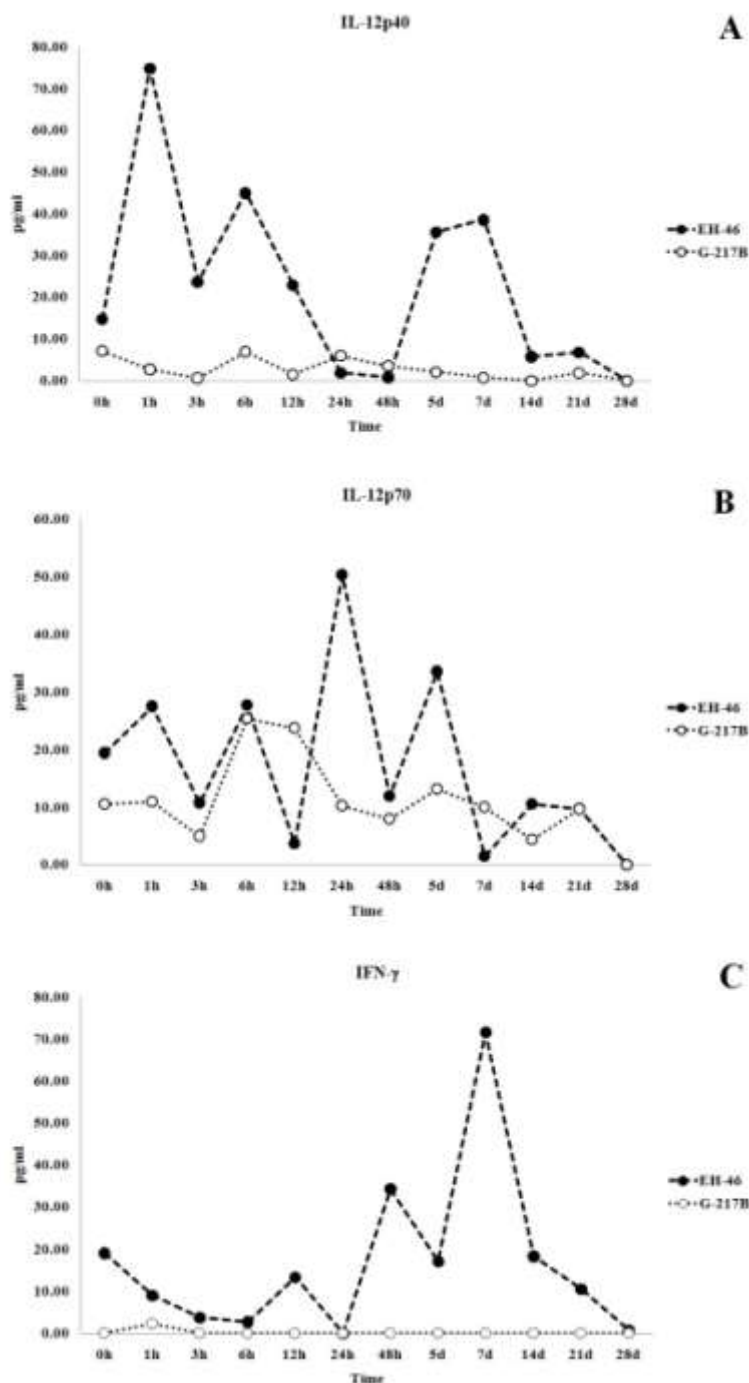


Fig. 3. Perfiles de IL-12p40, IL-12p70 e IFN- γ en homogeneizado de pulmón de ratones infectados por vía intranasal con propágulos del morfotipo-L. Se utilizaron las cepas de *H. capsulatum* EH-46 o G-217B. Los niveles de citoquinas (pg/ml) fueron detectados por el sistema MagPix. Cada valor de citoquina graficado fue corregido con sus respectivos valores basales determinados por el sistema MagPix en homogeneizados de pulmón de ratones no infectados (testigo). (A) IL-12p40, (B) IL-12p70 y (C) IFN- γ . Las lecturas de citoquinas se realizaron a diferentes tiempos después de la infección. (h = horas, d = días).

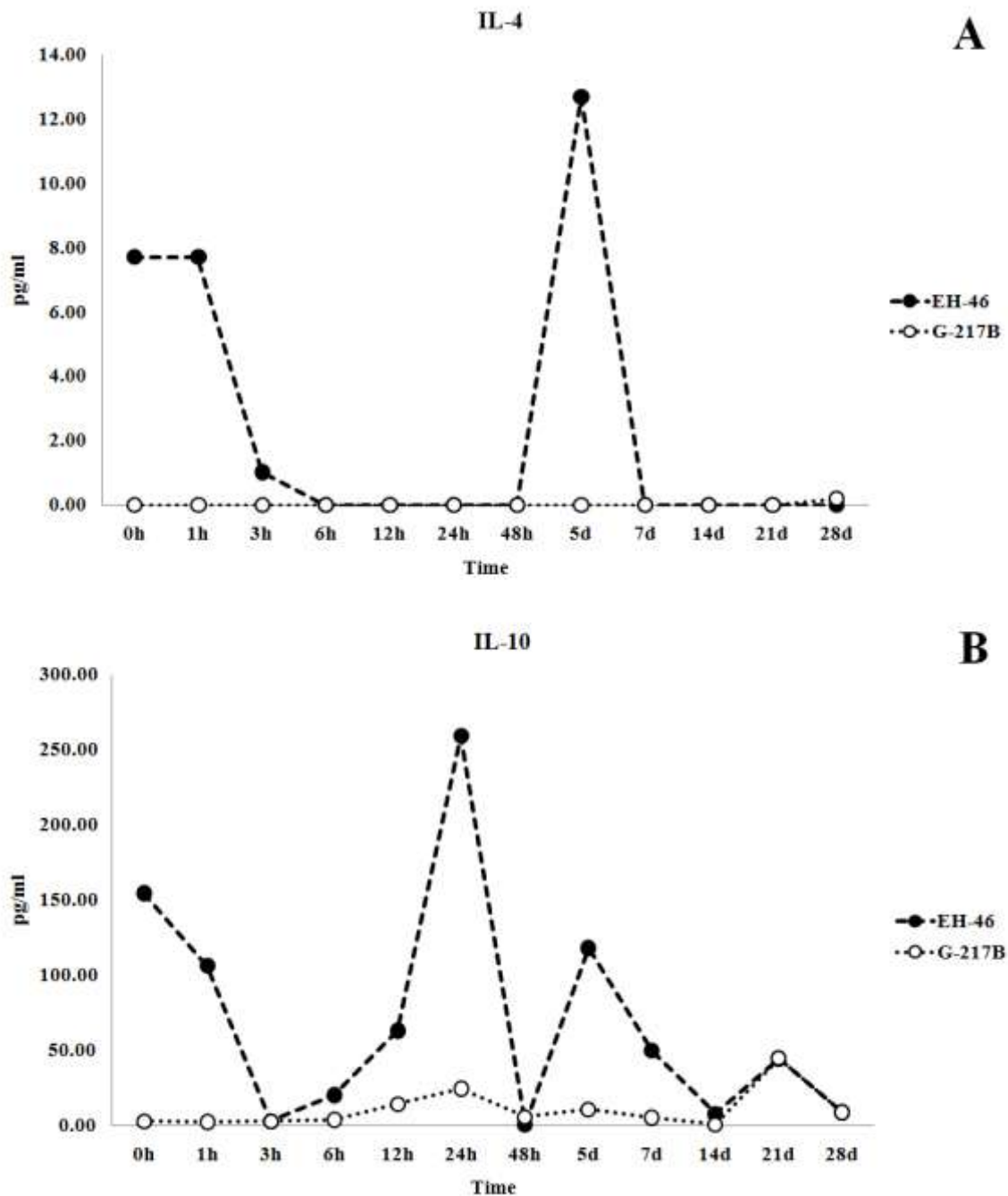


Fig. 4. Perfiles de IL-4 e IL-10 en homogeneizado de pulmón de ratones infectados por vía intranasal con propágulos del morfotipo-L. Se utilizaron las cepas de *H. capsulatum* EH-46 o G-217B. Los niveles de citoquinas (pg/ml) fueron detectados por el sistema MagPix. Cada valor de citoquina graficado fue corregido con sus respectivos valores basales determinados por el sistema MagPix en homogeneizados de pulmón de ratones no infectados (testigo). (A) IL-4 y (B) IL-10. Las lecturas de citoquinas se realizaron a diferentes tiempos después de la infección. (h = horas, d = días).

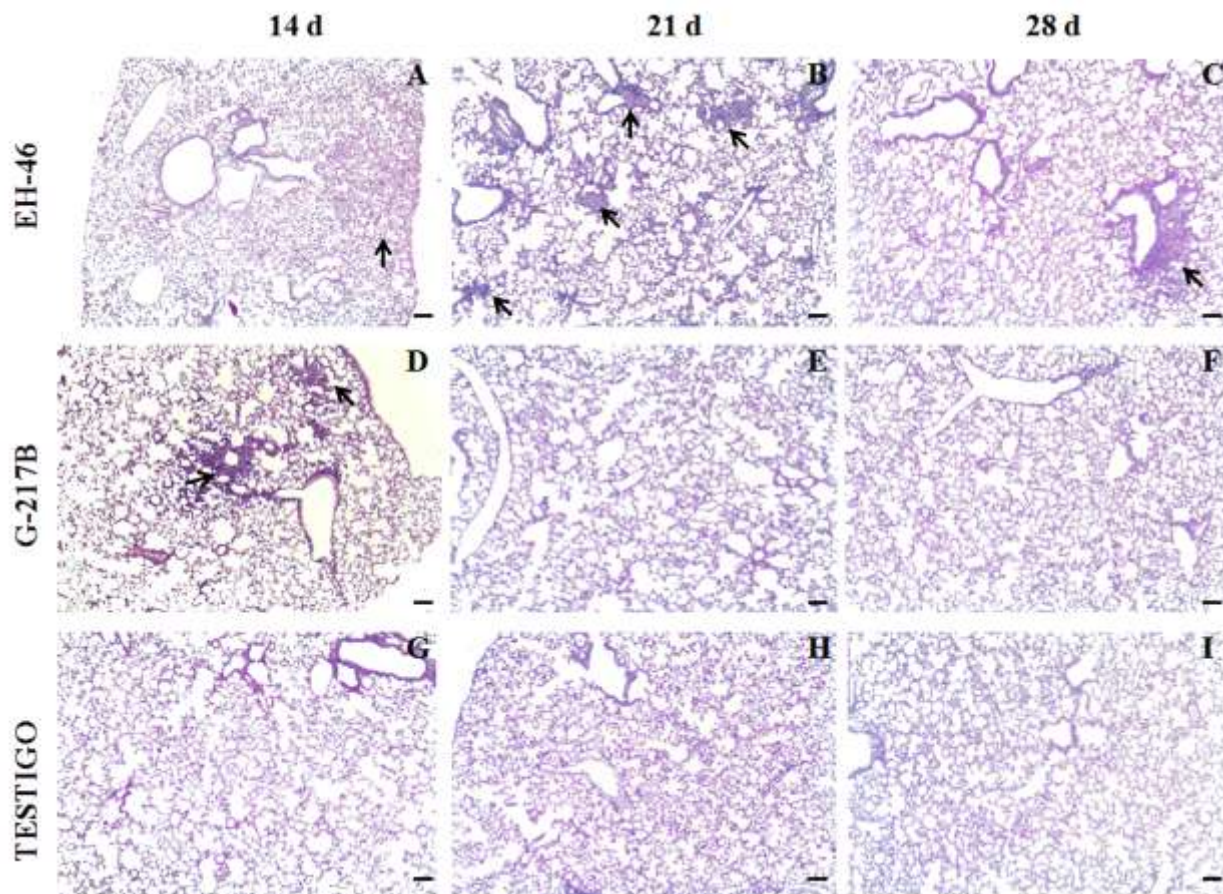


Fig. 5. Observación microscópica de secciones de pulmón de ratones infectados con el morfotipo-L de *H. capsulatum* a los 14, 21 y 28 días. Cepa EH-46 (A, B, C); cepa G-217B (D, E, F); ratones testigo no infectados (G, H, I). Las fotografías fueron tomadas a 40 X. Las flechas muestran: (A) infiltrado celular difuso en el 14 d; (B) granulomas incipientes distribuidos en todos los lóbulos pulmonares en el 21 d; (C) escasos cúmulos de infiltrado celular en el 28 d post-infección con la cepa EH-46; y (D) granulomas incipientes en algunas zonas pulmonares en el 14 d post-infección con la cepa G-217B. Tinción PAS, barras = 80 μ m, (d = día).

CAPÍTULO 7

CAPÍTULO 7

Discusión

En el presente estudio, en un modelo de ratones macho BALB/c inmunocompetentes, se indujo el desarrollo de histoplasmosis pulmonar, simulando una infección natural por la ruta intranasal utilizando propágulos fúngicos infecciosos del morfotipo-M de dos diferentes cepas virulentas de *H. capsulatum*: EH-46 (LAm A) y G-217B (NAm 2). Igualmente, se realizó la infección con propágulos del morfotipo-L, dado que este morfotipo es comúnmente utilizado para realizar investigaciones con este patógeno. Sin embargo, este morfotipo aunque es la forma parasitaria y virulenta de *H. capsulatum*, no es la partícula responsable de infectar huéspedes mamíferos en la naturaleza. Por lo tanto, la transición dimórfica en el huésped infectado debe ocurrir en las primeras etapas de la infección para permitir que el morfotipo-L parasitario virulento pueda establecerse y favorecer el progreso de la infección. La respuesta inmune fundamental del huésped se da para el morfotipo-L, sin embargo el tiempo y la diversidad de moléculas fúngicas expuestas durante el tránsito dimórfico de M a L son cruciales en los inicios del reconocimiento y el montaje de la defensa del huésped. Es importante destacar que el morfotipo-L, naturalmente no infeccioso, es el más utilizado en la mayoría de los trabajos de investigación experimental y, por lo tanto, éstos incurrir en sesgos interpretativos de los análisis de la primera etapa de la infección, la cual ha sido poco cuestionada y estudiada. Los propágulos infecciosos del morfotipo-M de *H. capsulatum* deben ser capaces de atravesar varias barreras del huésped y pueden soportar diferentes tipos de estrés durante su ruta por vías respiratorias y que pueden estar involucrados con el dimorfismo y la diseminación del patógeno antes de la llegada de los propágulos infecciosos a los pulmones. Por tal motivo, en el presente trabajo evaluamos el perfil de citoquinas en homogeneizados pulmonares y la respuesta inflamatoria a través del desarrollo de granulomas en cortes histológicos de pulmón de ratones infectados intranasalmente con el morfotipo-M o el morfotipo-L de *H. capsulatum*, de modo que la respuesta inmune pudiera ser valorada en tiempos cortos y largos post-infección. Esta estrategia fue diseñada para rastrear y analizar en el pulmón del huésped, el efecto del morfotipo-M en los tiempos iniciales de la infección fúngica y el curso de la respuesta inmune asociada a la aparición y establecimiento del morfotipo-L en los tiempos largos.

El análisis de las citoquinas pro-inflamatorias IL-1 β y TNF- α , sugiere que ambas citoquinas participan tanto en la respuesta inicial del huésped (tiempos cortos de post-infección) como durante el curso del proceso infeccioso, particularmente con ambos morfotipos fúngicos de la cepa EH-46, sobresaliendo la respuesta del huésped inducida con el morfotipo-M ([Sahaza et al. 2014b](#)).

En la infección experimental por *H. capsulatum* las citoquinas IL-6, IL-17 e IL-23, han sido menos estudiadas, sin embargo, se postula que estas citoquinas tienen un papel importante en el

control de la progresión clínica de la enfermedad (Deepe y Gibbons 2009; Kroentz y Deepe 2010; Wu et al. 2013). Estas citoquinas tienen la particularidad de presentarse tanto en la fase muy temprana como en la fase de consolidación de la infección, lo que las compromete posiblemente como reguladoras en la interface de la respuesta inmune innata y adaptativa. Los resultados con respecto a los perfiles de estas citoquinas, a lo largo del curso experimental de ratones infectados con el morfotipo-M o -L, revelaron que IL-6 tiene un curso similar con la inoculación de uno u otro morfotipo, sin embargo sus valores fueron más pronunciados al inducir la infección, de manera más cercana a la natural, utilizando un inóculo intranasal con el morfotipo infectivo (morfotipo-M) (Sahaza et al. 2014b), particularmente con la cepa EH-46. IL-17 e IL-23 presentaron un comportamiento interesante para los animales infectados con el morfotipo-M de la cepa EH-46 (Sahaza et al. 2014b), ya que la producción de ambas citoquinas fue desfasada en el tiempo post-infección, donde la elevación de IL-23 precede a la elevación de IL-17 en tiempos más tardíos. Este comportamiento particular no se discrimina cuando se utilizó como inóculo el morfotipo-L parasitario, virulento y no infectivo, siendo la producción de estas citoquinas discontinúa desde los tiempos tempranos de la infección. Una respuesta temprana de IL-17 durante la primera semana de la infección de ratones C57BL/6 infectados con el morfotipo-L de *H. capsulatum* ha sido reportada por Deepe y Gibbons (2009).

IL-22 nunca ha sido considerada anteriormente en la infección experimental con *H. capsulatum*. Los resultados alcanzados con esta citoquina, detectada por primera vez, demuestran su presencia en los homogeneizados de pulmón de ratones en la mayoría de los tiempos tempranos y tardíos post-infección probados. La presencia de esta citoquina durante todo el proceso de la infección por *H. capsulatum* podría estar asociada a los procesos de defensa y al mismo tiempo de reparación tisular de los ratones infectados, dado que IL-22 ha sido reportada como una citoquina muy importante en los procesos de protección del epitelio de la mucosa y reparación de los epitelios pulmonares dañados por patógenos (Zelante et al. 2011; Posiask et al. 2013).

En relación con IL-12, se sabe que ésta es necesaria para generar una inmunidad protectora contra la infección por *H. capsulatum* debido a su papel en la síntesis de IFN- γ por linfocitos T CD4 + y células NK (Marth y Kelsall 1997). En los resultados presentados, los niveles de producción de IL-12 en los homogeneizados de pulmón de ratones infectados con el morfotipo-M de la cepa EH-46 siempre fueron más altos y sostenidos en los tiempos post-infección, mientras que, en los animales infectados con el morfotipo-L se encontró un comportamiento variable, destacando los valores elevados previo al aumento de IFN- γ , del cual se sabe que es la citoquina activadora más potente de los macrófagos en el sitio de la infección y puede inhibir el crecimiento intracelular de *H. capsulatum* (Zhou et al. 1995; Allendoerfer y Deepe 1998; Heninger et al. 2006). De acuerdo con lo anterior, los resultados realizados con IFN- γ presentaron aumentos significativos sólo en aquellos animales inoculados con la cepa EH-46, independientemente del morfotipo, previo a la resolución de la enfermedad. Sin embargo, es interesante enfatizar que la cinética de producción de IFN- γ presentó un desfase en su aparición en relación al morfotipo fúngico utilizado, apareciendo más temprano en los animales infectados

con el morfotipo-L, lo anterior sugiere que el cambio dimórfico *in vivo* influye en el tiempo de la progresión de la infección.

En cuanto a las citoquinas anti-inflamatorias evaluadas en el presente estudio, IL-4 e IL-10, muy probablemente estén involucradas en la regulación de la respuesta pro-inflamatoria de acuerdo con el tipo de cepa de *H. capsulatum* utilizado. Es factible que la modulación del balance Th1/Th2 pueda estar asociado con la más intensa respuesta inflamatoria desarrollada por la cepa EH-46.

Con respecto al desarrollo de granulomas, se encontró que ambas cepas de *H. capsulatum* pueden inducir una respuesta inflamatoria con tendencia a la formación de granulomas. Sin embargo, destaca la rápida resolución de la respuesta inflamatoria menos extensas de los animales infectados con la cepa G-217B, a los 21 d comparado con los animales inoculados con la cepa EH-46, a los 28 d. Los granulomas se observaron principalmente en los pulmones de ratones infectados con la cepa EH-46 cuando la respuesta inmune adaptativa es particularmente efectiva (21 d post-infección). Los hallazgos histológicos sugieren que a partir del día 28 hubo una disminución en el número y extensión de granulomas, lo que podría indicar el principio de la resolución de la infección. Igualmente, como se observó en las citoquinas, comparando la infección del morfotipo-M con el morfotipo-L, se presentó una disminución en el tiempo y en la intensidad de la respuesta inflamatoria expresada en la formación de granulomas que probablemente favoreció la resolución de la enfermedad en los animales infectados.

Es importante señalar que el tipo de cepas de ratón utilizado puede influir en los resultados del perfil inmunológico de la histoplasmosis experimental. Por otro lado, tanto la edad como el sexo de los ratones son variables primordiales para definir datos repetitivos del comportamiento de la respuesta inmune al patógeno. En la histoplasmosis es común encontrar trabajos asociados a ratones A/J, BALB/c o C57BL/6, siendo este último más utilizado por algunos grupos de investigación que manejan animales predominantemente resistentes a la infección ([Sahaza et al. 2014a](#)). Para este estudio se ha utilizado un modelo animal susceptible a la infección con *H. capsulatum*, ratones machos BALB/c, el cual ha sido estandarizado en el laboratorio desde hace varios años y satisface las condiciones de seguimiento de una infección autolimitada.

Los resultados de la presente investigación utilizando dos cepas del hongo, EH-46 de México y G-217B de los Estados Unidos de América, de especies filogenéticas distintas, LAm A y NAm 2, respectivamente, revelaron diferencias significativas en el curso de la producción de las citoquinas y en el desarrollo de granulomas, lo que sugiere la relevancia de los PAMPs de cada cepa y sus respectivos morfotipos en el montaje, en tiempo y forma, de los mecanismos de defensa del huésped. Tanto es así que los resultados alcanzados con los dos morfotipos de la cepa EH-46 indujeron una mayor respuesta inflamatoria, reflejada tanto en una mayor producción de citoquinas como en un mayor desarrollo de granulomas. Sin embargo, la respuesta inducida primariamente por el morfotipo-M reveló marcadas diferencias en la intensidad y tiempo de resolución de la infección, en comparación con la infección inicial con el morfotipo-L. Es posible

que, en condiciones naturales, una de las primeras líneas de la defensa del huésped contra *H. capsulatum* puede implicar la producción de citoquinas que son estimuladas inicialmente por los PAMPs del morfotipo-M infeccioso. Cambios en la virulencia asociada a la mortalidad de animales, utilizando diferentes tipos de cepas de *H. capsulatum* procedentes de Norteamérica y América Latina han sido documentadas (Durkin et al. 2004).

Conclusiones

El morfotipo-M de la cepa EH-46 de *H. capsulatum*, procedente de México, inoculado vía intranasal en ratones machos BALB/c, permitió reproducir la histoplasmosis pulmonar autolimitada de modo similar como ocurre en la naturaleza, por lo que se logró evaluar el curso de la infección experimental a través de la identificación y cuantificación de citoquinas en homogeneizados pulmonares y de la respuesta inflamatoria en cortes de pulmón de ratones infectados.

La progresión de la histoplasmosis representa una relación multifactorial entre el estado inmune del huésped, la concentración de inóculo fúngico inicial, la virulencia del hongo, la diversidad y expresión de PAMPs según el morfotipo y la cepa fúngica utilizada (diferentes especies filogenéticas). Asimismo, influye en el curso de la infección la vía de entrada del patógeno y el modelo animal utilizado. Los resultados del presente trabajo sugieren que el morfotipo y la cepa de *H. capsulatum* intervienen no sólo sobre el establecimiento y el tiempo requerido para la autolimitación de la infección, sino también sobre los tiempos de aparición de los signos y síntomas propios que definen la enfermedad y la recuperación de la misma.

CAPÍTULO 8

CAPÍTULO 8

Literatura citada.

Allen HL, Deepe GS Jr. B cells and CD4-CD8- T cells are key regulators of the severity of reactivation histoplasmosis. *J. Immunol.* 2006;177:1763-71.

Allendoerfer R, Boivin GP, Deepe GS Jr. Modulation of immune responses in murine pulmonary histoplasmosis. *J. Infect. Dis.* 1997;175:905-14.

Allendörfer R, Brunner GD, Deepe GS Jr. Complex requirements for nascent and memory immunity in pulmonary histoplasmosis. *J. Immunol.* 1999;162:7389-96.

Allendoerfer R, Deepe GS Jr. Blockade of endogenous TNF- α exacerbates primary and secondary pulmonary histoplasmosis by differential mechanisms. *J. Immunol.* 1998;160:6072-82.

Berry CL. The development of the granuloma of histoplasmosis. *J Pathol.* 1969a;97:1–10.

Berry CL. The production of disseminated histoplasmosis in the mouse: The effects of changes in reticulo-endothelial function. *J Pathol.* 1969b;97:441–57.

Berry CL. Modification of the host response in experimental histoplasmosis. *J Pathol.* 1969c;97:653–64.

Cain JA, Deepe GS Jr. Evolution of the primary immune response to *Histoplasma capsulatum* in murine lung. *Infect. Immun.* 1998;66:1473-81.

Clemons KV, Darbonne WC, Curnutte JT, Sobel RA, Stevens DA. Experimental histoplasmosis in mice treated with anti-murine interferon-gamma antibody and in interferon-gamma gene knockout mice. *Microbes Infect.* 2000;2:997-1001.

Deepe GS Jr, Gibbons RS. T cells require tumor necrosis factor- α to provide protective immunity in mice infected with *Histoplasma capsulatum*. *J. Infect. Dis.* 2006;193:322-30.

Deepe GS Jr, Gibbons RS. Interleukins 17 and 23 Influence the Host Response to *Histoplasma capsulatum*. *J. Infect. Dis.* 2009;200:142-51.

Deepe GS Jr, Seder RA. Molecular and cellular determinants of immunity to *Histoplasma capsulatum*. *Res. Immunol.* 1998;149:397-406.

Durkin MM, Connolly PA, Karimi K, Wheat E, Schnizlein-Bick C, Allen SD, Alves K, Tewari RP, Keath E. Pathogenic differences between North American and Latin American strains of

Histoplasma capsulatum var. *capsulatum* in experimentally infected mice. J. Clin. Microbiol. 2004;42:4370-3.

Gildea LA, Morris RE, Newman SL. *Histoplasma capsulatum* yeasts are phagocytosed via very late antigen-5, killed, and processed for antigen presentation by human dendritic cells. J. Immunol. 2001;166:1049-56.

Goodwin RA Jr, Snell JD Jr. The enlarging histoplasmosis: concept of a tumor-like phenomenon encompassing the tuberculoma and coccidioidoma. Am. Rev. Respir. Dis. 1969;100:1-12.

Heninger E, Hogan LH, Karman J, Macvilay S, Hill B, Woods JP, Sandor M. Characterization of the *Histoplasma capsulatum*-induced granuloma. J. Immunol. 2006;177:3303-13.

Huffnagle GB, Deepe GS Jr. Innate and adaptive determinants of host susceptibility to medically important fungi. Curr. Opin. Microbiol. 2003;6:344-50.

Kroetz DN, Deepe GS Jr. CCR5 dictates the equilibrium of proinflammatory IL-17+ and regulatory Foxp3+ T cells in fungal infection. J. Immunol. 2010;184:5224-31.

Marth T, Kelsall BL. Regulation of interleukin-12 by complement receptor 3 signaling. J. Exp. Med. 1997;185:1987-95.

Matsuzaki G, Umemura M. Interleukin-17 as an effector molecule of innate and acquired immunity against infections. Microbiol. Immunol. 2007;51:1139-47.

Medeiros A, Sá-Nunes A, Soares EG, Peres CM, Silva CL, Faccioli LH. Blockade of endogenous leukotrienes exacerbates pulmonary histoplasmosis. Infect. Immun. 2004;72:1637-44.

Medeiros A, Sá-Nunes A, Turato WM, Secatto A, Frantz FG, Sorgi CA, Serezani CH, Deepe GS Jr, Faccioli LH. Leukotrienes are potent adjuvant during fungal infection: effects on memory T cells. J. Immunol. 2008;181:8544-51.

Mencacci A, Del Sero G, Cenci E, D'Ostiani EF, Bacci A, Montagnoli C, Kopf M, Romani L. Endogenous interleukin 4 is required for development of protective CD4+ T helper type 1 cell responses to *Candida albicans*. J. Exp. Med. 1998;187:307-17.

Mukhopadhyay S, Gal AA. Granulomatous lung disease: an approach to the differential diagnosis. Arch. Pathology Lab. Med. 2010;134:667-90.

Newman SL. Macrophages in host defense against *Histoplasma capsulatum*. Trends. Microbiol. 1999;7:67-71.

Ouyang W, Kolls JK, Zheng Y. The biological functions of T helper 17 cell effector cytokines in inflammation. Immunity. 2008;28:454-67.

Patiño MM, Williams D, Ahrens J, Graybill JR. Experimental histoplasmosis in the beige mouse. *J. Leukoc. Biol.* 1987;41:228-35.

Pociask DA, Scheller EV, Mandalapu S, McHugh KJ, Enelow RI, Fattman CL, Kolls JK, Alcorn JF. IL-22 is essential for lung epithelial repair following influenza infection. *Am. J. Pathol.* 2013;182:1286-96.

Romani L, Zelante T, De Luca A, Fallarino F, Puccetti P. IL-17 and therapeutic kynurenines in pathogenic inflammation to fungi. *J. Immunol.* 2008;180:5157-62.

Sahaza JH, Pérez-Torres A, Zenteno E, Taylor ML. Usefulness of the murine model to study the immune response against *Histoplasma capsulatum* infection. *Comp. Immunol. Microbiol. Infect. Dis.* 2014a;37:143-52.

Sahaza JH, Suárez-Alvarez RO, Estrada-Bárceñas DA, Pérez-Torres A, Taylor ML. Assessment of cytokines in the lungs of BALB/c mice after *Histoplasma capsulatum* intra-nasal infection with mycelial propagules. *Comp. Immunol. Microbiol. Infect. Dis.* 2014b (Enviado).

Suárez-Alvarez RO, Pérez-Torres A, Taylor ML. Adherence patterns of *Histoplasma capsulatum* yeasts to bat tissue sections. *Mycopathologia.* 2010;170:79-87.

Suárez-Alvarez R, Sahaza JH, Berzunza-Cruz M, Becker I, Curiel-Quesada E, Pérez-Torres A, Taylor ML. Dimorphism and dissemination of *Histoplasma capsulatum* occur in the nasal mucosa and cervical lymph nodes of bats and mice in a short-time after intranasal-infection with mycelial propagules. *Innate Immunity.* 2014. (Enviado).

Tewari R, Wheat LJ, Ajello L. 1998. Agents of histoplasmosis, p 373-393. *In* Ajello L, Hay RJ (ed). *Topley & Wilson's. Microbiology and microbial infections. Medical mycology.* Arnold & Oxford University Press Inc., New York, NY.

Wheat J. Histoplasmosis in the acquired immunodeficiency syndrome. *Curr. Top. Med. Mycol.* 1996;7:7-18.

Williams DM, Graybill JR, Drutz DJ. *Histoplasma capsulatum* infection in nude mice. *Infect. Immun.* 1978;21:973-77.

Wu SY, Yu JS, Liu FT, Miaw SC, Wu-Hsieh BA. Galectin-3 negatively regulates dendritic cell production of IL-23/IL-17-axis cytokines in infection by *Histoplasma capsulatum*. *J. Immunol.* 2013;190:3427-37.

Zhou P, Sieve MC, Bennett J, Kwon-Chung KJ, Tewari RP, Gazzinelli RT, Sher A, Seder RA. IL-12 prevents mortality in mice infected *Histoplasma capsulatum* through induction of IFN-gamma. *J. Immunol.* 1995;155:785-95.

Zelante T, Iannitti R, De Luca A, Romani L. IL-22 in antifungal immunity. *Eur. J. Immunol.* 2011;41:270-5.

ANEXOS

ANEXOS

Artículos enviados o publicados no asociados al trabajo de tesis

Anexo 1

Artículo publicado: Estrada-Bárcenas DA, Vite-Garín T, Navarro-Barranco H, de la Torre-Arciniega R, Pérez-Mejía A, Rodríguez-Arellanes G, Ramirez JA, Humberto **Sahaza J**, Taylor ML, Toriello C. Genetic diversity of *Histoplasma* and *Sporothrix* complexes based on sequences of their ITS1-5.8S-ITS2 regions from the BOLD System. Rev Iberoam Micol. 2014;31(1):90-4.

Anexo2

Artículo enviado: Sahaza JH, Reyes-Montes MR, Canteros CE, Taylor ML. Study of Temperature Sensitivity and Doubling Time of *Histoplasma capsulatum* Yeast Phase Using Clinical Strains from Different Regions of the Americas. BioMed Research International. 2014. (Enviado).

Anexo 1

Artículo publicado

Rev Iberoam Micol. 2014;31(1):90-94



Revista Iberoamericana
de Micología

www.elsevier.es/reviberoammicol



Mycologic Forum

Genetic diversity of *Histoplasma* and *Sporothrix* complexes based on sequences of their ITS1-5.8S-ITS2 regions from the BOLD System



Daniel Alfonso Estrada-Bárceñas^a, Tania Vite-Garín^b, Hortensia Navarro-Barranco^c, Raúl de la Torre-Arciniega^b, Amelia Pérez-Mejía^c, Gabriela Rodríguez-Arellanes^b, Jose Antonio Ramírez^b, Jorge Humberto Sahaza^{b,d}, María Lucia Taylor^{b,e}, Conchita Toriello^{c,*}

^a Colección Nacional de Cultivos Microbianos, Centro de Investigación y de Estudios Avanzados, Instituto Politécnico Nacional, México DF, México

^b Laboratorio de Inmunología de Hongos, Departamento de Microbiología y Parasitología, Facultad de Medicina, UNAM, México DF, México

^c Laboratorio de Micología Básica, Departamento de Microbiología y Parasitología, Facultad de Medicina, UNAM, México DF, México

^d Unidad de Micología Médica y Experimental, Corporación para Investigaciones Biológicas, Medellín, Colombia

ARTICLE INFO

Article history:

Received 30 August 2013

Accepted 9 October 2013

Available online 20 November 2013

Keywords:

*Histoplasma capsulatum**Sporothrix schenckii*

ITS region

iBOL

ABSTRACT

High sensitivity and specificity of molecular biology techniques have proven usefulness for the detection, identification and typing of different pathogens. The ITS (Internal Transcribed Spacer) regions of the ribosomal DNA are highly conserved non-coding regions, and have been widely used in different studies including the determination of the genetic diversity of human fungal pathogens. This article wants to contribute to the understanding of the intra- and interspecific genetic diversity of isolates of the *Histoplasma capsulatum* and *Sporothrix schenckii* species complexes by an analysis of the available sequences of the ITS regions from different sequence databases. ITS1-5.8S-ITS2 sequences of each fungus, either deposited in GenBank, or from our research groups (registered in the Fungi Barcode of Life Database), were analyzed using the maximum likelihood (ML) method. ML analysis of the ITS sequences discriminated isolates from distant geographic origins and particular wild hosts, depending on the fungal species analyzed.

This manuscript is part of the series of works presented at the "V International Workshop: Molecular genetic approaches to the study of human pathogenic fungi" (Oaxaca, Mexico, 2012).

© 2013 Revista Iberoamericana de Micología. Published by Elsevier España, S.L. All rights reserved.

Diversidad genética de los complejos *Histoplasma* y *Sporothrix* en función de las secuencias de sus regiones ITS1-5.8S-ITS2 del BOLD System

RESUMEN

Las técnicas de biología molecular han proporcionado instrumentos de alta sensibilidad y especificidad, útiles para la detección, identificación y tipificación de diferentes patógenos. Las regiones ITS (*Internal Transcribed Spacer*) del ADN ribosómico están altamente conservadas y no son codificantes. Estas regiones se han utilizado ampliamente en diferentes tipos de estudios, incluida la determinación de la diversidad genética de hongos patógenos del ser humano. La finalidad de este artículo es contribuir al conocimiento de la diversidad genética intra- e interespecífica de aislamientos de los complejos de *Histoplasma capsulatum* y *Sporothrix schenckii* a través del análisis de las secuencias disponibles de las regiones ITS en distintos bancos de secuencias. Las secuencias de las regiones ITS1-5.8S-ITS2, de cada hongo, depositadas en el GenBank, junto con las obtenidas por nuestros grupos de investigación (depositadas en la Fungal Barcoding of Life Database), se analizaron con el método de máxima probabilidad (ML, por sus

Palabras clave:

*Histoplasma capsulatum**Sporothrix schenckii*

Región ITS

iBOL

* Corresponding author.

E-mail address: ctoriello@unam.mx, c.toriellonajera@gmail.com (C. Toriello).

^{*} These authors participated in the design and coordination of the Mexican Thematic Net for Fungi Barcode of Life (MEXBOL) of the Consejo Nacional de Ciencia y Tecnología (CONACyT)-MEXICO and have equally contributed to this review.

siglas en inglés). El análisis ML de las secuencias de las regiones ITS discriminó aislamientos de orígenes geográficos distantes y de huéspedes salvajes particulares, de acuerdo con la especie fúngica analizada. Este artículo forma parte de una serie de estudios presentados en el «V International Workshop: Molecular genetic approaches to the study of human pathogenic fungi» (Oaxaca, México, 2012).

© 2013 Revista Iberoamericana de Micología. Publicado por Elsevier España, S.L. Todos los derechos reservados.

Reliable identification of pathogenic fungal species is fundamental to epidemiology in terms of biodiversity, geographical variation, and environmental changes. Species identification in fungi is particularly challenging because of their transient nature. Limitations to the studies of diversity in mammalian pathogenic fungi exist due to a lack of taxonomic specialists, and scarce and incomplete data for many taxonomic characters, which has been suggested by Suwannasai et al.¹⁷ and Tanticareon.¹⁹

Pheno- and genotyping of fungal strains have been used as important tools for identifying environmental sources of outbreaks as well as confirming the existence of pathogens in natural habitats. These different typing methods have used both conventional and molecular techniques.

Although phenotyping has continuously been used to study fungi, sensitive and specific genotyping methods are being developed to characterize fungal species, but different criteria must be met to be accepted by specialists. In many cases, genotyping methods compare DNA polymorphisms and classify fungal organisms according to the principles of molecular systematic. For *Histoplasma capsulatum* (etiological agent of the systemic mycosis histoplasmosis) and *Sporothrix schenckii* (etiological agent of the subcutaneous mycosis sporotrichosis) typing and classification, different molecular techniques have been applied, among them, various PCR methods using genomic sequences.^{7,8}

There is a wide array of molecular markers for microorganism identification and genotyping or molecular classification. Among them, the Internal Transcribed Spacer (ITS) regions stand out for the study of closely related taxa, due to genetic diversity associated with the high rate of evolutionary changes characteristic of these regions.¹² ITS consist of two variable non-coding regions (ITS1 and ITS2) inserted between the highly conserved small subunit 18S, the 5.8S, and the large subunit 28S of the rDNA gene cluster.¹²

ITS as a molecular target for fungal identification are supported by several unique characteristics: (i) The complete ITS region has a length between 600 and 800 bp and can be easily amplified, using universal primers that are complementary to rDNA sequences. (ii) The multicopy nature of the repeat regions of the rDNA allows for the amplification of the ITS regions from small, diluted or degraded DNA samples. (iii) Several studies have demonstrated that the ITS regions are highly variable among morphologically distinct fungal species.¹²

The usefulness of ITS markers has been documented in several studies of phylogeny and genotyping of *H. capsulatum*^{1,5,6,31} and *S. schenckii*.^{2-4,22}

The Mexican Barcode of Life project for the *H. capsulatum* and *S. schenckii* species complexes

The Mexican Barcode of Life (MEXBOL) resulted from the work of Mexican investigators as part of the international DNA barcoding (iBOL) project. MEXBOL is now part of a network with funding from the Consejo Nacional de Ciencia y Tecnología (CONACYT) and the Comisión Nacional para el Conocimiento y Uso de la Biodiversidad (CONABIO). The Natural Sciences and Engineering Research Council of Canada (NSERC) developed a Barcode of Life Database (BOLD) based on a specific informatics infrastructure. The cytochrome oxidase subunit 1 (COI), ribulose-bisphosphate

carboxylase (rbcL), maturase K (matK), and ITS regions are among the Barcode sequences used. In addition to the assembly of barcode information and maintenance of these records by the BOLD system, a copy of all sequence and key specimen data is archived at the National Center for Biotechnology Information (NCBI) or its sister genomic repositories, the DNA Data Bank of Japan (DDBJ) and the European Molecular Biology Laboratory (EMBL), when results are ready for public release.¹³

The identification of *H. capsulatum* and *S. schenckii* isolates from different sources and origins by the sequences of the ITS regions started in 2010 as a project for the MEXBOL network for fungi. To date there are 19 ITS1-5.8S-ITS2 sequences of *H. capsulatum* from the Laboratorio de Inmunología de Hongos and 10 sequences of *Sporothrix* spp. from the Laboratorio de Micología Básica, Departamento de Microbiología y Parasitología, Facultad de Medicina, UNAM, deposited in the BOLD System. Sequences were obtained from isolates that were previously pheno- and genotypically well identified.^{10,14,15}

Data regarding the natural hosts, sources, and samples of the 19 *H. capsulatum* and 10 *Sporothrix* spp. isolates are shown in Table 1. Fungal specimens are deposited in the Culture Collection of *H. capsulatum* from the Laboratorio de Inmunología de Hongos and the Culture Collection of Fungal Pathogens of the Laboratorio de Micología Básica, from the Departamento de Microbiología y Parasitología, Facultad de Medicina, UNAM. In addition, they are registered in the database of the World Federation for Culture Collection, with code number LIH-UNAM WDCM817 for *H. capsulatum* (http://www.wfcc.info/ccinfo/index.php/collection/by_id/817) and code number BMFM-UNAM WDCM834 for *Sporothrix* spp. (http://www.wfcc.info/ccinfo/index.php/collection/by_id/834).

Analysis of the genetic diversity of *H. capsulatum* and *S. schenckii* species complexes based on ITS sequences from MEXBOL project

Current data from our laboratory teams, using evolutionary and genetic distance analyses by maximum likelihood (ML) of ITS1-5.8S-ITS2 sequences of *H. capsulatum* or *Sporothrix* spp. from the BOLD System and GenBank datasets, produced robust results to aid in understanding the similarities and diversities among isolates either of *H. capsulatum* or *Sporothrix* spp. from different sources and geographic origins.

Sequences were generated by PCR assays with ITS5/ITS4 primers⁹ for *H. capsulatum* and ITS1F/ITS4 primers⁹ for *Sporothrix* spp. Fig. 1 shows the predicted products, 607 bp for *H. capsulatum* and 575 bp for *Sporothrix* spp., amplified by their respective primers. The ML trees generated are shown in Fig. 2.

Concerning *H. capsulatum*, Fig. 2A highlights the sequences of all isolates from different geographic origins and phylogenetic species that clustered together in a major group sustained by 99% of bootstrap values (BT). This finding confirms the high similarity of the isolates analyzed, separates a reference strain of *Ajellomyces dermatitidis* (nearby sister), and underlines the genetic distance from a heterologous pathogenic fungus, *Paracoccidioides brasiliensis*, used as an outgroup in the ML analysis. The ML tree topology of *H. capsulatum* sequences in Fig. 2A clearly confirms that inter-specific diversity among fungal pathogens that cause respiratory diseases

Table 1
Data of isolates of *Histoplasma* and *Sporothrix* complexes analyzed using the ITS1-5.8S-ITS2 region.

Isolate	Host or source sample	Species	Larcode accession number
EH-53	Human/Blood	<i>H. capsulatum</i> LAm A*	HIST001-13
EH-315*	Bat/Intestine	<i>H. capsulatum</i> Lineage*	HIST002-13
EH-317	Human/Blood	<i>H. capsulatum</i> LAm A*	HIST003-13
EH-373*	Bat/Lung	<i>H. capsulatum</i> LAm A*	HIST004-13
EH-375*	Bat/Lung	<i>H. capsulatum</i>	HIST005-13
EH-378*	Bat/Lung	<i>H. capsulatum</i>	—
EH-391*	Bat/Liver	<i>H. capsulatum</i> LAm A*	—
EH-393*	Bat/Spleen	<i>H. capsulatum</i>	HIST006-13
EH-394p†	Bat/Spleen	<i>H. capsulatum</i>	HIST007-13
EH-398p†	Bat/Lung	<i>H. capsulatum</i>	HIST008-13
EH-449†	Bat/Intestine	<i>H. capsulatum</i>	HIST009-13
EH-449p†	Bat/Lung	<i>H. capsulatum</i>	HIST010-13
EH-449p†	Bat/Lung	<i>H. capsulatum</i>	HIST011-13
EH-555p†	Bat/Lung	<i>H. capsulatum</i>	HIST012-13
EH-658††	Bat/Liver	<i>H. capsulatum</i>	HIST013-13
EH-670†	Bat/Spleen	<i>H. capsulatum</i>	HIST014-13
EH-670†	Bat/Liver	<i>H. capsulatum</i>	HIST015-13
EH-671p†	Bat/Lung	<i>H. capsulatum</i>	HIST016-13
EH-672†	Bat/Spleen	<i>H. capsulatum</i>	HIST017-13
EH-696p†	Bat/Lung	<i>H. capsulatum</i>	HIST018-13
EH-143	Human/Cutaneous	<i>S. schenckii</i>	IMFM001-13
EH-194	Environmental/Rose plant	<i>S. schenckii</i>	IMFM002-13
EH-195	Environmental/Coffee soil	<i>S. schenckii</i>	IMFM003-13
EH-197	Human/Cutaneous	<i>S. schenckii</i>	IMFM004-13
EH-230	Human/Cutaneous	<i>S. glabrosa</i>	IMFM005-13
EH-234	Human/Cutaneous	<i>S. schenckii</i>	IMFM006-13
EH-251	Environmental/Soil	<i>S. schenckii</i>	IMFM007-13
EH-252	Environmental/Soil	<i>S. schenckii</i>	IMFM008-13
EH-253	Environmental/Soil	<i>S. schenckii</i>	IMFM009-13
EH-254	Environmental/Soil	<i>S. schenckii</i>	IMFM010-13

* Phylogenetic species reported by Kasuga et al.†

† The sequence of this isolate has not yet been deposited in the BOLD System.

‡ *Mormoops megalophylla*.

§ *Arithus ituricus*.

¶ *Leptonycteris nivalis*.

‡ *L. curvirostris*.

* *Tadarida brasiliensis*.

is well sustained using ITS1-5.8S-ITS2 region sequence analyses. Besides, it should be emphasized that ITS could also distinguish intra-specific diversity among *H. capsulatum* isolates, evidenced by the formation of a subgroup sustained by 89% BT, which contains six fungal isolates recovered from a particular wild host (*Tadarida brasiliensis* bats), together with one isolate recovered from an

infected *Mormoops megalophylla* bat. This conclusion is consistent with results for these particular isolates using other molecular markers.^{20,21} In contrast, the ITS1-5.8S-ITS2 region sequence analysis in Fig. 2A could not discriminate cryptic species or clades of the *H. capsulatum* complex (NAm 1, NAam 2, LAm A, LAm B, African, Eurasian, and some lineages) and the taxonomic varieties

Histoplasma capsulatum (EH-658H)



Sporothrix schenckii (EH-234)

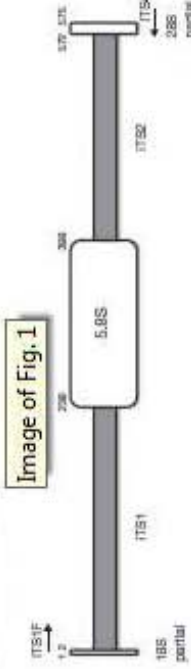


Image of Fig. 1

Fig. 1. ITS1-5.8S-ITS2 regions amplified from *Histoplasma* and *Sporothrix* samples. The schema depicts the regions amplified by the primers: ITS5 (5'-GCAGTAAAGCTGTAACAGG-3') and ITS4 (5'-TCCCTCCCTATTGATGCC-3') for *H. capsulatum*, and ITS1F (CTTGCTATTGACGGAGCTAA) and ITS4 for *Sporothrix* spp. The figure was modified from Saar and Nolans,¹⁶ according to *H. capsulatum* and *Sporothrix* spp. ITS region data.

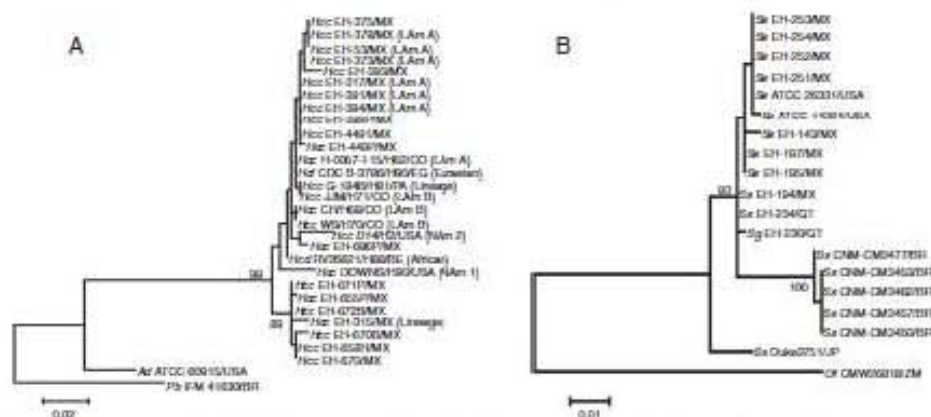


Fig. 2. Maximum likelihood (ML) trees of ITS1-5.8S-ITS2 regions amplified for *Histoplasma* (A) and *Sporothrix* (B) samples. PCR products using primers aforementioned in Fig. 1 for each fungal species were sequenced and aligned by MUSCLE program (MEGA version 5). The best model of evolution to generate the ML phylogenetic trees was obtained by Tamura and Nei gamma distribution.¹² A bootstrapping algorithm was achieved on the dataset for 1000 replicates, and values $\geq 70\%$ were recorded for each tree node. BOLD System sequence accession numbers are referenced in table 1. GenBank sequences for both fungal species were included as reference strains or as outgroups in the ML analyses. Accession numbers are as follows: for *H. capsulatum*: *H. capsulatum* var. *farciminosum* (Hcf) H90 (AF322387.1), *H. capsulatum* var. *capsulatum* (Hcc: H81 (AF322385.1), H71 (AF322384.1), H62 (AF322379.1), H2 (AF322377.1), H9 (AF322378.1), H70 (AF322383.1), H68 (AF322382.1), *H. capsulatum* var. *duboisii* (Hcd) H88 (AF322386.1); for *S. schenckii* (Ss): ATCC 14284 (AF364061.1), ATCC 2633 (FJ545232.1), CNM-CM3477 (EU126945.1), CNM-CM3453 (EU126941.1), CNM-CM3462 (EU126943.1), CNM-CM3457 (EU126942.1), CNM-CM3450 (EU126940.1), Duke3751 (AB089138.1). The GenBank sequence of *A. dermatitidis* (Ad) ATCC 60915 (AF322388.1) was used as reference strain, and *P. brasiliensis* (Pb) IFM 41630 (AB304423.1) as the outgroup for *H. capsulatum*; *O. fumeum* (Of) CMW26818 (FM051415.1) was used as outgroup for *Sporothrix* spp. Parenthesis indicate *H. capsulatum* clades or lineages as Kasuga et al.⁷ Abbreviations: Sg=*S. globosa*; BE=Belgium; BR=Brazil; CO=Colombia; EG=Egypt; GT=Guatemala; JP=Japan; MX=Mexico; PA=Panama; USA=United States of America; ZM=Zambia.

H. capsulatum var. *farciminosum*, *H. capsulatum* var. *capsulatum*, and *H. capsulatum* var. *duboisii*.

The tree generated for *Sporothrix* (Fig. 2B) shows three groups in relation with the outgroup, *Ophiostoma fumeum*. The first group was formed by two isolates from the United States of America, eight *S. schenckii* from Mexico, and one isolate of *S. schenckii* and one of *Sporothrix globosa* from Guatemala, with a BT of 93%. The second group was formed by five isolates of *S. schenckii*, all from Brazil, which was sustained by a BT of 100%. Finally, the third group included only one isolate of *S. schenckii* from Japan (Fig. 2B). Therefore, the ITS1-5.8S-ITS2 region sequence is a molecular marker that could discriminate *Sporothrix* species from different geographic regions; however, this marker could not discriminate between *Sporothrix* species.

Conclusions

ITS1-5.8S-ITS2 region sequences deposited in different databases could be utilized as a broad molecular marker for inter- and intraspecific genetic diversity of the *H. capsulatum* and *S. schenckii* species complexes. The intraspecific diversity of this genetic region could discriminate *H. capsulatum* or *Sporothrix* isolates according to their geographic distribution and association with environmental sources. However, ITS regions were unable to distinguish neither *H. capsulatum* species nor *Sporothrix* spp. among their respective phylogenetic, biological and/or taxonomic species complexes.

Conflict of interests

The authors have no conflict of interests.

Acknowledgments

MLT and CT thank the MEXBOL program of CONACyT-Mexico, ref. numbers: 122896 and 122481, respectively. RTA thanks

MEXBOL program of CONACyT, ref. 122481, for his scholarship. The authors thank Ingrid Mascher for editorial assistance.

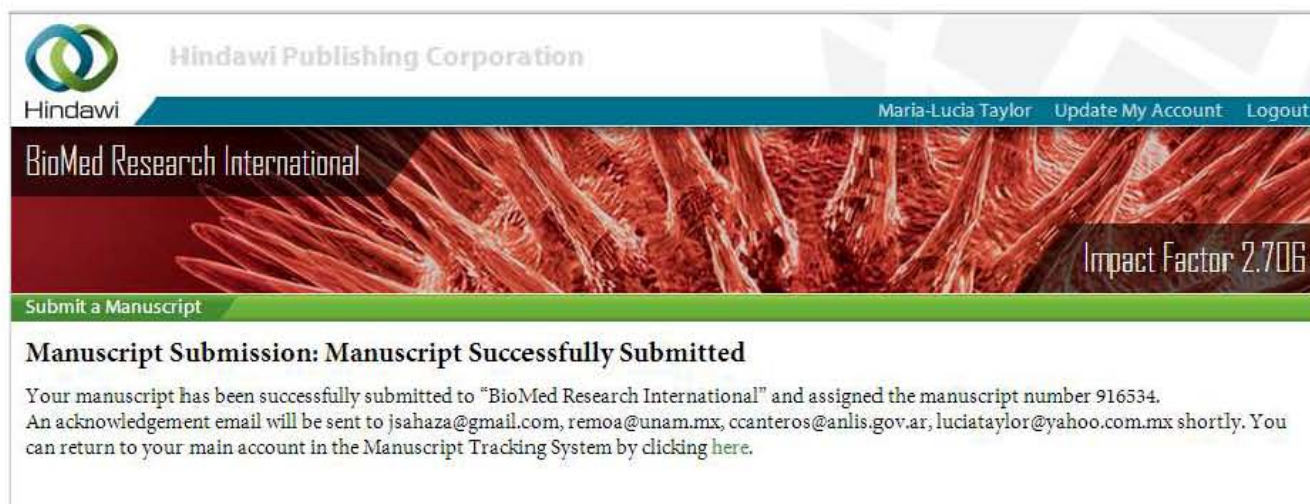
References

- Balajee SA, Hurst SF, Chang LS, Miles M, Beefer E, Hale C, et al. Multilocus sequence typing of *Histoplasma capsulatum* in formalin-fixed paraffin-embedded tissues from rats living in non-endemic regions reveals a new phylogenetic clade. *Med Mycol*. 2012;50:91-8.
- de Beer ZW, Harrington TC, Visser HF, Wingfield BD, Wingfield MJ. Phylogeny of the *Ophiostoma stenoceras-Sporothrix schenckii* complex. *Mycologia*. 2003;95:434-41.
- de Meyer EM, de Beer W, Summerbell RC, Moharram AM, de Hoog GS, Visser HF, et al. Taxonomy and phylogeny of new wood- and soil-inhabiting *Sporothrix* species in the *Ophiostoma stenoceras-Sporothrix schenckii* complex. *Mycologia*. 2008;100:647-61.
- Gutierrez-Galhardo MC, Zancopé-Oliveira RM, Francesconi De Valle AC, de Almeida-Paes R, Morais P, Silva Tavares E, et al. Molecular epidemiology and antifungal susceptibility patterns of *Sporothrix schenckii* isolates from a cat-transmitted epidemic of sporotrichosis in Rio de Janeiro, Brazil. *Med Mycol*. 2008;46:141-51.
- Jiang H, Bartlett M, Allen SD, Smith JW, Wheat LJ, Connolly PA, et al. Typing of *Histoplasma capsulatum* isolates based on nucleotide sequence variation in the Internal Transcribed Spacer regions of rDNA genes. *J Clin Microbiol*. 2000;38:241-5.
- Kasuga T, Taylor JW, White TJ. Phylogenetic relationships of varieties and geographical groups of the human pathogenic fungus *Histoplasma capsulatum* Darling. *J Clin Microbiol*. 1999;37:653-63.
- Kasuga T, White TJ, Koenig G, McEwen J, Restrepo A, Castañeda E, et al. Phylogeography of the fungal pathogen *Histoplasma capsulatum*. *Mol Ecol*. 2003;12:3383-401.
- Marimon R, Gené J, Cano J, Trilles L, Dos Santos Lázara M, Gutarro J. Molecular phylogeny of *Sporothrix schenckii*. *J Clin Microbiol*. 2006;44:3251-6.
- Martin KL, Ryplewicz PJ. Fungal-specific PCR primers developed for analysis of the ITS region of environmental DNA extracts. *BMC Microbiol*. 2005;5:28.
- Mesa-Arango AC, Reyes-Montes MR, Pérez-Mejía A, Navarro-Baranco H, Souza V, Zúñiga G, et al. Phenotypic and genotypic of *Sporothrix schenckii* isolates according to geographic origin and clinical forms of Sporotrichosis. *J Clin Microbiol*. 2002;40:3004-11.
- Muniz MM, Morais e Silva Tavares P, Meyer W, Nosanchuk JD, Zancopé-Oliveira RM. Comparison of different DNA-based methods for molecular typing of *Histoplasma capsulatum*. *Appl Environ Microbiol*. 2010;76:4438-47.
- Núñez RB, Kristianson E, Ryberg M, Hallenberg N, Larsson KH. Intraspecific ITS variability in the kingdom fungi as expressed in the international sequence databases and its implications for molecular species identification. *Evol Bioinformatics*. 2008;4:193-201.

13. Ratnasingham S, Hebert PDN. Bold: the barcode of life data system (<http://www.barcodinglife.org>). Mol Ecol Notes, 2007;7:355-64.
14. Reyes-Montes MR, Rodríguez-Arellanes G, Flores-Robles E, Taylor ML. Tipificación de aislados clínicos de *Histoplasma capsulatum* por métodos fenotípicos y genotípicos. Rev Inst Nal Enf Resp Mex. 1998;11:195-201.
15. Reyes-Montes MR, Taylor ML, Curiel-Quesada E, Mesa-Arango AC. Estado actual de la tipificación del hongo patógeno *Histoplasma capsulatum* var. *capsulatum*: una revisión de los hallazgos. Rev Iberoam Micol. 2000;17:121-6.
16. Saar DE, Polans NO. ITS sequence variation in selected taxa of *Pisum*. Pisum Genet J [Electronic Journal], 2000;32. Available at: <http://pisum.bionet.nsc.ru/pg/32/42.htm> [consulted on 15.01.13].
17. Suwannasai N, Martin MP, Phosri C, Sihanonth P, Whalley AJS, Spouge JL. Fungi in Thailand: a case study of the efficacy of an ITS barcode for automatically identifying species within the *Annulohypoxylon* and *Hypoxylon* genera. PLoS One. 2013;8:e54529.
18. Tamura K, Nei M. Estimation of the number of nucleotide substitutions in the control region of mitochondrial DNA in humans and chimpanzees. Mol Biol Evol. 1993;10:512-26.
19. Tantichareon M. Introduction to Thai biodiversity. In: Jones EBC, Tantichareon M, Hyde KD, editors. Thai fungal diversity. Pathum Thani: Biotec; 2004. p. 1-16.
20. Taylor ML, Chávez-Tapia CB, Rojas-Martínez A, Reyes-Montes MR, Bobadilla-Del Valle M, Zúñiga G. Geographical distribution of genetic polymorphism of the pathogen *Histoplasma capsulatum* isolated from infected bats, captured in a central zone of Mexico. FEMS Immunol Med Microbiol. 2005;45:451-8.
21. Taylor ML, Hernández-García L, Estrada-Bárceñas DA, Salas-Lizana R, Zancopé-Oliveira RM, García de la Cruz S, et al. Genetic diversity of microsatellite (GA)_n and their flanking regions of *Histoplasma capsulatum* isolated from bats captured in three Latin-American countries. Fungal Biol. 2012;116:308-17.
22. Watanabe S, Kawasaki M, Mochizuki T, Ishizaki H. RFLP analysis of the internal transcribed spacer regions of *Sporothrix schenckii*. Jpn J Med Mycol. 2004;45:165-75.

Anexo 2

Artículo enviado



The screenshot shows the top navigation bar of the Hindawi website. On the left is the Hindawi logo, followed by the text "Hindawi Publishing Corporation". On the right, there are links for "Maria-Lucia Taylor", "Update My Account", and "Logout". Below this is a banner for "BioMed Research International" with a background image of red, fibrous biological structures. The banner also displays "Impact Factor 2.706" and a "Submit a Manuscript" button. The main content area features a green header with the text "Manuscript Submission: Manuscript Successfully Submitted". Below this, a paragraph of text provides details about the submission, including the manuscript number 916534 and a list of email addresses: jsahaza@gmail.com, remoa@unam.mx, ccanteros@anlis.gov.ar, and luciataaylor@yahoo.com.mx. A link is provided to return to the Manuscript Tracking System.

Manuscript Submission: Manuscript Successfully Submitted

Your manuscript has been successfully submitted to "BioMed Research International" and assigned the manuscript number 916534. An acknowledgement email will be sent to jsahaza@gmail.com, remoa@unam.mx, ccanteros@anlis.gov.ar, luciataylor@yahoo.com.mx shortly. You can return to your main account in the Manuscript Tracking System by clicking [here](#).

Study of Temperature Sensitivity and Doubling Time of *Histoplasma capsulatum* Yeast Phase Using Clinical Strains from Different Regions of the Americas

Jorge H. Sahaza,^{1,2} María del Rocío Reyes-Montes,¹ Cristina E. Canteros,³ and Maria Lucia Taylor¹

¹*Departamento de Microbiología-Parasitología, Facultad de Medicina, Universidad Nacional Autónoma de México (UNAM), Circuito Interior, Ciudad Universitaria, Av. Universidad 3000, México D.F., 04510, Mexico*

²*Unidad de Micología Médica y Experimental, Corporación para Investigaciones Biológicas, Carrera 72 A No. 78 B 141, Medellín, Colombia*

³*Departamento Micología, INEI ANLIS “Dr. Carlos G. Malbrán”, Av. Vélez Sarsfield 563 (1281), Buenos Aires, Argentina*

Correspondence should be addressed to Maria Lucia Taylor; luciataylor@yahoo.com.mx; emello@unam.mx

Short title: Clinical strains of *H. capsulatum* phenotyping

Abstract

The yeast phase of 22 *Histoplasma capsulatum* clinical strains from Mexico, Argentina, Colombia, and Guatemala and three reference strains (one from Panama and two from the United States) were screened for thermosensitivity at 40°C and doubling time at 37 and 40°C phenotypes. Growth kinetics at 0, 3, 6, 12, 24, and 30 h of incubation at both temperatures were performed for all strains studied. The percentage of yeast growth inhibition at 40°C was estimated. Doubling time at 37 and 40°C was determined from the growth curve data for each strain. Highlight differences in the growth kinetics of *H. capsulatum* strains at 37 and 40°C. The Downs strain from the United States was the only one of the strains to exhibit thermosensitivity at 40°C. Growth inhibition below 33.8% supported the predominance of thermotolerant phenotype at 40°C in most studied strains. The doubling time means found for different strains were 5:18 h \pm 1:19 h at 37°C and 5:48h \pm 1:54 h at 40°C. This is the first report that underscores the predominance of thermotolerant and delayed doubling time phenotypes in *H. capsulatum* clinical strains from different regions of the Americas.

Keywords: *H. capsulatum*, Y-phase, thermotolerance, thermosensitivity, doubling time

1. Introduction

The saprobe-geophilic multicellular morphotype (mycelium, M-phase) of the dimorphic fungus *Histoplasma capsulatum* develops at 25-28°C, its optimal environmental temperature. Aerosolized infective propagules of the M-phase, mainly microconidia and small hyphal fragments, can produce a respiratory infection when inhaled by humans and other mammals. Depending on the immunocompetence of the host, the inoculum size, and/or the virulence of the *H. capsulatum* strain, the infection can lead to severe illness [1, 2]. The unicellular morphotype (yeast, Y-phase) of this pathogen is related to intracellular parasitism in susceptible (immunocompromised) hosts, and it can grow at 37°C in special culture media [1].

The dimorphic transition of *H. capsulatum* is of particular interest because it is necessary for the manifestation of fungal virulence [3]. Under laboratory conditions, the M- to Y-transition can be reversibly induced by temperature switches from 25-28°C (M-phase) to 35-37°C (Y-phase) [4].

Most of the phenotypic studies of *H. capsulatum* have focused on its morphology, physiology, and biochemical properties [5-11]. Based on thermosensitivity at 40°C and avirulence for mice of the Y-phase of the Downs strain, an atypical strain described by Gass & Kobayashi [12] that was isolated from an elderly patient with disseminated histoplasmosis coursing with vaginal lesions, Spitzer et al. [13] reported that fungal isolates from patients with AIDS-associated histoplasmosis from St. Louis, Missouri, United States, shared these two phenotypic characteristics, like the Downs strain. This association was confirmed by molecular methods, which revealed that the St. Louis isolates had a polymorphic mtDNA profile similar to that of the Downs strain. Consequently, the St. Louis isolates were included in Class 1 together with the Downs strain, according to the classification proposed by Vincent et al. [14].

Most phenotypic studies of *H. capsulatum* have been conducted with a limited number of strains, highlighting the reference strains: Downs (low virulence) [12] and G-217B (high virulence) [6, 8] from the United States and the G-186B (high virulence) [15] from Panama. The reported spectrum of phenotype characteristics must be revised accurately in a broad number of strains to ensure their corroboration. Given that *H. capsulatum* is distributed between 54°N [16] and 38°S [17] latitudes, its phenotypes could be used to discriminate among several strains from different geographic distributions, which will contribute to the understanding of the diversity of this pathogen.

The aim of the present study was to phenotype strains of *H. capsulatum* isolated from patients from different regions of the Americas, regarding the Y-phase characteristics of thermosensitivity at 40°C and doubling time (Dt) at 37 and 40°C.

2. Materials and Methods

2.1 *Histoplasma capsulatum*. Clinical strains, 11 from Mexico, five from Argentina, five from Colombia, one from Guatemala, the reference strain G-186B from Panama (ATCC-26030), and two reference strains from the United States, G-217B (ATCC-26032) and Downs (ATCC-38904) were studied. The details for these 25 strains are shown in Table 1.

All strains studied were previously well-characterized and they are deposited in the *H. capsulatum* Culture Collection of the Fungal Immunology Laboratory of the Department of Microbiology and Parasitology, School of Medicine, UNAM (LIH-UNAM) (www.histoplas-mex.unam.mx). *H. capsulatum* specimens of the collection have been well-preserved in sterile distilled water and on Sabouraud-agar with mineral oil, since their first isolation. This collection is registered in the World Data Centre on Microorganisms (WDCM) database of the World Federation for Culture Collections as WDCM817 LIH-UNAM.

2.2 *H. capsulatum* Y-phase transition. The M-phase of each *H. capsulatum* strain studied was initially cultured at 25-28°C on mycobiotic-agar (Bioxon, Becton-Dickinson, Mexico City). Afterwards, each strain was grown in a synthetic medium [18] and incubated at 37°C in an orbital shaker at 200 rpm. The culture medium was replaced every 72 h, until Y-phase was achieved within one or two weeks. Once the dimorphic transition was complete, the Y-phase culture was incubated at 37°C for 24-48 h in brain-heart infusion (BHI)-broth (Bioxon) supplemented with 0.1% L-cysteine and 1% glucose. Yeasts were harvested by centrifuging at 800 g for 15 min, washed twice with fresh BHI-broth, and preserved at -80°C in the presence of fetal calf serum (GIBCO, Grand Island Biological Co. NY) and dimethyl sulfoxide at a 9:1 ratio, until required.

2.3 Thermosensitivity and growth inhibition percentage (GI%) assays. After gradual defrosting, the Y-phase of each strain was grown in supplemented BHI-broth. The culture was incubated at 37°C for 24-48 h, the estimated time required to enter the logarithmic growth phase (log-phase).

Log-phase cultures of each strain were transferred to fresh supplemented BHI-broth and incubated at 37°C for 24 h. Yeasts were centrifuged at 800 x g for 15 min and the pellet was used for each assay. To reach the desired optical density (OD), yeasts were suspended in 10 mL of supplemented BHI-broth. Each suspension was initially diluted 1:10 and, subsequently, serially diluted until 1:2048, in 200 µL per well of a 96-wells microplate (Nunc, Roskilde, Denmark). Each well in the first microplate column was filled with 200 µL of supplemented BHI-broth (blank), and serial dilutions were made from the second to the last columns. The microplate wells were read using a Labsystems Multiskan MS reader (Labsystems, Helsinki, Finland) at 405 nm, and each OD value was automatically adjusted with the blank. For each strain, a 0.2 OD yeast dilution was used to fill eight wells per microplate column with 200 µL of the yeast suspension. Each growth curve assay (growth kinetics) was set up in triplicate either at 37 or 40°C. Optical density readings were taken at 0, 3, 6, 12, 24, and 30 h of incubation at both temperatures, and OD values were averaged using $n = 12$ per each OD strain value, for each time tested. The results were plotted as OD versus incubation times at both temperatures tested.

The percentage of yeast growth inhibition at 40°C was estimated based on the equation: $GI\% = 1 - (OD_{t_x} - OD_{t_0} \text{ at } 40^\circ\text{C} / OD_{t_x} - OD_{t_0} \text{ at } 37^\circ\text{C}) \times 100$, where t_x is the OD value at each time tested and t_0 represents the zero time.

2.4 Doubling time (Dt) assay. Dt at both 37 and 40°C was determined from the growth curve data for each strain. The Dt value for each strain was calculated according to the following equation: $Dt = OD_{t_0} / \mu$, where μ = the slope of the growth curve [19].

The overall mean Dt value for all 25 strains studied was estimated to establish the lowest and highest Dt values \pm SD.

2.5 Statistics. All thermosensitivity and Dt data were statistically analyzed using the Student's t test (Microsoft Excel 2010 for Windows). For all assays, means \pm standard deviation (SD) were determined. A significant difference for P values ($P \leq 0.01$) was considered when $\alpha = 0.001$.

3. Results

Out of 25 *H. capsulatum* strains studied, 20 were isolated from patients with the disseminated

clinical form of histoplasmosis (eight of them came from patients with mucosal lesions), three strains were isolated from patients with localized pulmonary histoplasmosis, and two strains (the GeM strain from Colombia and the G-217B reference strain from the United States) were not associated with any data of clinical and immune conditions of the respective patients.

In addition, 15 strains (ten from Mexico, three from Argentina, and two from Colombia) were from patients with human immunodeficiency virus (HIV+), one strain from a systemic lupus erythematosus Colombian patient and the Downs reference strain from the United States was originally isolated from an 86-years-old patient with rheumatoid arthritis, and finally, eight strains (one from Mexico, two from Argentina, two from Colombia, one from Guatemala, and two reference strains, G-217-B from United States and G-186B from Panama) were associated with patients that had no report of HIV+ or other immunosuppressive states (Table 1).

3.1 Thermosensitivity and GI% assays. For the growth kinetic assays (Figures 1(a-d) and 2(a-d)), all OD data at 0 h of incubation (t_0) were recorded in the range of 0.164 ± 0.002 and 0.286 ± 0.001 at 37°C and of 0.129 ± 0.006 and 0.288 ± 0.001 at 40°C (data not shown). This allowed to ensure that the initial yeast-population at t_0 of all *H. capsulatum* strains studied were as homogeneous as possible. The SD confirmed the minimal variation of readings within the same population.

Differences in the lag (latency), log (exponential), stationary, and decline *H. capsulatum* growth phases were detected at 37 and 40°C , for the incubation time points assayed as can be seen in Figures 1(a-d) and 2(a-d), respectively.

Most of the strains exhibited similar growth kinetics at both 37 (Figures 1(a-d)) and 40°C (Figure 2(a-d)). Several strains did not exhibit a lag-phase at 37°C (Figure 1(a-d)), reaching the log-phase before 3 h and the stationary-phase between 6 and 24 h, depending on the strain studied. In contrast, the lag-phase was well defined in the DMic993444 strain from Argentina, four strains from Mexico (EH-317, EH-324, EH-328, and EH-356), and the Downs strain from the United States (Figure 1(a), (c), and (d)). Most strains reached stationary-phase at 30 h of culture, without evidence of a decline in the yeast population. One strain from Argentina (DMic993444) and the Downs strain reached the log-phase after a 12 h lag-phase (Figure 1(a) and (d)).

The Downs strain was the only one that did not grow at 40°C as shown in Figure 2(d),

confirming its thermosensitive phenotype at this temperature. Overall, out of 25 strains studied, 12 strains (three from Mexico, five from Argentina, three from Colombia, and one from Guatemala) developed GI values from 15.6 to 33.8% at 30 h of incubation at 40°C (Table 2).

The differences in growth kinetics between the reference strains G-217B (thermotolerant prototype at 40°C) and Downs (thermosensitive prototype at 40°C) were significant ($P \leq 0.01$) at the t6, t12, t24, and t30 incubation time points at 37°C, whereas differences in growth kinetics of both strains at 40°C were not applicable due to the lack of growth of the Downs strain at this temperature as aforementioned.

Based on growth kinetics at 37 and 40°C (Figures 1(a-d) and 2(a-d)), most of the studied strains were defined as thermotolerant, irrespective of the clinical form and the immune condition of the patient from whom they were isolated. However, the kinetic of strain DMic993444 (isolated from an Argentinean patient coursing a disseminated clinical form with mucosal lesions) at 37°C is noteworthy since it showed significant differences ($P \leq 0.01$) from strain G-217B at 6-30 h of incubation times and from the Downs reference strain at the t24 and t30 incubation time points (Figure 1(a) and (d)). Because strain DMic993444 also exhibited growth at 40°C at 24 and 30 h of incubation times in contrast to the Downs strain, it could be considered to have a thermotolerant phenotype. However, this strain presented significant differences ($P \leq 0.01$) in OD values from t3 to t30 incubation time points at 40°C when compared with the thermotolerant G-217B strain (Figure 2(a) and (d)).

The determinations of GI% at 40°C allowed verifying the thermosensitive phenotype of all strains studied (Table 2). With the exception of the Downs strain, the remaining strains exhibited thermotolerant phenotype, because all developed low GI (below 33.8%) (Table 2).

3.2 Dt assays. Dt was calculated at both 37 and 40°C for each strain (Table 3). The Dt interval obtained for the different *H. capsulatum* strains varied from 1:36 h (EH-319, Mexican strain) to 8:30 h (MZ 2, Colombian strain) with a mean of 5:18 h \pm 1:19 h at 37°C; and varied from 1:54 h (EH-319, Mexican strain) to 9:42 h (DMic01739, Argentinean strain) with a mean of 5:48 h \pm 1:54 h at 40°C (Table 3).

Two strains (EH-319 and EH-326) from Mexican patients with AIDS-associated disseminated histoplasmosis presented the fastest Dt, with values lower than the averages of all Dt values at 37 and 40°C. Whereas, four strains with mucosal lesions (EH-359 from Mexico,

DMic993446 and DMic01739 from Argentina, and MZ 2 from Colombia) and one strain with the pulmonary clinical form (H.1.02.W from Guatemala) were considered to present the most delayed Dt, showing Dt mean values higher than those found at 37 and 40°C (Table 3). Interestingly, strain DMic993444 (Argentina) presented Dt values close to the means obtained for *H. capsulatum* at both temperatures (Table 3), despite its very long lag-phase (Figures 1(a) and 2(a)). The Dt value calculated for the Downs strain at 37°C was one of the longest revealed in this study (Table 3). This characteristic was not applicable at 40°C for the Downs strain due to its thermosensitivity.

Out of 25 strains of *H. capsulatum* studied, 17 showed an increase in Dt from 37 to 40°C; six exhibited decreased Dt; one strain maintained the same Dt value at both temperatures; whereas the Downs strain did not grow at 40°C, as mentioned above (see details in Table 3).

4. Discussion

The data shown in Table 1 indicate that most of the studied *H. capsulatum* strains were obtained from 1991 to 2001. They were selected for this study due to the limited number of sub-cultures in suitable media after their first isolation. Certainly, they did not develop critical phenotypic changes by the fact that they were taken from their original cultures, as explained in the requirements of the LIH-UNAM *H. capsulatum* collection (see Materials and Methods). In contrast, reference strains G-186B, G-217B, and Downs were isolated many years ago, in the 1960s- and 1970s, and have been sub-cultured successively.

Some phenotypic characteristics (e.g., serotypes, chemotypes, isozymes, and fatty acid profiles) of the two *H. capsulatum* morphotypes have been explored to group and/or classify fungal strains [5, 7, 11, 20, 21]. However, in some cases, these data were analyzed partially, overlooking important associations with critical aspects of the interaction between the fungus and its environment. In the last decades, studies of *H. capsulatum* related to the search thermosensitivity phenotypes associated with fungal virulence were conducted by Keath et al. [22], Medoff et al. [9], and Spitzer et al. [13]. However, their *H. capsulatum* isolates came from circumscribed geographic areas that are not representative of the genetic and phenotypic fungal changes that could be occurring in other regions in the Americas.

The present work focused on searching for the relation between scarcely explored

phenotypic characteristics of *H. capsulatum* Y-phase (thermosensitivity and doubling time), which represents an innovative report since most of the studied *H. capsulatum* strains are closely related to their original cultures, and their phenotypic behavior could be considered as naive. The data obtained for the 25 studied strains are reliable because they incorporated the results of multiple measurements, such as growth kinetics at 37 and 40°C, the GI% at 40°C, and the original Dt estimation at both temperatures. The results showed that all studied strains were thermotolerant at 40°C, with the exception of the Downs reference strain. Interestingly, the Downs strain is also associated with avirulence in a murine model, and according to Spitzer et al. [13], a potential association between virulence and thermotolerance in the *H. capsulatum* Y-phase could be inferred. However, no associations between *H. capsulatum* temperature sensitivity with clinical forms of histoplasmosis and immune status of the patients were found.

It is noteworthy that, in the present study, we found delayed Dts for most of the studied samples at 40°C, indicating that exposure to this temperature delays the growth of thermotolerant yeasts, but did not kill them. This finding, under *in vivo* infection conditions, suggests that host defense mechanisms might include the restriction of fungal dissemination via febrile inflammatory processes.

One novel finding was that the strain DMic993444, which was isolated from an Argentinean histoplasmosis patient who coursed with a disseminated form with mucosal lesions, presented a long lag-phase at both 37 and 40°C, suggesting a probable delay in adaptation to the experimental condition.

The Dt values at 37°C found for most studied strains are compatible for pathogens with low rate of growth and consistent with the previous description of the optimal culture conditions of *H. capsulatum* [8, 15].

Despite the involuntary biases that must be considered in the gathering and handing of patient's records and the number of samples supporting our data, the present findings provide relevant information on the phenotypic behavior of *H. capsulatum* strains irrespective of their association with clinical forms of the disease and their different geographic origins in the Americas. An appropriate number of fungal strains were tested, and, undoubtedly, this type of study will advance the knowledge on the possible manifestations of the pathogen in susceptible hosts.

Competing Interests

The authors declare that they have no competing interests.

Authors' Contribution

Jorge H. Sahaza, María del Rocío Reyes-Montes, and Maria Lucia Taylor contributed equally to the design of this study. Jorge H. Sahaza conducted all the experiments. Cristina E. Canteros contributed to data interpretation and to improve the manuscript. María del Rocío Reyes-Montes and Maria Lucia Taylor were supervisors of this study. All of the authors read and approved the final version of the manuscript.

Acknowledgements

This research was financially supported by a grant from the National Council of Science and Technology (CONACYT) from Mexico (Ref-166052). This paper constitutes collateral fulfillment of the requirements of the Graduate Program in Biological Sciences of the UNAM. JHS thanks the Graduate Program in Biological Science of the UNAM and the scholarship of CONACYT-Mexico (Ref-245151). The authors thank Ingrid Mascher for editorial assistance.

References

- [1] R. Tewari, L. J. Wheat, and L. Ajello, "Agents of histoplasmosis." in *Medical Mycology. Topley and Wilson's, Microbiology and Microbial Infections*, L. Ajello and R. J. Hay, Eds., pp. 373-407, Arnold and Oxford University Press, New York, NY, USA, 1998.
- [2] M. L. Taylor, R. M. Reyes-Montes, and C. B. Chávez-Tapia, "Ecology and molecular epidemiology findings of *Histoplasma capsulatum* in Mexico," in *Research Advances in Microbiology*, R. M. Mojan and M. Benedik, Eds., pp. 29-35, Global Research Network, Kerala, India, 2000.
- [3] D. M. Retallack and J. P. Woods, "Molecular epidemiology, pathogenesis, and genetics of the dimorphic fungus *Histoplasma capsulatum*," *Microbes and Infection*, vol. 1, no. 10, pp. 817-

825, 1999.

- [4] B. Maresca and G. S. Kobayashi, "Dimorphism in *Histoplasma capsulatum*: a model for the study of cell differentiation in pathogenic fungi," *Microbiological Reviews*, vol. 53, no. 2, pp. 186-209, 1989.
- [5] J. E. Domer, J. G. Hamilton, and J. C. Harkin, "Comparative study of the cell walls of the yeast-like and mycelial phases of *Histoplasma capsulatum*," *Journal of Bacteriology*, vol. 94, no. 2, pp. 466-474, 1967.
- [6] M. D. Berliner, "Primary subcultures of *Histoplasma capsulatum*. I. Macro and micro-morphology of the mycelial phase," *Sabouraudia*, vol. 6, no. 2, pp. 111-118, 1968.
- [7] J. E. Domer, "Monosaccharide and chitin content of cell walls of *Histoplasma capsulatum* and *Blastomyces dermatitidis*," *Journal of Bacteriology*, vol. 107, no. 3, pp. 870-877, 1971.
- [8] M. D. Berliner, and N. Biundo Jr, "Effects of continuous light and total darkness on cultures of *Histoplasma capsulatum*," *Medical Mycology*, vol. 11, no. 1, pp. 48-51, 1973.
- [9] G. Medoff, B. Maresca, and A. M. Lambowitz, "Correlation between pathogenicity and temperature sensitivity in different strains of *Histoplasma capsulatum*," *The Journal of Clinical Investigation*, vol. 78, no. 6, pp. 1638-1647, 1986.
- [10] G. Medoff, M. Sacco, B. Maresca, D. Schlessinger, A. Painter, G. S. Kobayashi, and L. Carratu, "Irreversible block of the mycelial-to-yeast phase transition of *Histoplasma capsulatum*," *Science*, vol. 231, no. 4737, pp. 476-479, 1986.
- [11] R. Zarnowski, M. Miyazaki, A. Dobrzyn, J. M. Ntambi, and J. P. Woods, "Typing of *Histoplasma capsulatum* strains by fatty acid profile analysis," *Journal of Medical Microbiology*, vol. 56, no. 6, pp. 788-797, 2007.
- [12] M. Gass and G. S. Kobayashi, "Histoplasmosis. An illustrative case with unusual vaginal and joint involvement," *Archives of Dermatology*, vol. 100, no. 6, pp. 724-727, 1969.
- [13] E. D. Spitzer, E. J. Keath, S. J. Travis, A. A. Painter, G. S. Kobayashi, and G. Medoff, "Temperature-sensitive variants of *Histoplasma capsulatum* isolated from patients with acquired immunodeficiency syndrome," *The Journal of Infectious Diseases*, vol. 162, no. 1, pp. 258-261, 1990.
- [14] R. D. Vincent, R. Goewert, W. E. Goldman, G. S. Kobayashi, A. M. Lambowitz, and G. Medoff, "Classification of *Histoplasma capsulatum* isolates by restriction fragment polymorphisms. *Journal of Bacteriology*, vol. 165, no. 3, pp. 813-818, 1986.

- [15] M. D. Berliner, “*Histoplasma capsulatum*: effects of pH on the yeast and mycelial phases in vitro,” *Medical Mycology*, vol. 11, no. 3, pp. 267-270, 1973.
- [16] H. Anderson, L. Honish, G. Taylor et al., “Histoplasmosis cluster, golf course, Canada,” *Emerging Infectious Diseases*, vol. 12, no. 1, pp. 163-165, 2006.
- [17] L. M. Calanni, R. Pérez, S. Brasili et al., “Brote de histoplasmosis en la provincia de Neuquén, Patagonia Argentina,” *Revista Iberoamericana de Micología*, vol. 30, no. 3, pp. 193-199, 2013.
- [18] R. P. Tewari and H. Kegel, “Suppressive effect of streptomycin on the phagocytic activity of mouse peritoneal macrophages for *Histoplasma capsulatum*,” *Mycopathologia et Mycologia Applicata*, vol. 44, no. 3, pp. 231-240, 1971.
- [19] D. Moore, G. D. Robson, and A. P. J. Trinci, “Whole organism biotechnology”, in *21st Century Guidebook to Fungi*, pp. 460-464, Oxford University Press, New York, NY, USA, 2011.
- [20] L. Kaufman and S. Blumer, “Ocurrence of serotypes among *Histoplasma capsulatum* strains,” *Journal of Bacteriology*, vol. 91, no. 4, pp. 1434-1439, 1966.
- [21] P. Gaur, R. W. Lichtwardt, and J. L. Hamrick, “Isozyme variation among soil isolates of *Histoplasma capsulatum*,” *Experimental Mycology*, vol. 5, no. 1, pp. 69-77, 1981.
- [22] E. J. Keath, A. A. Paiter, G. S. Kobayashi, and G. Medoff, “Variable expression of a yeast-phase-specific gene in *Histoplasma capsulatum* strains differing in the thermotolerance and virulence,” *Infection and Immunity*, vol. 57, no. 5, pp. 1384-1390, 1989.

TABLE 1: Data from all *H. capsulatum* clinical strains studied

Strain	Year of isolation	Geographic origin	Clinical form of the disease	Patient immuno-compromise
EH-316	1993	MX	D	HIV+
EH-317	1992	MX	D	HIV +
EH-319	1991	MX	D	HIV +
EH-323	1993	MX	D	HIV +
EH-324	1994	MX	D	HIV +
EH-325	1996	MX	D	HIV +
EH-326	1996	MX	D	HIV +
EH-328	1991	MX	D	HIV +
EH-355	1996	MX	D	HIV +
EH-356	1996	MX	D	HIV +
EH-359	1995	MX	DML	ND
DMic993444	1999	AR	DML	ND
DMic993445	1999	AR	DML	ND
DMic993446	1999	AR	DML	HIV +
DMic993267	1999	AR	DML	HIV +
DMic01739	2001	AR	DML	HIV +
LA	1996	CO	D	HIV +
AP	ND	CO	D	ND
WE	1996	CO	P	HIV +
MZ 2	1995	CO	DML	SLE
GeM	2001	CO	ND	ND
H.1.02.W	1995	GT	P	ND
G-186B [*]	1967	PA	P	ND
G-217B [†]	1973	US	ND	ND
Downs [‡]	1969	US	DML	RA

AR, Argentina; CO, Colombia; GT, Guatemala; MX, Mexico; PA, Panama; US, United States; D, disseminated; DML, disseminated with mucosal lesions; P, pulmonary; HIV, human immunodeficiency virus; SLE, systemic lupus erythematosus; RA, rheumatoid arthritis; ND, not determined. References: ^{*}Berliner [15]; [†]Berliner [6]; [‡]Gass & Kobayashi [12].

TABLE 2: Growth inhibition percentage (GI%) of *H. capsulatum* yeasts at 40°C

Strain	GI%*				
	3 h	6 h	12 h	24 h	30 h
EH-316	2.5	0.7	12.7	5.7	15.6
EH-317	0.0	0.0	1.4	5.0	6.2
EH-319	2.8	17.1	11.4	15.7	33.8
EH-323	0.0	0.0	0.0	2.7	0.7
EH-324	0.0	0.0	0.0	5.9	4.3
EH-325	0.0	0.0	0.0	2.8	0.0
EH-326	0.0	0.0	0.0	6.4	5.6
EH-328	0.0	0.0	0.0	4.7	0.9
EH-355	0.0	0.0	0.3	4.8	0.0
EH-356	0.0	0.0	0.0	0.0	0.0
EH-359	0.0	0.7	14.1	31.9	28.7
DMic993444	NA	NA	NA	16.5	28.6
DMic993445	5.0	0.0	25.7	15.2	24.2
DMic993446	0.0	18.5	28.3	28.8	26.6
DMic993267	3.1	12.3	16.5	19.0	15.9
DMic01739	0.0	0.4	18.0	25.3	21.2
LA	0.0	0.0	10.8	12.5	23.2
AP	0.0	0.0	0.0	6.7	2.2
WE	0.0	0.0	0.0	2.5	1.8
MZ 2	0.0	0.0	17.7	25.1	27.9
GeM	0.0	5.1	16.9	18.6	17.7
H.1.02.W	0.0	0.0	6.7	12.4	17.5
G-186B	0.0	0.0	5.7	5.2	1.9
G-217B	0.0	0.0	0.0	8.2	5.3
Downs	NA†	NA	NA	NA	NA

*The GI% was estimated according to the equation given under Materials and Methods. †NA (not applicable), due to the lack of yeast growth at 40°C.

TABLE 3: Doubling times (Dt) of *H. capsulatum* yeasts at 37 and 40°C

Strain	Dt (h:min)†		Dt changes*
	37°C	40°C	
EH-316	4:36	5:00	↑
EH-317	5:12	6:00	↑
EH-319	1:36	1:54	↑
EH-323	4:06	5:18	↑
EH-324	4:30	4:36	↑
EH-325	5:00	6:24	↑
EH-326	3:18	3:18	↔
EH-328	4:42	4:48	↑
EH-355	4:24	5:36	↑
EH-356	5:12	4:48	↓
EH-359	6:54	8:54	↑
DMic993444	6:06	6:42	↑
DMic993445	5:18	4:54	↓
DMic993446	6:36	7:24	↑
DMic993267	5:36	7:36	↑
DMic01739	6:42	9:42	↑
LA	5:18	4:42	↓
AP	4:24	3:18	↓
WE	5:42	4:24	↓
MZ 2	8:30	7:42	↓
GeM	5:00	7:06	↑
H.1.02.W	7:24	8:00	↑
G-186B	5:42	5:48	↑
G-217B	3:30	4:24	↑
Downs	7:36	NA†	NA
Means‡	5:18 ± 1:19	5:48 ± 1:54	

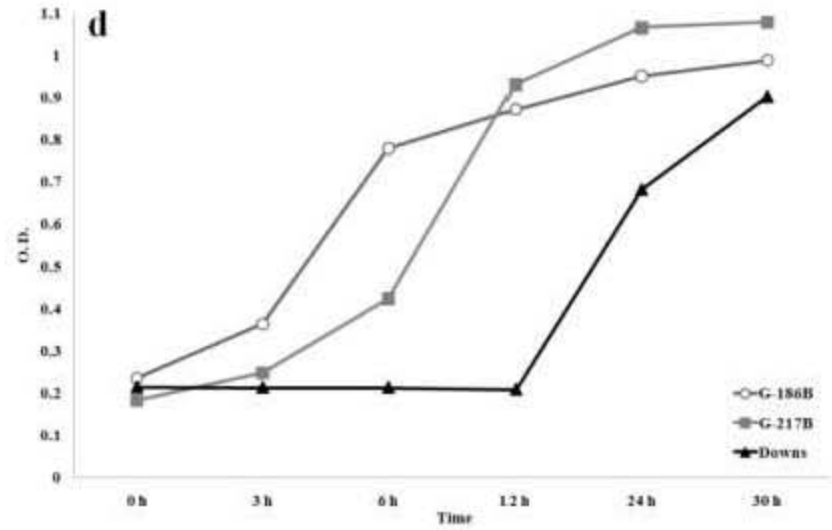
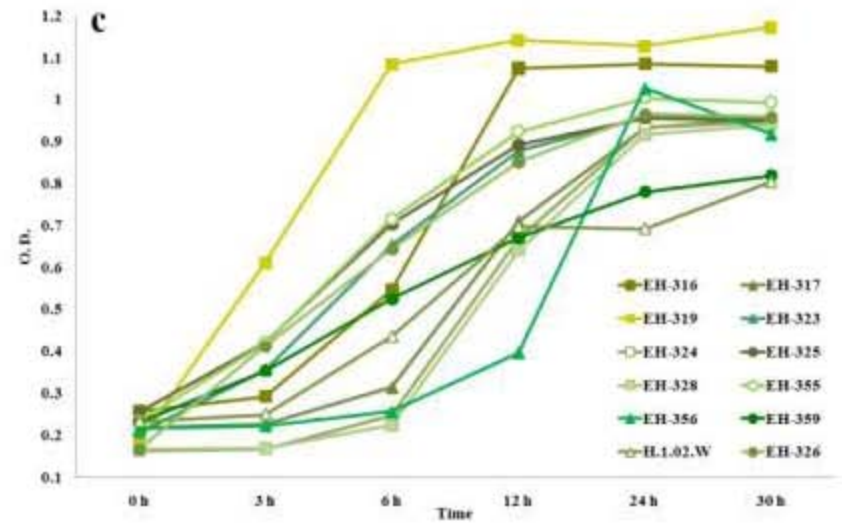
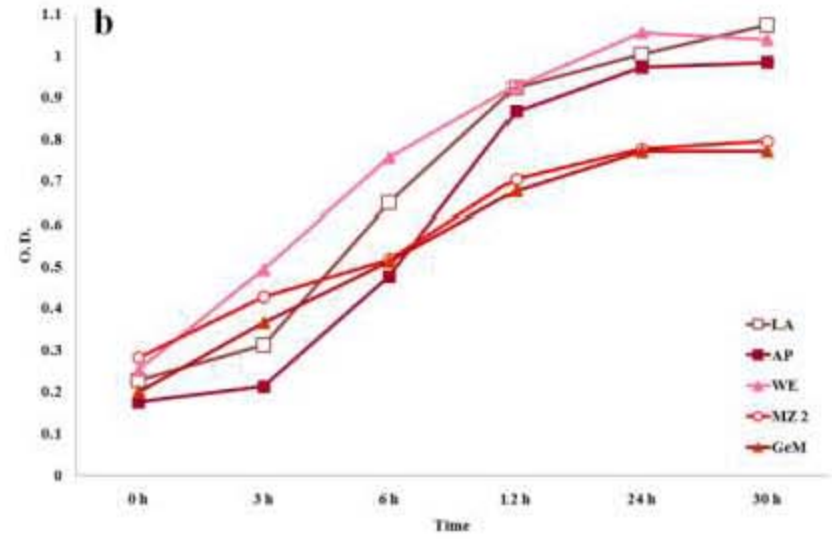
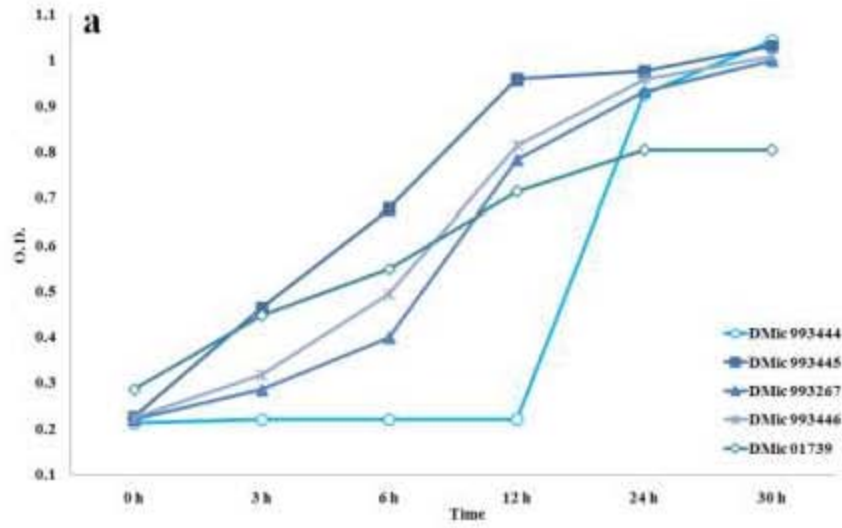
*The Dt estimation was performed according to the equation described under Materials and Methods. †NA (Not applicable). ↑Increasing Dt at 40°C; ↓Decreasing Dt at 40°C; ↔Same Dt values at both temperatures. ‡Data at 37 and 40°C are presented as mean of *H. capsulatum* yeast Dt values ± SD, on the basis of three independent assays, using $n = 12$ per each OD value.

Figure legends

FIGURE 1: Growth kinetics of *H. capsulatum* yeasts at 37°C. The OD readings for each time tested were measured in a Multiskan reader at 405 nm; the yeast growth conditions and growth curve construction are described under Materials and Methods. (a) Strains from Argentina; (b) strains from Colombia; (c) strains from Mexico and Guatemala; and (d) reference strains. On the basis of three independent assays ($n = 12$ per each OD value), significant differences in growth kinetics were recorded for $P \leq 0.01$ along the incubation time points tested.

FIGURE 2: Growth kinetics of *H. capsulatum* yeasts at 40°C. The OD readings for each time tested were measured in a Multiskan reader at 405 nm; the yeast growth conditions and growth curve construction are described under Materials and Methods. Strains, assays, and analyses are the same as those for Figure 1.

37 °C



40 °C

